Summer 8-15-2015

# Growth Factor Gradient Formation and Release from PEG Microspheres for Nerve Regeneration.

Jacob Roam
*Washington University in St. Louis*

WASHINGTON UNIVERSITY IN ST. LOUIS

School of Engineering and Applied Science
Department of Biomedical Engineering

Dissertation Examination Committee:

Donald Elbert, Chair

Dennis Barbour

Shelly Sakiyama-Elbert

Jin-Yu Shao

Matthew Wood

# Growth Factor Gradient Formation and Release from PEG Microspheres for Nerve Regeneration.

By

Jacob Levi Roam

A dissertation presented to the
Graduate School of Arts & Sciences
of Washington University in
partial fulfillment of the
requirements for the degree
of Doctor of Philosophy

August 2015
Saint Louis, Missouri

# Table of Contents

# List of Figures

# List of Tables

# Acknowledgements

Foremost, I would like to thank Don Elbert, my advisor, for everything you have done for me over nearly 6 years. Without your having taken a chance on me and giving me a job in your lab, there is little chance that I would have made it into a program of this caliber. Your guidance, advice, and patience for me, as well as your own scientific creativity has not only been invaluable in getting me to this point, but will also serve as inspiration for years to come.

I would also like to thank Shelly Sakiyama-Elbert for her advice and help going all the way back to my first year rotation in her lab. I would like to thank Matt Wood for his advice, planning, assistance, materials, animals, and everything else over this past year. I thank the rest of my thesis committee, Jin-Yu Shao and Dennis Barbour, for their time and advice as well. I would also like to thank Ying Yan for all his time and surgical work with my conduits.

I would like to thank all the members of the Elbert lab, Megan Flake, Casey Donahoe, Amanda Smith, and Peter Nguyen, for everything they've done over the years; endlessly helping me find things, generally keeping me straight, and just making our lab a great place to work. Special acknowledgement should go to Peter Nguyen, who ran the lab with me for these last couple years; it was quite an adventure. I would also like to thank the members of the Sakiyama-Elbert lab for all their help and for making such a great inter-lab community.

Finally, I need to thank my family and friends for all of their love and support. To my parents, Frank and Carol Roam, you have supported me in every conceivable way, given me sage council at every turn, and provided me love and encouragement beyond anything most people could dream. You are, without exaggeration, the best parents in the world. To my wife, Jessie, you make all of this, every day, every experiment, every word typed, every sigh heaved, every moment worthwhile.

**Jacob Levi Roam**

*Washington University in St. Louis*

*August 2015*

*Now to Him who is able to do exceedingly abundantly above all that we ask or think, according to the power that works in us, to Him be glory in the church by Christ Jesus to all generations, forever and ever. Amen.*

*(Ephesians 3:20-21)*

ABSTRACT OF THE DISSERTATION

Growth Factor Gradient Formation and Release from

PEG Microspheres for Nerve Regeneration.

By Jacob Levi Roam

Doctor of Philosophy in Biomedical Engineering

Washington University in St. Louis, 2015

Professor Donald Elbert, Chair

Many biological processes depend on concentration gradients in signaling molecules. Thus, introduction of spatial patterning of proteins, while retaining activity and releasability, will be critical for the field of regenerative medicine. In particular, the area of nerve regeneration is in need of innovations to improve outcomes. Only about 25% of surgical patients with peripheral nerve damage (~200,000 surgical interventions performed each year) regain full motor function with less than 3% regaining sensation. The use of nerve guidance conduits (NGC's) which are filled with biomimetic scaffolds is one treatment being explored. These scaffolds, however, lack the spatial patterning of proteins found in native tissue. Glial-cell line derived neurotrophic factor (GDNF), a potent stimulator of axon regeneration, is one such protein that, if contained within the scaffold and conformed to a particular concentration profile, could greatly enhance neural regeneration. The object of this work is to utilize poly(ethylene glycol) (PEG) microspheres to accomplish this spatial patterning of GDNF and apply it to NGC's.

First, an approach utilizing the controllability of the PEG microsphere's density (buoyancy) was explored. By creating the microspheres under varying conditions, incubation time and temperature, the cross-linking and, thus, the swelling rate of the microspheres could be

controlled. This created microspheres of different densities that, upon centrifugation, would orient themselves within a scaffold, creating a gradient in the different microsphere types. GDNF loaded into a batch of microspheres would thusly be oriented within the scaffold along with that particular microsphere batch. Through this, gradients in GDNF were created. Heparin was also added to the microspheres to allow for reversible binding of GDNF.

Next, gradients in reversibly bound GDNF were formed through sequential centrifugation of microsphere batches. For instance, a layer of GDNF loaded microspheres were formed into a scaffold followed by a layer of microspheres without GDNF on top of them. This created an initial step gradient in GDNF that, given time to release, would form a linear concentration gradient. Gradients formed by this method were visualized by fluorescent confocal microscopy and compared to Fickian models. Some conditions yielded profiles more linear than the model predictions, which persisted for over a week.

Lastly, the sequential gradient formation was modified and applied to NGC's. Before the scaffolds were ready for *in vivo* implantation, functionalities such as cell initiated degradability, cell adhesion, and inter-microsphere cross-linking were added. A plasmin degradable peptide sequence (GCGGVRNGGK) was incorporated into the microspheres. CLICK agents, laminin, and heparin (via a new binding chemistry) were attached to the microspheres to add inter-microsphere cross-linking, add cell adhesion, and heparin binding functionalities, respectively. GDNF gradient formation and activity retention were confirmed with these fully functionalized microspheres. Microsphere scaffolds with linear gradients in GDNF were then formed in silicone tubes which were transplanted into rats with severed sciatic nerves.

# Chapter 1

# Introduction

## 1.1 Synopsis and Objectives of Thesis

The primary objective of this work is to create functional nerve guidance conduits (NGC's) containing poly(ethylene glycol) microspheres incorporating a linear concentration gradient in glial cell-derived neurotrophic factor (GDNF). Concentration gradients of signaling molecules are important in wound healing, as well as embryogenesis, immunity, angiogenesis, and nerve cell signaling (X. Cao & Shoichet, 2001; Parent & Devreotes, 1999; Singh, Morris, Ellis, Detamore, & Berkland, 2008; H. Song & Poo , 2001). In particular, chemotaxis, the preferential movement of cells up a concentration gradient of signaling molecules, is known to be dependent upon the steepness of a concentration gradient as opposed to the average concentration of the molecule (Knapp, Helou, & Tranquillo, 1999; K. Moore, MacSween, & Shoichet, 2006; Parent & Devreotes, 1999). Utilization of such gradients may be critical to the advancement of nerve regeneration. Because scaffolds formed from hydrogels made of synthetic polymers show significant promise in regenerative medicine (Drury & Mooney, 2003; E. a. Scott, Nichols, Kuntz-Willits, & Elbert, 2010; Tessmar & Göpferich, 2007), this research sought to create gradients with PEG microsphere scaffolds. Because these microsphere scaffolds are formed in a modular manner (Nichols, Scott, & Elbert, 2009; E. a. Scott et al., 2010), distinct disadvantages, such as scaling issues and difficulty in pumping polymerizing solutions (X. Cao & Shoichet, 2001; Kapur & Shoichet, 2004; Knapp et al., 1999; H. Song & Poo , 2001), incurred by other gradient making systems can be circumvented (Rivest et al., 2007; E. a. Scott et al., 2010; Serban & Prestwich, 2008).

This work details two approaches to this problem. First, microspheres of varying densities (buoyancies) were fabricated which, upon centrifugation would orient themselves into scaffold containing a gradient in microspheres (Roam, Xu, Nguyen, & Elbert, 2010). The density (buoyancy) of the microspheres could be altered via their cross-link density which is controllable by varying incubation times and temperatures at microsphere formation (Nichols et al., 2009). Proteins such as protamine and GDNF were bonded to the microspheres which were then mixed with microsphere of different densities containing no bond protein. After centrifugation and microsphere scaffold formation, gradients in these proteins were observed. In order to avoid damage to the GDNF potentially caused by the covalent bonding and to maintain releasability, the study sought to use heparin, which promotes electrostatic (reversible) binding of heparin-binding proteins (Nie, Baldwin, Yamaguchi, & Kiick, 2007; Sakiyama-Elbert & Hubbell, 2000; Tae, Scatena, Stayton, & Hoffman, 2006). Heparin was incorporated into the microspheres via an EDC/NHS activation of carboxylic acids (Tae et al., 2006), and gradients in reversibly bound protamine and GDNF were formed.

The second approach, which eliminated much of the complexity and variability of the first approach, was to centrifuge different batches of microspheres sequentially in order to form distinct layers (Roam, Nguyen, & Elbert, 2014). GDNF electrostatically bound into one of the layers by heparin would slowly release from that layer into the unoccupied layer, forming a gradient. The gradients were tracked over time by fluorescent confocal microscopy and compared to predictions by fickian models. In some cases, particularly the simple two-tier initial step gradient, this system formed gradients more linear than the predictions and maintained them for over a week. This success led to the third portion of this work which sought to implement this second gradient making system within NGC's.

Before the scaffolds were ready for in vivo testing, however, certain functionalities needed to be added to the microspheres. Cell initiated degradability, inter-microsphere cross-linking, and cell

adhesion needed to be incorporated into the microsphere in order for the scaffolds to be functional for nerve regeneration. While cell initiated degradability will be necessary simply to make room in the conduit for the extending nerve, replication the native degradability of natural biomaterials, such as fibrin, has the added benefit of stimulating the regeneration process (Ehrbar et al., 2007; M P Lutolf & Hubbell, 2005). This study implemented peptide sequences sensitive to plasmin, a second enzyme that plays a key role in cell migration, especially during wound healing (West & Hubbell, 1999). To promote scaffold stability, it will be necessary for the microspheres to cross-link to one another. In order to accomplish this under physiological conditions without using agents that might interact with the GDNF, other ambient proteins, or the extending nerves themselves, this study utilized bioorthogonal Click reactions (Nwe & Brechbiel, 2009). Click agents had already been attached to the Elbert lab's PEG microspheres (Nguyen, Snyder, Shields, Smith, & Elbert, 2013). To allow extending nerves to attach to and subsequently grow through our scaffold, laminin, a basement membrane protein that influences cell adhesion, neurite outgrowth, growth cone movement, and acts as a neuronal cue (Culley et al., 2001; Evans et al., 2007; Swindle-Reilly et al., 2012), was attached to the microspheres. The gradient making capability of scaffold made from these fully functionalized microspheres was confirmed, and the GDNF released by them was verified to have maintained its activity. Finally, NGC's containing scaffolds made from these fully functionalized microspheres and gradients in GDNF were implanted into rats with severed sciatic nerves.

The following introduction will highlight the key principles that support this thesis work regarding synthetic biomaterials and peripheral nerve injury. Current research involving the design of biomaterial scaffolds and delivery of growth factors will be discussed.

## 1.2 Biological Gradients

It has long been known that concentration gradients in biological molecules are crucial to the guidance of cells (Fisher, Merkl, & Gerisch, 1989; Parent & Devreotes, 1999). Cells rely on directional sensing to determine the direction and proximity of extracellular stimuli, whether chemical or topographical, that control differentiation, survival, and proliferation and direct cell migration. Chemotaxis, immunity, angiogenesis, wound healing, embryogenesis, neuronal patterning, and many other processes are critically dependent upon this directionality, and the sensing of gradients is one important way cells are able to gather this information. Cells react to chemoattractants by a number of means including G protein–linked signaling pathways and activation of the Rho family of small guanosine trisphosphatases (GTPases) to induce actin polymerization (Parent & Devreotes, 1999). Concentration differences as low as 2% between the front and the back of the cell can be detected, and, thus, the relative steepness of a gradient rather than the mean concentration of a molecule will heavily affect the actions of a cell (Tranquillo, 1988).

### 1.2.1 Gradients and Nerves

Chemical gradients are also critical to neuronal guidance. More than a century ago, Cajal suggested that the migration of neuroblasts and growth cones might be guided by gradients of chemical substances secreted by the target cells (Cajal, 1995). Micropipettes containing NGF placed near growing chick dorsal root ganglia (DRG) allowed the NGF to diffuse out, creating a gradient and directing the extending neurites from the DRG to the micropipette (Gundersen & Barrett, 1979). Song, et al, found that gradients of brain-derived neurotrophic factor (BDNF) can trigger an attractive turning response of the growth cone of Xenopus spinal neurons *in vitro* (H. Song & Poo , 2001; H. J. Song, Ming, & Poo, 1997). The Shoichet lab has shown that growing PC12 exposed to a gradient in

nerve growth factor (NGF) will orient themselves in the direction of that gradient (X. Cao & Shoichet, 2001). A later study by the same lab showed that PC12 cells would extend neurites up a gradient of immobilized NGF (Kapur & Shoichet, 2004). These studies show the potential for application of gradients to tissue engineering systems, especially those intended for nerve regeneration. Specifically engineered gradients in neuronal cues could be critical for the advancement of peripheral nerve injury treatment therapies.

### 1.2.2 Strategies for Gradient Fabrication

A number of systems currently exist for fabricating growth factor concentration gradients. On the microscopic scale, chemical gradients can be formed around single cells, or very small colonies, through the pulsatile application of picoliters of a growth factor solution near the cell (Parent & Devreotes, 1999; H. Song & Poo , 2001; H. J. Song et al., 1997). This is extremely small scale, only useful for single-cell level experimentation and not really suitable for *in vivo* experimentation, or clinical treatments. The most widely used form of gradient creation is simple diffusion of a molecule into a gel. A pre-loaded gel can be allowed to release in one direction, forming the gradient, or one side of a gel can be exposed to a solution of the desired growth factor allowing the growth factor to diffuse into it; from there the gel can be used as diffusion is happening, removed once diffusion into the gel has created a gradient, or (X. Cao & Shoichet, 2001; Dodla & Bellamkonda, 2008, 2006; X Yu, Dillon, & Bellamkonda, 1999). Knapp, et al. used this method to create a gradient in chemotactic factor in a collagen gel that, when seeded with fibroblasts, would provide a unique assay for cell chemotaxis (Knapp et al., 1999). This method, however, is lacking in robustness, as only certain gradient profiles can be formed, and the gradients will not persist for long once removed from the growth factor source, though the latter difficulty has been overcome by covalently bonding the growth factor into the gel after the diffusional gradient has formed (Dodla & Bellamkonda, 2006;

Vepari & Kaplan, 2006). Kipper, et al also devised a unique variation on this system. By slowly pumping a solution containing a "coupling agent" though a fibrin gel, they ensured that different points in the gel would be exposed to the agent for gradually increasing times, thus having the agent bond to the gel in a gradient of concentrations (Kipper, Kleinman, & Wang, 2007).

A number of more controlled means of creating gradients have been conceived. Gradients have been made by modularly layering polymer scaffolds, with each layer containing different concentrations of the target molecule (Mapili, Lu, Chen, & Roy, 2005; Suri et al., 2011). Printing techniques have allowed for the 2D patterning of molecules on a surface, making a gradient on which cells can be cultured (Campbell, Miller, Fisher, Walker, & Weiss, 2005; Rosoff et al., 2004). Similar to the printing methods, photo-patterning has also allowed for the precise placement of molecules into a gradient profile (Iha et al., 2009; Stefonek & Masters, 2007). By creating gradients in light exposure over the length of a scaffold with photo-reactive elements, gradients in the molecules captured in those reactions are formed (Deforest, Sims, & Anseth, 2010; Polizzotti, Fairbanks, & Anseth, 2008). Gradients in lentiviral vector mediated GDNF production were created along a nerve through multiple injections of the vector in varying amounts (Eggers et al., 2013). Oh, et al. created gradients of growth factors by using polycaprolactone (PCL) microfibers that, upon centrifugation would pack together in a gradient of densities, the top being loosely packed and the bottom being heavily packed (Oh, Kim, & Lee, 2011). Davidenko, et al created a gradient in scaffold structure by thermal means, with a heating element placed to one side of a solution of heat-reactive constituents creating a temperature gradient in the solution that would cause the scaffold to form with a gradient of properties (Davidenko et al., 2012).

Microfluidic devises have been employed by many groups for the fabrication of gradients (Khademhosseini & Langer, 2007). By combining polymerizing solutions with varying

concentrations of a target molecule within microfluidic chambers, gradients can be formed in a very precise, controlled manner (Chung et al., 2009; Edalat, Sheu, Manoucheri, & Khademhosseini, 2012; J. He et al., 2010; Zaari, Rajagopalan, Kim, Engler, & Wong, 2004). He, et al created centimeter-long gradients in an RGD adhesion peptide within a microfluidic channel through passive-pump-induced forward flow followed by evaporation-induced backward flow, with the hydrogel material containing the gradient synthesized via photopolymerization (J. He et al., 2010). Microfluidic chips have also been engineered, capable of producing testing platforms with precise gradient profiles in numerous molecules (Cosson, Kobel, & Lutolf, 2009). This method is obviously lacking due to its small scale, but the process has been scaled up in the form of a device called a "gradient maker."

Commercially available gradient makers are made up of the two chambers of polymerizing solutions, one of which containing the molecule of interest, connected by a pumping system capable of modulating the ratio of one solution to the other (Kapur & Shoichet, 2004). The Shoichet group has used this technology extensively to make gradients in growth factors, especially nerve growth factor (NGF), to test the responsiveness of PC12 cells and DRG's to gradients and to biomaterial scaffolds with gradients for nerve regeneration (Kapur & Shoichet, 2004; K. Moore et al., 2006). Other groups have used the system to similar ends, created gels with gradients and culturing cells on those gels to evaluate the effect of the gradient (DeLong, Moon, & West, 2005; Lühmann, Hänseler, Grant, & Hall, 2009). Microspheres containing the target molecule could also be formed into a gradient within the greater polymer scaffold through this technology (X. Wang et al., 2009). Scott, et al. used the system to create a gradient containing gel capable of sustained, zero-order release (D. C. Scott & Hollenbeck, 1991). This system has the distinct disadvantage of the viscous polymer solutions being difficult to pump, and considering *in vivo* applications, air bubbles and harsh chemicals involved in polymerization are a concern.

Many of these difficulties can be overcome by creating gradient containing scaffolds by modular means through the use of microparticles. One method involves making microspheres, some of which encapsulate a growth factor, and injecting the microspheres with and without the growth factor into a mold at varying rates, much like the gradient maker, to form the gradient (Dormer, Singh, Wang, Berkland, & Detamore, 2010; Singh et al., 2008). Scott, et al. created modular microsphere scaffolds with varying properties within the scaffold. Though concentration gradients were not created, they theorized that their system would be very conducive to that use (E. a. Scott et al., 2010). This work seeks to expand upon that idea.

## 1.3 Poly(ethlyene glycol) Biomaterials

Poly(ethylene glycol) (PEG), also referred to as poly(ethylene) oxide at high molecular weights, is a synthetic polymer composed of ethylene oxide monomers. Described as a "stealth material" and long approved by the FDA for clinical use, PEG has a general formula of HO-(CH2-CH2-O)n-H and is strongly hydrophilic (Bailey & Koleske, 1967; Peppas, Hilt, Khademhosseini, & Langer, 2006). PEG is a highly favored material for many therapeutic applications due to its resistance to protein adsorption and cell adhesion. Here, I will discuss its potential as hydrogel scaffold for NGC's.

### 1.3.1 History of PEG materials

Most materials implanted *in vivo* trigger a foreign body response caused by their adsorbtion of proteins from the blood over long periods of time, walling off the implant in a fibrotic capsule (Ratner, Hoffman, Schoen, & Lemons, 2013). Coagulation studies in the early 1970s first reported PEG's ability to prevent cell adhesion (George, 1972). Not long after, it was demonstrated that protein adsorption could be decreased by including PEG in copolymers (K. Furasawa, 1977), with

subsequent studies confirming this (Brash & Uniyal, 1979; Whicher & Brash, 1978). Only a few years later, it was shown that PEG surfaces incurred lower platelet adhesion than PVP surfaces (Mori et al., 1982). Merrill made a strong argument that PEG may be one of the least thrombogenic materials available (Edward W Merrill & Salzman, 1983), convinced by multiple studies performed by his own lab as well as results other labs (E W Merrill et al., 1982; Sa Da Costa, Brier-Russell, Salzman, & Merrill, 1981; V Sa da Costa, D Brier-Russell, G Trudel, D.F Waugh, E.W Salzman, 1980).

A wave of research into "PEGylation" of previously studied materials as well as PEG-copolymers emerged based on these findings supporting PEG as a non-thrombogenic material. Hill-West et al. found that coating the surface of the artery treated by balloon angioplasty with PEG-diacrylate nearly eliminated restenosis normally induced by the procedure (Hill-West, Chowdhury, Slepian, & Hubbell, 1994). In an attempt to prevent adhesions that frequently occur as a result of certain surgical procedures, Hubbell developed a PEG-polylactide surgical sealant (Sawhney, Pathak, & Hubbell, 1993). Though results in humans were relatively difficult to assess, these sealants performed relatively well in small animals and were later adapted for use in lung (Porte et al., 2001) and brain (Preul, Campbell, Bichard, & Spetzler, 2007) surgeries.

### 1.3.2 PEG Resistance to Protein Adsorption

PEG has the unique ability to form a "hydration shell" due to each PEG unit being hydrated by three water molecules (indicated by both Raman scattering and NMR analysis) and the resultant hydrogen bonding; these shells possibly extending several hundred angstroms from the PEG backbone (Horne, Almeida, Day, & Yu, 1971; Kjellander & Florin, 1981; K. J. Liu & Parsons, 1969; Maxfield & Shepherd, 1975; Muller & Rasmussen, 1991). PEG is thought to have considerable

resistance to non-specific protein adsorption as a result of both this hydration shell and steric repulsive forces of the polymer chains (Jeon, Lee, Andrade, & de Gennes, 1991; McPherson, Shim, & Park, 1997). The effects of these repulsive forces can be enhanced by increased packing of the polymer chains and longer chain lengths. Thus, as the molecular weight and density are increased, the resistance of PEG to protein adsorption is amplified (Jeon et al., 1991). Adding to the resistance, PEG's overall neutral charge, in combination with the hydration shell, provides very few binding sites for proteins to attach via electrostatic forces (Ostuni, Chapman, Holmlin, Takayama, & Whitesides, 2001; Whitesides, 1993). In multiple studies, PEG chains have been reacted to the surfaces of proteins and enzymes, preventing immunologic recognition as well as clearance of these biomolecules when injected into the blood stream ( a. Abuchowski, McCoy, Palczuk, van Es, & Davis, 1977; A. Abuchowski, van Es, Palczuk, & Davis, 1977). Immunologic resistance could be accomplished through the covalent attachment of higher molecular weight PEG chains at lower densities of coupling.

Though its resistance to protein adsorption makes PEG desirable for use as a biomaterial, it does lack some of the advantageous structural properties possessed by other polymers currently used in the manufacturing of implanted devices. Frequently, to combat this deficiency, PEG is used in the formation of hydrogels (Nguyen et al., 2013; Roam et al., 2014; Sawhney et al., 1993; Wacker, Scott, Kaneda, Alford, & Elbert, 2006; Zisch et al., 2003) or grafted or coated onto the surfaces of other materials (Burchenal et al., 2002; Heuberger, Drobek, & Spencer, 2005; Ma, Hyun, Stiller, & Chilkoti, 2004; McPherson et al., 1997). The development of PEG-based materials commonly uses PEG derivatives, due to the hydroxyl moiety's low reactivity. Numerous methods for the highly efficient synthesis of PEG derivatives were developed by Harris *et al*. These methods initially formed either a PEGtosylate or PEG-mesylate that could be displaced in subsequent reactions with minimal chain cleavage (Harris et al., 1984). Dacron surfaces with PEG-diisocyanate grafted onto them were

shown to have significantly decreased platelet adhesion and fibrinogen adsorption (Burchenal et al., 2002). Generation of surface radicals with UV light allowed for the attachment of PEG to Dacron via graft polymerization (Uchida, Uyama, & Ikada, 1994). Cell in-growth matrices have been formed using four-arm PEG-VS hydrogels by covalently retaining integrin-binding RGD peptides and substrates for matrix metalloproteinases (Zisch et al., 2003).

### 1.3.3 Chemical Functionalization of PEG

The hydroxyl end-groups of PEG can be functionalized with vinyl-sulfones which, subsequently, can be utilized for hydrogel formation via crosslinking of PEG molecules, biological factor retention, and covalent attachment to surfaces of materials, all under mild physiological conditions (Wacker et al., 2006; Zisch et al., 2003). In the presence of nucleophiles, α,β conjugated compounds undergo Michael-type nucleophilic addition reactions. Vinyl sulfone has been shown to participate in such reactions in a pH dependent manner (Masri & Friedman, 1988). Under neutral conditions thiol-containing molecules will readily alkylate PEG-VS, and under slightly basic conditions amine-containing molecules will do the same. This allows for conjugation to proteins via selective reactivity with either cysteines or lysines. It is, therefore, possible to attach biological molecules containing cysteines and/or lysines to PEG-VS containing gels under mild physiological conditions, thereby avoiding denaturation or unwanted side-reactions. Lutolf, et al, successfully used this ability to conjugate hydrogels with cell adhesion peptides and to crosslink enzymatically degradable peptides into them (M P Lutolf et al., 2003).

### 1.3.4 Poly(Ethylene Glycol) Scaffolds

Tissue engineering scaffolds are able to promote tissue healing and/or regeneration by providing structures with specially designed mechanical and biochemical properties necessary for

maintaining cell viability and directing cell proliferation and differentiation (Place, George, Williams, & Stevens, 2009). The goal of current advancements in scaffolds is to design a biomaterial makeup capable of eliciting specific cellular interactions and responses at the molecular level while minimizing unfavorable nonspecific biological activity (Hench & Polak, 2002). PEG derivatives and copolymers, with their chemical versatility and specificity, have been the focus of many emerging strategies to create these scaffolds. The Hubbell group, who have focused on developing PEG hydrogel scaffolds under mild conditions via the vinyl sulfone derivative of PEG, has achieved in situ formation of cell niches of cells migrating and proliferating within a scaffold through the fabrication of cell-laden PEG-VS hydrogels crosslinked with MMP-degradeable peptides (M P Lutolf et al., 2003). Malda et al, used poly(ethylene glycol)-terephthalate, a completely synthetic PEG copolymer, fibers in porous scaffolds for the engineering of articular cartilage to enhance scaffold stiffness, achieving elastic moduli up to 4.33 MPa (Malda et al., 2004, 2005).

In the quest to achieve an ideal tissue engineering scaffold, scaffolds containing high percentages of PEG have been fabricated to minimize nonspecific protein adsorption and cell adhesion while maintaining a hydrogel structure desirable for achieving high levels of water content and nutrient transfer. Some of these scaffolds have also allowed for the incorporation of biomolecules either at the backbone level or in the form of end-group conjugation to impart specific bioactivity and/or cell-initiated mechanisms of degradation (Jo et al., 2010; Lih, Yoon Ki Joung, Jin Woo Bae, & Ki Dong Park, 2008; Marquardt & Willits, 2011; Miller et al., 2010; Raeber, Lutolf, & Hubbell, 2005; Zisch et al., 2003). However, it would be extremely advantageous for these scaffolds to fabricated with a rapid, scalable, and modular process (Lampe, Antaris, & Heilshorn, 2013; E. a. Scott et al., 2010; R. a. Scott, Elbert, & Willits, 2011; Serban & Prestwich, 2008). Porosity at multiple length scales to provide niches for embedded cells and routes of vascularization (E. a. Scott et al., 2010; H. Wang, Leeuwenburgh, Li, & Jansen, 2012; Wu et al., 2011), adjustable stiffness to mimic the

physical characteristics of different types of tissues (Lampe et al., 2013; Serban & Prestwich, 2008), and gradients in various properties (Dormer et al., 2010; Roam et al., 2014, 2010; E. a. Scott et al., 2010; Singh et al., 2008; X. Wang et al., 2009) could be incorporated into scaffolds through modular means.

## 1.4 Peripheral Nerve Injury and Treatment

Peripheral nerve injury (PNI) affects up to up 1-3% of all traumatic injuries, approximately 500,000 Americans each year, with as many as 360,000 upper limb extremity injuries alone (Kelsey & Praemer A., 1997; Pfister et al., 2011; Taylor, Braza, Rice, & Dillingham, 2008). PNIs often result in chronic or permanent loss of motor function and sensation due to the limited regenerative capacity of the peripheral nervous system (PNS), leading to over 8.5 million restricted activity and 5 million bed/rest disability days (Kelsey & Praemer A., 1997). A $1.68 billion industry has emerged to combat PNS injury and neuropathy, given its high prevalence compared to spinal cord injury, which has led to a significant focus on faster regeneration (Brattain, 2012).

Depending on the type and severity of nerve trauma, surgical intervention may be needed to aid in axonal regeneration to distal end organs, such as muscle or skin. Less than 25% of patients with PNI's recover proper motion and less than 3% recover full sensation despite the nearly 200,000 surgeries performed each year in an attempt to regain lost motor and sensory function, (Archibald, Shefner, Krarup, & Madison, 1995; Mackinnon SE & AL Dellon, 1988; Madison, Archibald, & Krarup, 1992). Currently, clinical options to bridge nerve gaps include nerve autografts, acellular nerve allografts (ANAs), and hollow biomaterials conduits (Szynkaruk, Kemp, Wood, Gordon, & Borschel, 2012). The gold standard of these treatments are autografts obtained from the patient, as they support the adequate regeneration without eliciting an immune response. However, a better

clinical alternative is still needed due to distinct disadvantages such as donor site morbidity, increased surgery time, risk, and cost, as well as size and phenotype mismatch (Brenner, Dvali, Hunter, Myckatyn, & Mackinnon, 2007; Moradzadeh et al., 2008). ANAs, while similarly providing physical guidance to regenerating axons through the underlying basal lamina, induce a limited immune response due to the removal of cellular components. Hollow conduits can provide a basic level of regenerative support, but due to insufficient growth supporting factors they often fail in large (>1cm) nerve gaps (Whitlock et al., 2009).

### 1.4.1 Causes of Peripheral Nerve Injury and Obstacles to Repair

PNIs are most often the result of lacerations, gunshot wounds, stretch or traction, compression, drug injection, and surgical injury (Eser, Aktekin, Bodur, & Atan, 2009; Robinson, 2000). Systemic diseases, such as diabetes, chronic inflammation, kidney disorders, vascular damage, repetitive stress, cancer, and toxins also contribute to PNI's, though to a lesser extent (NINDS, 2014). Correct regeneration to the end organ targets (muscle and skin) can be hindered by significant fibrous scarring and large gaps between the proximal and distal nerve stumps. Because of this, complete recovery rarely occurs and leads to chronic pain, loss of function, and muscle atrophy. Swelling and fibrous scar build up are major inhibitors of complete reinnervation and functional recovery (Burnett & Zager, 2004; Stroncek & Reichert, 2007). This scarring around the proximal nerve stump can stop regenerating axons in their tracks and can even cause them to swirl if not surgically removed (Burnett & Zager, 2004). Surgical intervention is almost always required in such injuries. Any scarring must be removed, and the proximal and distal stumps must be reconnected either though direct end to end anastomosis or grafting techniques (Quan & Bird, 1999; Siemionow & Sonmez, 2007). In many surgical cases, however, direct end-to-end anastomosis (reconnection) is not the optimal treatment due to several disadvantages (G Lundborg & Rydevik, 1973; Trumble & Shon, 2000; Wolford &

Stevao, 2003). Strategies to bridge axons from the proximal to distal nerve stumps and, thus, overcome these difficulties have been undertaken.

# 1.5 Methods for PNI Treatment

## 1.5.1 Biological Treatments

Surgeons repairing severely crushed, lacerated or neuromas containing peripheral nerves, in order to find tissue suitable for surgical reconnection, may be forced to remove a significant portion of the damaged area (Trumble & Shon, 2000). This removal of damaged tissue that could lead to scar formation can leave a considerable gap that could cause unwanted tension if the two stumps were simply brought together. This prevents standard end-to-end coaptation of the nerve stumps from being a viable option for small injuries. Nerve "bridges" must be employed in these cases to join the proximal and distal stumps while avoiding any negative effects of tension. Autologous nerve grafts, or autografts, have proven to be the gold standard for these bridges in clinical situations. For the autograft, a minor nerve of the patient, such as the medial antebrachial cutaneous nerve (MABCN), the lateral antebrachial cutaneous nerve, or more typically, the sensory saphenous or sural nerves in the leg, is harvested and sutured to the proximal and distal stumps (Schonauer, Marlino, Avvedimento, & Molea, 2012). The loss of small, minor nerves like these will not impair motor function. Because they are harvested from the patient, immunosuppressants, used in the case of grafts taken from cadavers, are not necessary. Grafts such as these generally result in the best regeneration possible. Though autografts have shown great aptitude to promote regeneration, there are a number of negative aspects to them as well. As previously stated, the loss of a minor, sensory nerve will not generally impair motor function. However, morbidity at the donor site will cause loss of sensation and, potentially, chronic pain. Surgery time, cost, and risk of infection are all increase with the

addition of a second surgical site (Pfister et al., 2011; Schonauer et al., 2012). Lastly, in large diameter motor nerves, grafts of matching phenotype are more effective in promoting regeneration than small sensory nerves (Brenner et al., 2006; Moradzadeh et al., 2008). This is due to not only the size mismatch, but also sensory vs. motor phenotype mismatch. Research has been looking at alternative solutions for grafting nerve defects in order to overcome these obstacles.

Chiu et al found that the use of autologous vein grafts can lead to positive sensory recovery in 1982. Autologous vein grafts address two of the main drawbacks of autografts in their accessibility and lack of donor-site morbidity. These vein grafts can be harvested and used to act as conduits between the nerve stumps. The study, using a rat sciatic nerve model, reported the use of 1 cm vein grafts resulting in ordered nerve regeneration, healing of plantar ulcers, and nearly normal muscle fibers of the gastrocnemius muscle (Chiu, Janecka, Krizek, Wolff, & Lovelace, 1982). Many following studies sought to translate the technique to human regenerative success. Walton et al., using 1-3 cm vein grafts in patients with acute digital nerve repair, reported return of sensation in 50% of cases (Walton, Brown, Matory, Borah, & Dolph, 1989). However, use of these vein grafts tended to delay nerve repair, resulting in poor regeneration and functional recovery. A subsequent Chiu et al. study, along with these previous results, did show that autologous nerve grafts result in favorable sensory recovery when limited to small defects (3 cm) in nonessential sensory nerves that affect a limited end organ target area (Chiu & Strauch, 1990). Various factors such as vessel wall collapse, physical structure, and neurotrophic support could explain the lack in success past 3 cm gaps (Demir et al., 2014; Schonauer et al., 2012; Strauch et al., 1996). Another issue is their lack of neurotrophic factors which promote regeneration and functional recovery. Multiple attempts have been made to rectify this issue by treating grafts with growth factors, such as NGF, seeding olfactory ensheathing cells, and by placing minced nerve tissue or muscle within the graft (Lokanathan et al., 2014; Pu et al., 1999; Sahin et al., 2014). Thus, autologous vein grafts, while promising, lack many of the

necessary physical characteristics needed to enhance functional regeneration in large diameter, long gap nerve defects.

The acellular nerve allograft (ANA) is one of the most promising clinical alternatives to autografts. Nerve allografting provides a nearly unlimited source of tissue, as they are harvested from cadaveric donor nerves, and circumvents issues of donor site morbidity, associated risks of multiple surgeries, etc. found in autograft. The major dowside of allografts, however, is their need for proper immunosuppression of the host patient to prevent rapid rejection (Siemionow & Sonmez, 2007).

## 1.5.2 Synthetic Nerve Guidance Conduits

Research into commercially viable materials for nerve grafts in hopes of replacing autografts, with their numerous downsides and limited availability, began in the 1980s. Because clinicians seeking to bridge the proximal and distal nerve stumps were principally seeking a conduit to that could be easily handled and sterilized, the first conduits were simple hollow tubes made of nonresorbable silicone (G Lundborg, Gelberman, Longo, Powell, & Varon, 1982). These conduits led to compression of the nerve due to the lack of degradation, which impeded regeneration and required a second surgery to remove (G Lundborg & Dahlin, 1992; G Lundborg et al., 1982; Göran Lundborg, 2000). It was quickly determined that certain requirements would need to be met if nerve guidance conduits (NGC) were to be a viable clinical solution for promoting regeneration. The ideal NGC would need to be biocompatible, biodegradable, flexible, have physical and mechanical properties that support nerve regeneration, nutrient permissible, and growth permissive (Kehoe, Zhang, & Boyd, 2012). This led to the development of conduits made of collagen, poly (lactic-co-glycolic acid) (PLGA), and poly (glycolic acid) (PGA) to meet these basic requirements (Daly et al., 2012; Nectow, Marra, & Kaplan, 2012; S. Wang & Cai, 2010). Collagen conduits are bioresorbable, made of a

native ECM protein that supports axon growth, and biocompatible on the large scale, many of the properties considered ideal for regeneration. Conduits consisting of a hollow tube with a porous wall made from type I collagen are sold from Neurogen® and have been shown to be capable of encouraging regeneration across small nerve defects in animal models (Kemp, Syed, Walsh, Zochodne, & Midha, 2009). Unfortunately, of using natural polymers, such as collagen, to form NGCs incurs two shortcomings, batch-to-batch variability in collagen production and poor mechanical properties to support regenerating axon cables (Ciardelli & Chiono, 2006; Schmidt & Leach, 2003).

Due to these drawbacks, companies began investigating NGCs made from synthetic polymers, which elicit a lower immune and inflammatory response and have highly tunable mechanical and degradation properties. Bioresorbable conduits made from PGA (Neurotube®) and PLGA have shown promise in promoting axonal regeneration (S. Wang & Cai, 2010). These conduits, which are easy off-the-shelf products that can be sterilized and handled without difficulty, have shorter surgery time than autografts and minimize risk of infection, distinct advantages in a clinical setting. These conduits continue to fail clinically in large diameter, large nerve defects, despite all these positive attributes. Part of this discrepancy between small and large diameter nerves is due to the volume within the conduit increasing by the power of 2 as the diameter of the nerve increases (A. M. Moore et al., 2009; Pfister et al., 2011). Accordingly, to properly compare results of regenerating tissue between small and large diameter nerves, the gap length must be decreased by that same factor to keep the volumes equal. This volumetric effect, especially the effect on concentrations of biological factors and mechanical properties, must be taken into account if large defects are to be bridged by conduits, or even biological grafts, such as ANAs or vein grafts. Conduits must be designed in a way that will support axonal regeneration physically, biochemically, and functionally. The following

sections will cover current strategies to engineer scaffolds with these stipulations to promote peripheral nerve regeneration.

### 1.5.3 Engineering Topographical Cues within Conduits

Most commercially available NGCs are hollow tubes or nerve wraps that lack native nerve architecture, and many groups are working to remedy this by developing materials that contained within conduits could provide guidance to extending nerves after injury. Highly aligned, porous biomaterial scaffolds have been developed by several groups using both natural (Cullen et al., 2012; Davidenko et al., 2012; Pawar et al., 2011; Suri et al., 2011) and synthetic materials (Fan et al., 2011; L. He et al., 2009; Yang et al., 2009) seeking to guide regenerating axons by providing longitudinally aligned substrates. Conduit porosity might also play an important role along with intraluminal porosity and topography. Oh et al. observed increased longitudinal regeneration in conduits with nanopores, while conduits with micropores incurred regeneration into the pores suggesting that increased porosity may decrease axonal regeneration toward the distal nerve segment (Oh et al., 2012). Daly et al. showed the use of ultrastructured, grooved collagen fibers within aligned conduits aid regenerating axons *in vivo*. Electrospinning is one of the most popular methods of creating aligned biomaterial substrates. Electrospun scaffolds have been shown to promote cell migration and guide neurite extension from DRGs *in vitro* (Mukhatyar et al., 2011). Electrospun scaffolds are often fabricated from synthetic materials, such as PCL (Greiner & Wendorff, 2007; Kijeńska, Prabhakaran, Swieszkowski, Kurzydlowski, & Ramakrishna, 2012; Lee et al., 2012; Ng et al., 2001; Xie, MacEwan, Li, Sakiyama-Elbert, & Xia, 2009; Xie, Willerth, et al., 2009), poly-acrylonitrile (PAN) (Kim, Haftel, Kumar, & Bellamkonda, 2008), and poly-L-lactic acid (PLLA) (Kijeńska et al., 2012), and natural materials, such as silk, collagen, and blends of silk and PLLA (Moroder et al., 2011; S. Y. Park et al., 2012). Aligned electrospun fibers, compared to randomly aligned electrospun fiber mats,

promoted significantly enhanced axon regeneration in a sciatic nerve injury model, yielding increased nerve fiber number, electrical activity, and motor reinnervation (Kim et al., 2008; Moroder et al., 2011; Neal et al., 2012; Zhu et al., 2011).

Artificial Bands of Büngner, structures created by Schwann cells, were created by Ribeiro-Resende et al. through aligned collagen and poly--caprolactone (PCL) filament constructs. These aligned microfilaments could be seeded with Schwann cells and, thereafter, promote enhanced, oriented outgrowth of dorsal root ganglia (DRG) neurites in vitro (Ribeiro-Resende, Koenig, Nichterwitz, Oberhoffner, & Schlosshauer, 2009). This study also achieved increased Schwann cell orientation, providing better axonal guidance in turn, by using combination of topographical cues, as well as what they termed "polarizing" differentiation factors, nerve growth factor (NGF), neuregulin-1, and transforming growth factor-β (TGF-β). The Schwann cell imprinted molds have been used to mimic the native Bands of Büngner architecture by the Hoffman-Kim group (Bruder, Lee, & Hoffman-Kim, 2007). Created from aligned Schwann cell substrates, these cell topographical molds were capable of promoting highly aligned neurite outgrowth from DRG neurons *in vitro*. This group then adapted this Schwann cell-mimicked topography into conduits capable of influencing DRG neurite extension, as well as cell migration patterns (Richardson, Rementer, Bruder, & Hoffman-Kim, 2011). These studies show the importance in designing scaffolds that provide structure similar to that of native nerve architecture, as well as topological guidance for regenerating axons to the distal target of innervation.

## 1.5.4 Engineering Chemical Cues within Conduits

In addition to topographical cues, incorporating important growth factors and adhesion cues, such as neurotrophic factors (NF) and extracellular matrix (ECM) proteins will also critical to

engineering NGC's, if not more so. The role of laminin in nerve regeneration has been well studied, due to its mediation of cell survival, axon extension and cell adhesion through specific peptide sequences, IKVAV and YIGSR, as well as important integrin signaling (Jurga et al., 2011; Marquardt & Willits, 2011; Neal et al., 2012; Swindle-Reilly et al., 2012; Zustiak, Durbal, & Leach, 2010). Cao et al. developed a number of laminin-based systems. Laminin was covalently attached to linear ordered collagen scaffolds to promote axonal regeneration. Cilliary neurotrophic factor (CNTF) and brain-derived neurotrophic factor (BDNF) were delivered using laminin via laminin-binding domains (LBD) within the proteins. While laminin alone improved myelinated axon number *in vivo*, additional improvement in axon regeneration and conduction velocity of the regenerating sciatic nerve through the controlled delivery of CNTF through the LBD (J. Cao et al., 2011). The LBD was also employed for controlled delivery of BDNF and CNTF, which showed improved compound muscle action potential (CMAP) activity of rat facial nerves (J. Cao et al., 2013). Incorporation of biochemical factors including laminin, CNTF, BDNF, and many others (tested and untested) indicate that these cues can further enhance functional outcomes in addition to structural effects from the collagen scaffold.

ECM proteins found in the native nerve architecture have also been successfully incorporated into biomaterial scaffolds to enhance neurite outgrowth *in vitro* and *in vivo*. Fibronectin, an ECM protein that is important for cell migration and adhesion via integrin binding to the RGD peptide, has been shown to promote neurite extension *in vitro* when combined with various polymer scaffolds such as aligned electrospun PAN-methacrylate, collagen, and PEG (Mukhatyar et al., 2011; Zhou, Blewitt, Hobgood, & Willits, 2012). Synthetic polymers have also been modified by collagen in order to promote enhanced neurite outgrowth and axon regeneration (Lee et al., 2012; R. Scott, Marquardt, & Willits, 2010). Lampe, et al. created elastin-like protein hydrogels, providing RGD binding sites and mimicking native nerve mechanical properties, which increased neurite extension

from DRG's significantly *in vitro* (Lampe et al., 2013). Biomaterial scaffolds with optimal adhesion properties for regenerating axons could be fabricated using these tunable hydrogels.

Scaffolds from both synthetic and natural polymers have been functionalized to deliver NFs and ECM proteins through various chemical crosslinking methods. Affinity peptides have proven useful for the controlled delivery of NF's in a number of studies. Shepard, et al. used to functionalize PEG hydrogels in order to locally deliver viral vector constructs for NGF, as well as NGF, promoting increased neurite outgrowth from DRGs *in vitro* (Shepard et al., 2011). Wood, et al. created NGC's containing fibrin matrices with an affinity peptide system for delivery of NGF and GDNF , which promoted enhanced motor regeneration, target reinnervation and functional recovery (A. M. Moore et al., 2010; Wood, Borschel, & Sakiyama-Elbert, 2009; Wood et al., 2010). Heparin, which reversibly binds many NF's, has also been added to many systems for controlled delivery (Joung, Bae, & Park, 2008; Nie et al., 2007; Oh et al., 2011; Roam et al., 2014; Sakiyama-Elbert & Hubbell, 2000; Tae et al., 2006). NFs and ECM proteins can be delivered in a controlled manner from non-reversible chemical conjugation methods, as well as these affinity-based systems, and may provide an ideal solution for *in vivo* regeneration (Cho, Choi, Jeong, & Yoo, 2010; Hsieh et al., 2011; Roam et al., 2010; R. a. Scott et al., 2011; Vulic & Shoichet, 2012; Xu, Yan, & Li, 2011).

## 1.6 Glial-Cell Line Derived Neurotrophic Factor

Originally isolated from the supernatant of a rat glioma cell-line, GDNF is a part of the cysteine-knot family of the transforming growth factor- (TGF-) superfamily that has been found to be effective in increasing dopaminergic neuron survival (Airaksinen & Saarma, 2002; Saarma, 2000). GDNF has since been utilized in treatment strategies for diseases affecting dopaminergic and motor neuron populations after it was demonstrated that GDNF to also promotes motor neuron survival

(Airaksinen & Saarma, 2002; Arce et al., 1998; Chu et al., 2012; Herrán et al., 2013). GDNF binds to a GDNF-family receptor (GFR), as do most factors in the GDNF-family of ligands, particularly a co-receptor for Ret, receptor tyrosine kinase called GFR1 (Hase et al., 2005). GFR1 is anchored to the plasma membrane using lipid rafts, which has been shown to be an important component in GDNF signaling (Hase et al., 2005; Iwase, Jung, Bae, Zhang, & Soliven, 2005). Ret is actively recruited to this lipid raft following the binding of GDNF to the glycosylphosphatidylinositol (GPI)-anchored GFR1, which allows for autophosphorylation (Airaksinen & Saarma, 2002). Ret, a proto-oncongene found in neurons, activates its intracellular tyrosine kinase domain upon binding, contributing to downstream signaling via the activation of Src-family kinases. Dopaminergic, motor, parasympathetic, sympathetic, and sensory neuron survival are all aided by this signaling pathway (Bennett et al., 1998). Upregulation of GDNF and its receptors may be induced initially by PNI (Hoke, Bell, & Zochodne, 1998; A. Höke, Cheng, & Zochodne, 2000). However, decreased levels of GDNF signaling, which may cause failures in functional regeneration and result in neuropathic pain, has been displayed subsequently in cases of chronic denervation of nerves ( a Höke, Gordon, Zochodne, & Sulaiman, 2002; Nagano et al., 2003). Thus, GDNF has been studied extensively for its ability to enhance both motor and sensory neuron regeneration in PNI (A. Höke, 2006). Chen, et al. found that GDNF, delivered via a simple local intramuscular injection, significantly improved motor neuron survival, as well as elongation of both sensory and motor nerves (Chen, Chu, Chen, & Li, 2010). Painful neuropathies have been treated with intrathecal delivery and even topical applications of GDNF with some success (Boucher et al., 2000; Hedstrom, Murtie, Albers, Calcutt, & Corfas, 2014; A. Höke, 2014). A number of methods used to locally deliver GDNF to sciatic nerves have resulted in significant improvement in axonal regeneration (Fine, Decosterd, Papaloïzos, Zurn, & Aebischer, 2002; Wood, Moore, et al., 2009). Most significantly, however, GDNF delivery, in addition to just increasing nerve fiber number, has shown the ability to promote proper motor

reinnervation leading to enhancement in functional motor recovery (Lin et al., 2011; A. M. Moore et al., 2010; Wood, Moore, et al., 2009).

### 1.6.1 Strategies for Controlled Delivery of GDNF

Because GDNF has been shown so clearly to positively affect nerve regeneration, the issue becomes how to effectively and precisely deliver it in a controlled manner. Drug clearance occurs rapidly in the body, so the ability to control or sustain the delivery of a compound, in this case GDNF, should dramatically improve its effectiveness (Panyam & Labhasetwar, 2003). The simplest mode of delivery is systemic injection. However, the targeted areas rarely get a sufficiently high and sustained enough dosage to have the desired effect. A wide range of systems, including cell and gene-based delivery, affinity-based systems, and diffusion and degradation-based methods, have been conceived and tested, with varying degrees of success, to treat PNI with local delivery of GDNF (Magill et al., 2010; Ramburrun et al., 2014).

GDNF, as well as a variety of other growth factors, has been targeted for gene delivery and transfer, and PNI therapies using this have shown promise (De Winter et al., 2013; Mason, Tannemaat, Malessy, & Verhaagen, 2011). In chronically damaged sciatic nerves, intramuscular injections of GDNF adenovirus lead to improved myelination and behavioral outcomes (J.-Y. Shi et al., 2011). This method was also employed in treating diabetic neuropathy resulting in improving neurological functions due to increased sensory neuropeptide and the GDNF signaling cascade levels for 21-35 days (G.-S. Liu et al., 2009; J.-Y. Shi et al., 2011). Injection of GDNF lentiviral vectors directly into injured peripheral nerves increased local GDNF production and improved sensory axon recovery and pain levels, but also led to at the site of GDNF production, termed the "candy-store effect" (Eggers et al., 2008; Tannemaat et al., 2008). Cell-based delivery of GDNF using retroviral

(Q. Li, Ping, Jiang, & Liu, 2006), lentiviral (Eggers et al., 2013; Hoyng et al., 2014; Santosa et al., 2013; Shakhbazau et al., 2013; Y. Shi, Zhou, Tian, & Wang, 2009), and non-viral transfection (Kraus et al., 2010) techniques have been used in multiple *in vitro* and *in vivo* studies, yielding some positive results, though many incurred problems with cell death and, once again, motor neuron entrapment at the delivery site.

Multiple strategies using diffusion-based local delivery of growth factors, including GDNF, has been developed by many groups. The simple systems soak biomaterial sponges, bulk gels, and electrospun scaffolds in GDNF, relying on passive diffusion of the growth factor through the material to reach regenerating axons (Catrina, Gander, & Madduri, 2013; Chew, Mi, Hoke, & Leong, 2007; Fine et al., 2002; Madduri, di Summa, Papaloïzos, Kalbermatten, & Gander, 2010; Madduri, Feldman, Tervoort, Papaloïzos, & Gander, 2010). Release from these systems is generally not sustained for long periods of time, and the burst release profile usually generated by this passive diffusion is normally cleared away quickly. Degradable, hollow microspheres containing GDNF have been explored a few groups (Aubert-Pouëssel et al., 2004; Clavreul et al., 2006; Wood et al., 2012; Xiao & Zhang, 2010). Degradable microspheres allow for a 2-phase release system in which GDNF can diffuse slowly out of the microspheres, followed by a larger release as the microspheres degrade. PLGA microspheres loaded with GDNF and contained within a NGC, as discussed previously, has led to significant improvements in axonal regeneration and functional motor output, even after delayed repair (Borschel et al., 2012; Wood et al., 2012, 2013). The release of GDNF from PLGA microspheres has been further slowed by the addition of another diffusive barrier in the form of a PCL conduit (Kokai, Bourbeau, Weber, McAtee, & Marra, 2011; Kokai, Ghaznavi, & Marra, 2010). Materials such as silk, chitosan, and PCL have also been used to effectively deliver GDNF in a sustained manner (X. Wang et al., 2007; Wen et al., 2011; Wu et al., 2011).

The use of affinity-based delivery systems (ABDS), which rely on electrostatic interactions between growth factors and other molecules, such as glycosaminoglycans (GAGs), to slow their release by sequestration, provides a good alternative to the uncontrolled passive diffusion or release from materials. As previously mentioned, the heparin-based delivery system (HBDS) is an affinity-based system that has been well characterized and used in a multitude of tissue regeneration studies (Sakiyama-Elbert & Hubbell, 2000; Wood et al., 2010). Heparin, which is the most negatively charged, highly sulfated GAG and one of the negatively charge biological molecules, has been used intensively for anti-coagulation applications for decades (Howell & Holt, 1918; Salek-Ardakani, Arrand, Shaw, & Mackett, 2000). Many growth factors, which have an affinity for heparin, can be immobilized by its inclusion within a scaffold. Sakiyama-Elbert, et al. non-covalently attached heparin to fibrin through a bi-domain peptide sequence in order to sequester growth factors within fibrin scaffolds (Sakiyama, Schense, & Hubbell, 1999; Sakiyama-Elbert & Hubbell, 2000). Wood et al. showed, *in vitro*, this method created controlled release of GDNF for up to two weeks and increased neurite extension (Wood, Borschel, et al., 2009) and later showed, *in vivo*, resulted in increased axon regeneration, fiber width, motor neuron survival and muscle reinnnervation, and, most importantly, functional motor recovery for a 13-mm gap repaired with a silicone conduit (A. M. Moore et al., 2010; Wood et al., 2010; Wood, Moore, et al., 2009).

# Chapter 2*

# The formation of protein concentration gradients mediated by density differences of poly(ethylene glycol) microspheres

## 2.1 Abstract

A critical element in the formation of scaffolds for tissue engineering is the introduction of concentration gradients of bioactive molecules. We explored the use of poly(ethylene glycol) (PEG) microspheres fabricated via a thermally induced phase separation to facilitate the creation of gradients in scaffolds. PEG microspheres were produced with different densities (buoyancies) and centrifuged to develop microsphere gradients. We previously found that the time to gelation following phase separation controlled the size of microspheres in the de-swollen state, while crosslink density affected swelling following buffer exchange into PBS. The principle factors used here to control microsphere densities were the temperature at which the PEG solutions were reacted following phase separation in aqueous sodium sulfate solutions and the length of the incubation period above the 'cloud point'. Using different temperatures and incubation times, microspheres were formed that self-assembled into gradients upon centrifugation. The gradients were produced with sharp interfaces or gradual transitions, with up to 5 tiers of different microsphere types. For proof-of-concept, concentration gradients of covalently immobilized proteins were also assembled. PEG microspheres containing

* Chapter 2 has been adapted from the following manuscript:
J. Roam, H. Xu, P. Nguyen, D. Elbert. The formation of protein concentration gradients mediated by density differences of poly(ethylene glycol) microspheres. Biomaterials, 31 (2010), pp. 8642–8650

heparin were also fabricated. PEG-heparin microspheres were incubated with fluorescently labeled protamine and used to form gradient scaffolds. The ability to form gradients in microspheres may prove to be useful to achieve better control over the kinetics of protein release from scaffolds or to generate gradients of immobilized growth factors.

## 2.2 Introduction

Concentration gradients of signaling molecules are important in embryogenesis, wound healing, immunity, angiogenesis, and nerve cell signaling (X. Cao & Shoichet, 2001; DeLong et al., 2005; Fisher et al., 1989; Kapur & Shoichet, 2004; Knapp et al., 1999; K. Moore et al., 2006; Parent & Devreotes, 1999; Rosoff et al., 2004; Singh et al., 2008; H. Song & Poo , 2001; H. J. Song et al., 1997; X. Wang et al., 2009). Therefore, introducing gradients of bioactive signals into scaffolds according to some spatial blueprint may be crucial to the engineering of tissues or organs. In particular, chemotaxis, the preferential movement of cells up a concentration gradient of signaling molecules, is known to be dependent upon the steepness of a concentration gradient as opposed to the average concentration of the molecule (Knapp et al., 1999; K. Moore et al., 2006; Parent & Devreotes, 1999). This may have particular importance in the development of scaffolds for nerve regeneration. Shoichet et al., have demonstrated that concentration gradients of nerve growth factor immobilized on a scaffold can be used to enhance the directionality of extending dendrites (Kapur & Shoichet, 2004; K. Moore et al., 2006). Bellamkonda et al., showed that gradients of laminin-1 could also turn growing dorsal root ganglia towards the increasing concentration and gradients of laminin-1 and nerve growth factor could promote regeneration of the sciatic nerve in rats (Dodla & Bellamkonda, 2008, 2006).

Scaffolds formed from hydrogels made of synthetic polymers show significant promise in regenerative medicine (Drury & Mooney, 2003; E. a. Scott et al., 2010; Tessmar & Göpferich, 2007). Biological functions, such as cell adhesion or cell-initiated degradability, may be incorporated within these hydrogels using functional peptides or proteins (Almany & Seliktar, 2005; DeLong et al., 2005; M P Lutolf & Hubbell, 2005; E. a. Scott et al., 2010; Zhang, Wang, Wang, Zhang, & Suggs, 2006). However, bulk hydrogel scaffolds are typically homogenous structures without macroporosity or spatial organization, much different than native tissue. Modular strategies to produce heterogeneous scaffolds from hydrogel microparticles show promise in addressing these limitations (Khademhosseini & Langer, 2007; Rivest et al., 2007).

A number of systems have been used to produce gradients in scaffolds, including pulsatile application of picoliters of growth factor solutions, diffusion of molecules into a gel, and gradient makers in which polymerizing solutions exit two different chambers in varying ratios (X. Cao & Shoichet, 2001; Kapur & Shoichet, 2004; Knapp et al., 1999; H. J. Song et al., 1997). However, these methods have distinct disadvantages, such as scaling issues and difficulty in pumping polymerizing solutions. Assembling different types of microparticles in a modular manner may provide the versatility necessary to engineer the properties of bioactive scaffolds, including formation of gradients (Du, Lo, Ali, & Khademhosseini, 2008; Rivest et al., 2007; E. a. Scott et al., 2010; Serban & Prestwich, 2008; Yeh et al., 2006). Mechanical microparticle production techniques (e.g. micromolding, microfluidics, 3D printing, etc.), which are most common, may have scalability issues, as even small scaffolds can require billions of microparticles to form (Boland, Xu, Damon, & Cui, 2006; Liu Tsang & Bhatia, 2004; E. a. Scott et al., 2010; Um, Lee, Pyo, & Park, 2008; Yeh et al., 2006). Previously, we have fabricated PEG hydrogel microspheres in solution via a thermally induced phase separation (E. a. Scott et al., 2010). The microspheres were produced by reacting multiarm-

PEG derivatives in the presence of kosmotropic salts that induced a phase separation upon incubation at 37 °C or above. The method can be performed rapidly and at large scales. Different functionalities, such as cell adhesion, degradability, and drug delivery, have already been imparted to these microspheres as well (E. a. Scott et al., 2010).

The current study explored how to engineer gradients into scaffolds made from these PEG microspheres. We have found that varying the temperature of the phase separation and the amount of time the PEG is allowed to react above the cloud point allows us to control both the size and the density (buoyancy) of the microspheres. The size of microspheres in their de-swollen state is controlled primarily by the time to reach the gel point, while the swelling following buffer exchange into PBS is determined by crosslink density(Nichols et al., 2009). The swelling of the microsphere should greatly affect the density of the microspheres by changing the ratio of solvent to polymer. By incubating batches of microspheres for different amounts of time, a range of densities can be produced. The formation of scaffolds from the microspheres is enhanced by centrifugation, exploiting small density differences to introduce gradients while simultaneously crosslinking the microspheres together to form a scaffold. Proteins can be covalently bound to the microspheres or electrostatically attached using heparin in varying concentrations to form concentration gradients of those proteins. The methods described herein may allow for the development of gradient-containing scaffolds for a variety of tissue engineering and drug delivery applications.

## 2.3 Materials and Methods

Unless otherwise noted, all reagents were purchased from Sigma–Aldrich.

### 2.3.1 PEG synthesis and labeling

Eight-arm PEG-OH (PEG8-OH; mol. Wt. 10,000; Shearwater Polymers, Huntsville, AL) was used to synthesize PEG8-vinylsulfone (PEG8-VS) and PEG8-amine as previously described (Wacker et al., 2006). PEG macromonomers were dissolved separately at 200 mg/mL in Dulbecco's phosphate buffered saline (PBS; 8 mm sodium phosphate, 2 mm potassium phosphate, 140 mm sodium chloride, 10 mm potassium chloride, pH 7.4) and sterile filtered with 0.22 μm syringe filters (Millipore). Dylight-488 NHS-ester (Pierce), Dylight-633 NHS-Ester (Pierce), and Dylight-549 Maleimide (Pierce) were dissolved in dimethyl formamide at 10 mg/mL and added to the PEG8-amine solutions at 1600:1, 20:1, or 200:1 mol:mol ratios, respectively, and incubated at 25 °C overnight protected from light.

### 2.3.2 Microsphere formation

Labeled or unlabeled PEG8-amine solutions were combined with PEG8-VS solutions at a 1:2 ratio. If the solutions were to be used for microsphere formation at 37 °C, the solutions were pre-reacted at 37°C for 5–6 h until a mean dPCS = 100 nm was observed by dynamic light scattering (E. a. Scott et al., 2010). The PEG solutions (pre-reacted or otherwise) were diluted to 20 mg/mL PEG with PBS and 1.5 m sodium sulfate (in PBS) to a final sodium sulfate concentration of 0.6 m. The PEG8-VS/PEG8-amine solutions were then incubated above the cloud point at 37°C, 70°C, or 95°C for various times (Fig 2.1). Suspensions of microspheres were subsequently buffer exchanged into

PBS 2× to remove the sodium sulfate by: (1) diluting the microsphere solution 3:1 with PBS and titurating, (2) centrifuging at 14,100 g for 2 min, (3) removing the supernatant.

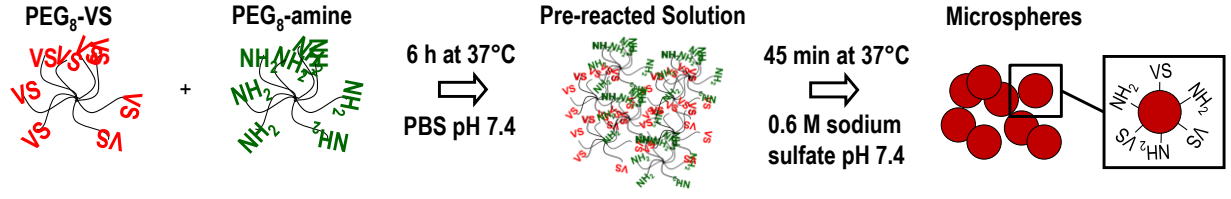


**Figure 2.1. Microsphere Formation**

## 2.3.3 Gradient formation

The glass walls of Pasteur pipettes were passivated with PLL(375)-g[7]-PEG(5) (D. L. Elbert & Hubbell, 1998; Kenausis et al., 2000). The pipettes were filled with a 20 mg/mL PLL-g-PEG solution, incubated for 30 s, and washed with DI water. After sufficient drying time, the tips of the pipettes were sealed with silicone aquarium sealant (DAP Inc., Baltimore, MD). To form scaffolds, the microspheres were resuspended in 10% Fetal Bovine Serum in DMEM (Invitrogen) after the final PBS wash and combined with other labeled microsphere solutions in the Pasteur pipette. The pipette was placed in a 15 mL conical vial and centrifuged at 1000 g for 10 min and then incubated overnight at 37 °C before viewing (Fig 2.2).

## 2.3.4 Confocal microscopy

Fluorescence microscopy was performed with a Nikon Eclipse C1/80i confocal microscope. Microsphere gradients were imaged while still in the Pasteur pipettes with a 10× objective (0.30 DIC L WD 7.4). Multiple images were taken along the length of the pipette and processed using EZ-C1 3.70 FreeViewer software (Nikon Instruments Inc.) and then combined.

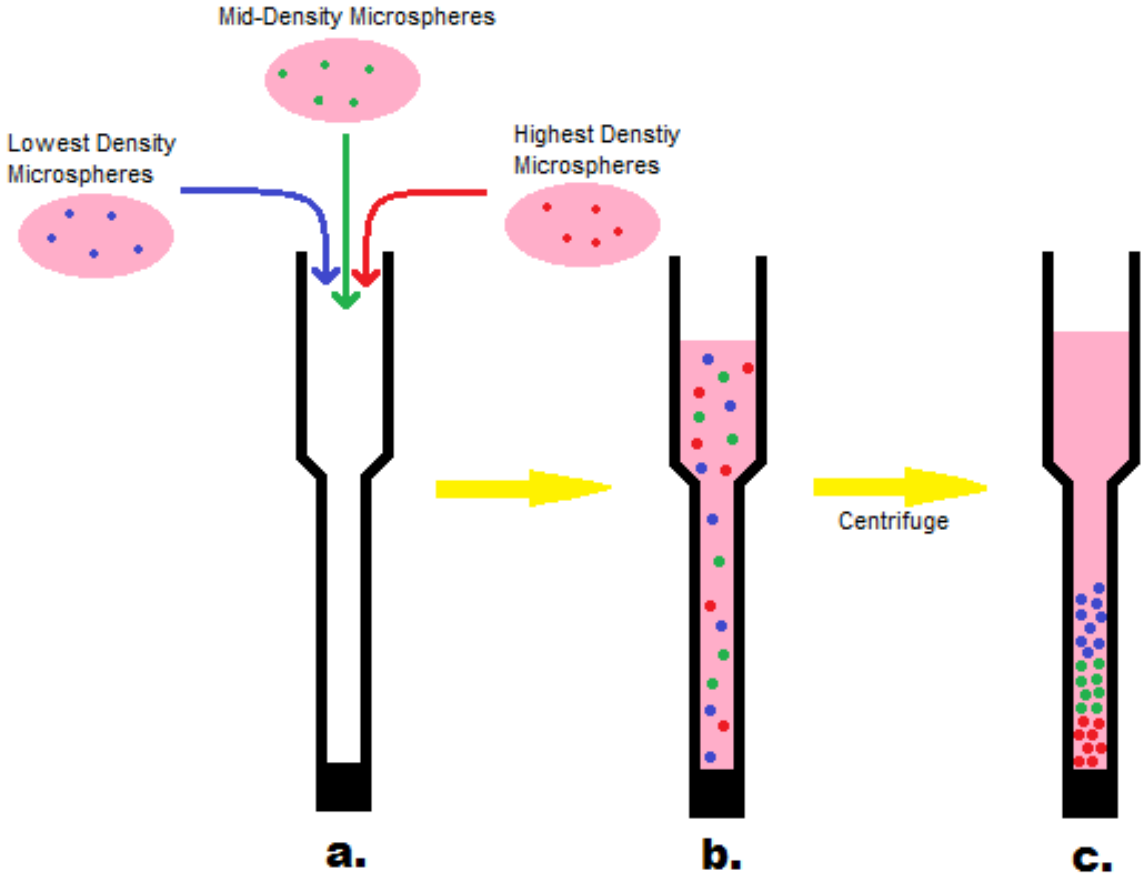


**Figure 2.2. Gradient formation.** (a) Microspheres with the same chemical structure but with different densities were produced from PEG precursors labeled with different fluorescent dyes. The microspheres were suspended in 10% serum and added to a PLL-*g*-PEG treated Pasteur pipette. (b) The microspheres were initially well mixed. (c) Upon centrifugation, the microspheres separated themselves based on their relative densities.

## 2.3.5 GDNF labeling

Recombinant human glial cell line-derived neurotrophic factor (100 µg/mL, GDNF, R&D Systems, Minneapolis, MN) was reconstituted in PBS. Dylight-488 was added to the solution for a final concentration of 50 µg/mL and incubated overnight at room temperature. Cysteine (200 µg/mL) was added and incubated overnight as well. Bovine serum albumin (0.1%; BSA) was then added to the solution to reduce adsorption to the vials. SDS-PAGE showed that while BSA did receive a small amount of labeling, the much smaller quantity of GDNF was labeled to a much greater extent (Note:

For the covalent attachment of GDNF at 37 °C, cysteine was not added, and the BSA was revealed by SDS-PAGE to have become significantly labeled.).

## 2.3.6 Protein attachment to microspheres

The labeled GDNF/BSA solution was diluted by half in PBS and added in place of the PBS along with the sodium sulfate solution and unlabeled PEG solutions (pre-reacted or otherwise). The combined solution was then incubated and washed as before to form microspheres.

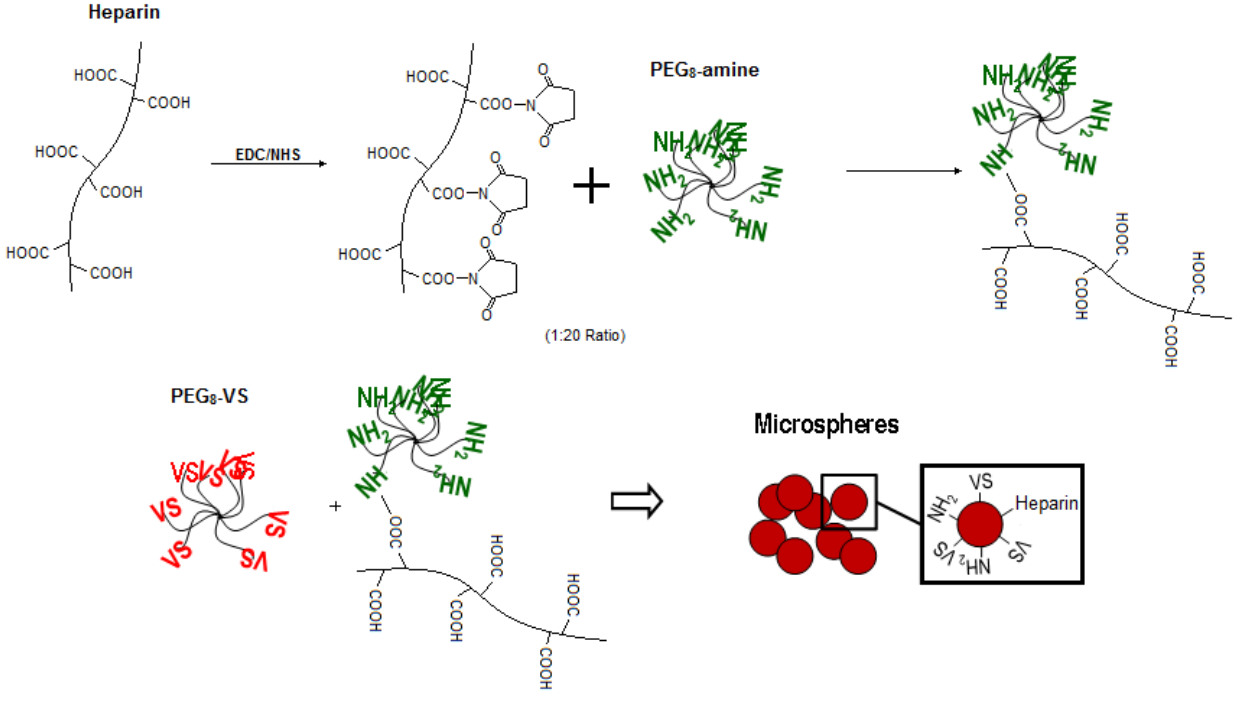


**Figure 2.3. Heparin Attachment**

## 2.3.7 Heparin attachment

A solution of 500 mm N-(3-Dimethylaminopropyl)-N′-ethylcarbodiimide hydrochloride (EDC), 200 mm N-Hydroxy-succinimide (NHS), and 50 mg/mL heparin sodium salt (mol. wt. ~18,000) in MES buffer (10 mm, pH 6.0) was incubated at room temperature for 30 min. The

activated heparin solution was then added to a 200 mg/mL solution of PEG8-amine at a 20:1 PEG8-amine to heparin mol:mol ratio and incubated at room temperature for another 30 min before refrigeration. Microspheres were formed as before using the heparin-conjugated PEG8-amine along with PEG8-VS in a 1:2 ratio (Fig. 2.3).

## 2.3.8 Protamine labeling

Protamine sulfate salt from salmon (10 mg/mL, Grade X) was dissolved in 50 mm sodium borate buffer (pH 8.5). Dylight-488 was added to the solution for a final concentration of 50 μg/mL and incubated overnight at room temperature. As before, a PD-10 Sephadex G-25M column (Supelco, Bellefonte, PA) was used to remove any unbound Dylight-488. The column was washed with ~20 mL PBS before adding the labeled protamine solution. After the sample entered the column, 2.4 mL of PBS was added and allowed to flow through. The labeled protamine was eluted with 20 mL PBS, and the flow through was collected in 0.5–0.75 mL fractions. The fluorescence of each fraction was measured with a fluorometer and the protein-containing fraction with peak fluorescence was retained. The final concentration of labeled protamine in the peak fraction was ~1 mg/mL.

## 2.3.9 Protamine attachment to heparin microspheres

After the PBS washes, the microspheres were spun down, and the supernatant was removed. The labeled protamine solution was diluted to 25 μg/mL in PBS and added to the dehydrated microspheres. The microspheres were incubated with the protamine solution at room temperature overnight.

## 2.4 Results

### 2.4.1 Formation of Microsphere Gradients

Density measurements of microspheres with Histopaque-1077 and Histopaque-1119 demonstrated that microspheres under all formation conditions migrated to the interface of the two solutions. This showed that all the microspheres had specific gravities between 1.077 and 1.119. Thus density differences across the spectrum of formation conditions were quite subtle. To determine if the density differences between microspheres were sufficient to generate microsphere gradients, PEG8-amine was fluorescently labeled using one of three different dyes and used to form microspheres with different densities. In all of the experiments presented here, microspheres in any one scaffold were formed at the same temperature (37, 70 or 95 °C) but incubated above the cloud point for different lengths of time. Microspheres with different densities were centrifuged together in the presence of 10% serum to form scaffolds (we previously demonstrated that microspheres crosslink together in the presence of serum proteins to form solid materials) (E. a. Scott et al., 2010). The distribution of the fluorescent dyes in the scaffold was visualized using a scanning confocal fluorescence microscope.

The scaffolds were formed in the bottoms of Pasteur pipettes. Each scaffold was about 2 cm long. The glass walls provided a good optical platform for the scanning confocal microscopy. However, early experiments showed substantial streaking of microspheres along the walls of the pipette. Evidently, some microspheres were adhering to the glass walls and not migrating properly. The presence of amines in the microspheres makes them net cationic, (Nichols et al., 2009) probably promoting adhesion to the anionic silanol groups on the glass. The glass was thus coated with PLL-g-PEG to prevent the microspheres from adhering to the glass walls. This eliminated the streaking of microspheres and allowed the formation of distinct gradients.

We found that incubation of the PEG at 70 °C provided the greatest range and control of densities of the microspheres while keeping the polydispersity to a minimum. To demonstrate the full range of densities, a 2-tier scaffold was made using the highest and the lowest density microspheres (Fig. 2.4). The incubation times above the cloud point used to produce these two types of microspheres were 11 and 45 min. Times less than 11 min did not produce microspheres. Times greater than 45 min led to the aggregation of the microspheres into a gel-like structure.

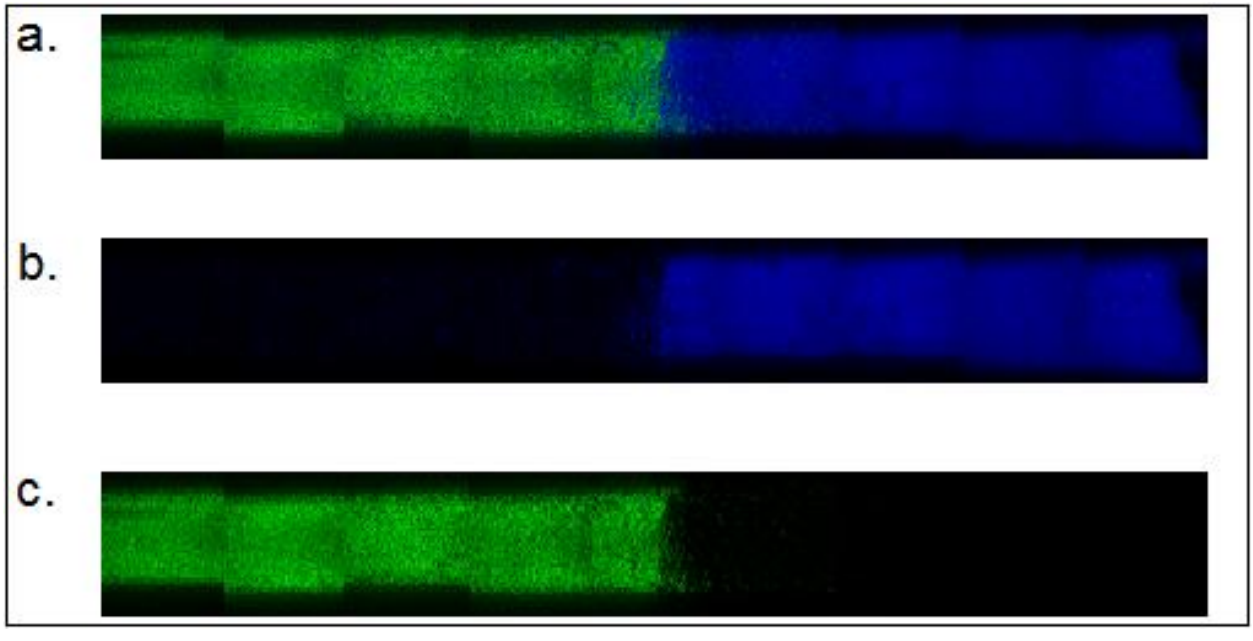


**Figure 2.4. Two-tier gradient with sharp interface.** Microspheres were formed above the cloud point at 70˚C. Dylight-488 (green) labeled microspheres were incubated above the cloud point for 45 minutes. Dylight-633 (blue) labeled microspheres incubated above the cloud point for 11 minutes. (a) combined channels, (b) blue only, (c) green only.

Next, we determined how many tiers with sharp interfaces could be produced in these scaffolds. The maximum number of clearly defined tiers of microspheres that we were able to form was three (Fig. 2.5). We previously showed a nonlinear relationship between density, and incubation time, with large changes in swelling (and presumably density) soon after microspheres begin to form, but with a long plateau with a slow rate of change in swelling at longer incubation times (Nichols et

al., 2009). Incubation times resulting in well-defined 3-tier gradient were 11, 17, and 45 min. If we tried to achieve more than 3 tiers, the tiers began to blend together. This blending, however, could be useful if gradual transitions between levels were desired, so we formed 5-tier gradients as well (Fig. 2.6). The best incubation times for forming 5-tiered gradient scaffolds were 11, 12, 16, 26, and 45 min. In this 5-tier gradient, the transitions from level to level became nearly seamless.

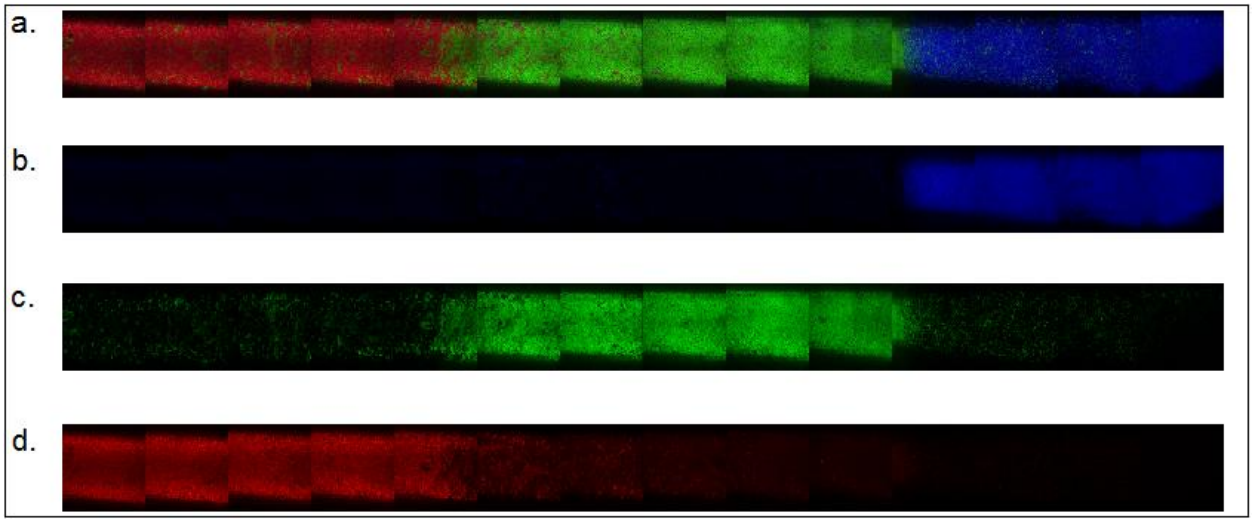


**Figure 2.5. Three-tier gradient with sharp interfaces.** Microspheres were formed above the cloud point at 70˚C. Dylight-488 (green) labeled microspheres were incubated above the cloud point for 45 minutes. Dylight-549 (red) labeled microspheres were incubated above the cloud point for 17 minutes. Dylight-633 (blue) labeled microspheres were incubated above the cloud point for 11 minutes. (a) combined channels, (b) blue only, (c) green only, (d) red only.

Though this 5-tier gradient may provide great control over the form of the gradient, a simple 2-tier gradient with a gradual transition between levels might also be desirable. At the standard 70 °C formation temperature, either two distinct layers or no detectable gradient were formed. Exploring another temperature (95 °C) resulted in more success. The higher temperature resulted in microspheres with densities different enough to separate into tiers but close enough to have a region with substantial overlap. We found the most successful incubation times at 95 °C for a gradual transition 2-tier gradient were 3 and 5 min (Fig.2.7).

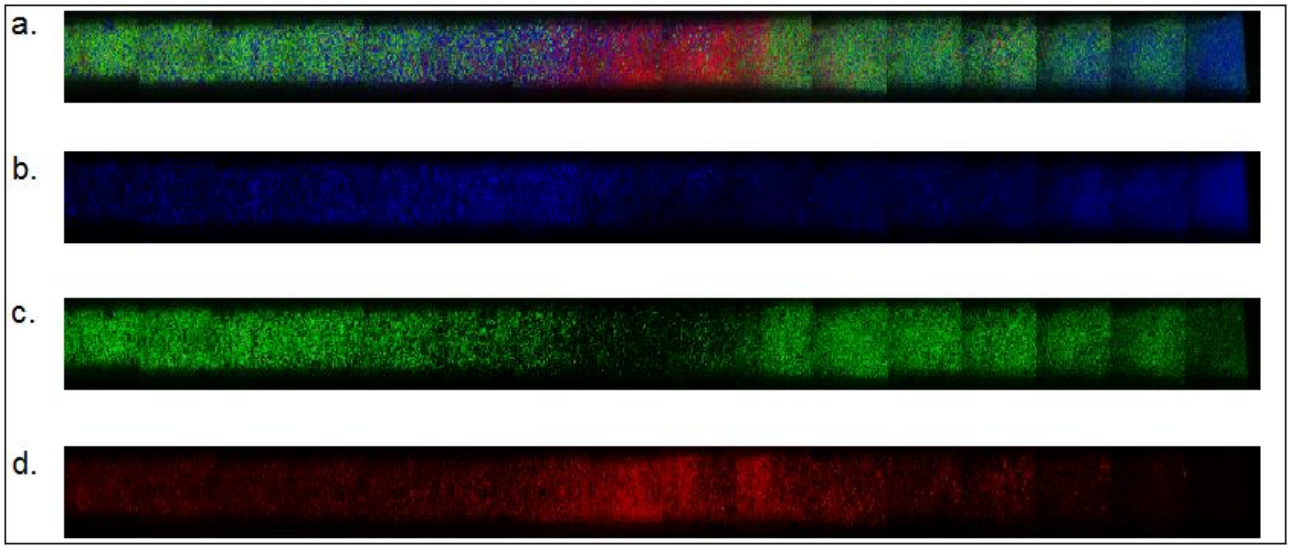


**Figure 2.6. Five-tier gradient.** Microspheres were formed above the cloud point at 70˚C. Dylight-488 (green) labeled microspheres were incubated above the cloud point for 12 or 45 minutes. Dylight-549 (red) labeled microspheres were incubated above the cloud point for 16 minutes. Dylight-633 (blue) labeled microspheres were incubated above the cloud point for 11 or26 minutes. (a) combined channels, (b) blue only, (c) green only, (d) red only.

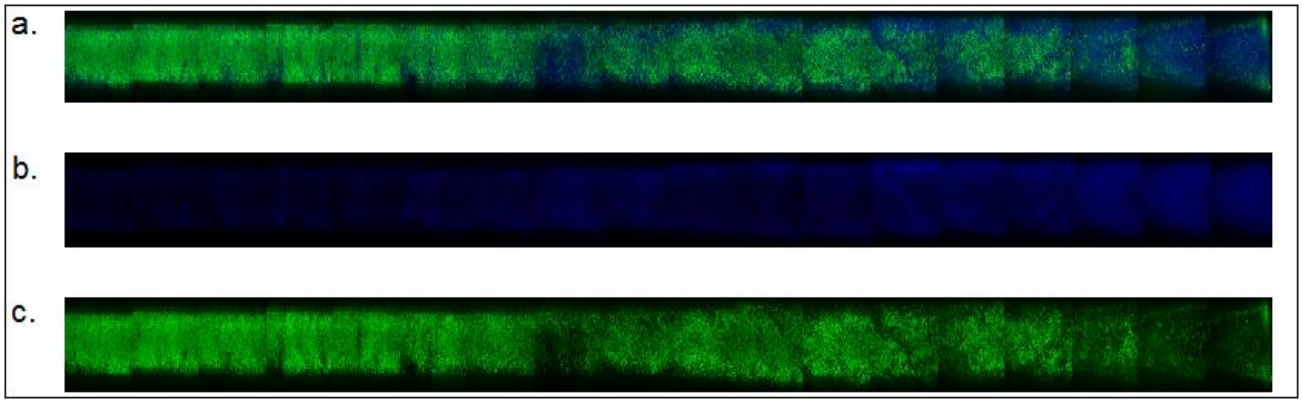


**Figure 2.7. Two-tier gradient with gradual transition.** Microspheres were formed above the cloud point at 95˚C. Dylight-488 (green) labeled microspheres were incubated above the cloud point for 5 minutes. Dylight-633 (blue) labeled microspheres were incubated above the cloud point for 3 minutes. (a) combined channels, (b) blue only, (c) green only.

## 2.4.2 Formation of Protein Gradients

We are particularly interested in producing conduits for nerve regeneration, and GDNF has been shown to enhance motor nerve regeneration (Barras, Pasche, Bouche, Aebischer, & Zurn, 2002; Fine et al., 2002). To directly visualize the GDNF in the scaffolds, we fluorescently labeled the protein with Dylight-488. A simple 2-tier gradient of Dylight-488 labeled GDNF was made using the 2-tier gradient scheme that produced sharp interfaces. The denser microspheres were formed in the presence of the fluorescently labeled proteins to promote covalent attachment. The less dense microspheres were labeled with Dylight-633 so that these microspheres could be visualized in the scaffold. Covalent coupling of proteins to one of the microsphere types did not affect gradient formation (Fig. 2.8).

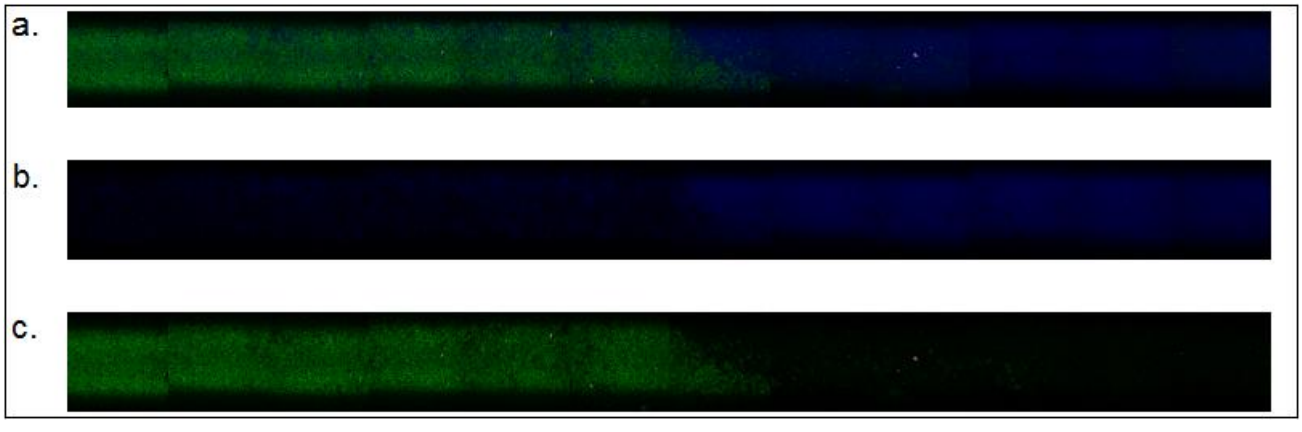


**Figure 2.8. Two-tier gradient with covalently coupled BSA/GDNF.** Microspheres were formed above the cloud point at 70˚C. Dylight-488 (green) labeled BSA/GDNF was covalently coupled to PEG precursors during microsphere formation. The PEG/protein microspheres were incubated above the cloud point for 45 minutes. Dylight-633 (blue) labeled microspheres were incubated above the cloud point for 3 minutes (no protein is coupled; dye is covalently coupled to PEG precursor). (a) combined channels, (b) blue only, (c) green only.

Due to the high temperature of microsphere formation (70 °C), the proteins were likely denatured. At physiological temperature, 37 °C, the only gradients that were produced were 2-tier gradients with gradual transitions between levels (Fig. 2.9). The incubation times above the cloud

point for forming the 2-tier gradient at physiological temperature were 20 and 65 min. As before, the denser microspheres were formed in the presence of the labeled protein to ensure covalent attachment, while the lighter microspheres were labeled with Dylight-633.

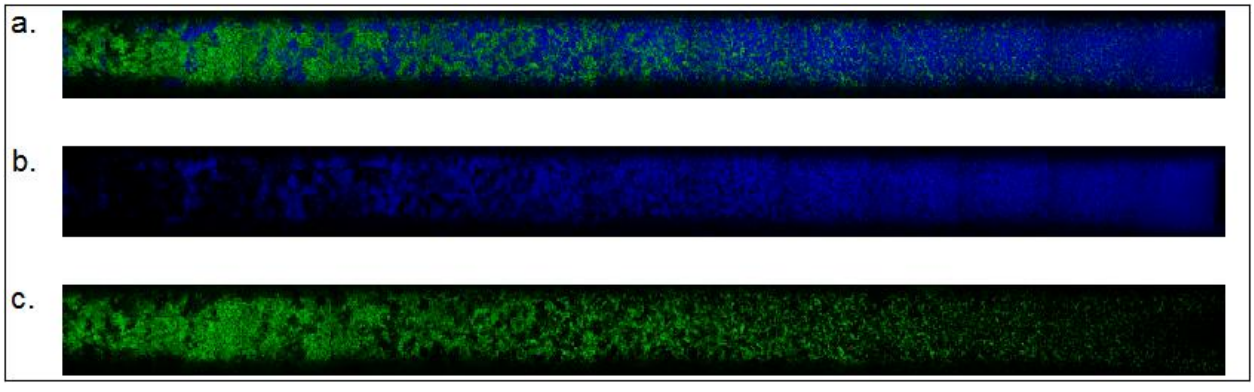


**Figure 2.9. Two-tier gradient with covalently coupled BSA/GDNF formed at 37°C.** Microspheres were formed above the cloud point at 37˚C. Dylight-488 (green) labeled BSA/GDNF was covalently coupled to PEG precursors during microsphere formation. The PEG/protein microspheres were incubated above the cloud point for 65 minutes. Dylight-633 (blue) labeled microspheres were incubated above the cloud point for 20 minutes (no protein coupled, dye bound to PEG precursor). (a) combined channels, (b) blue only, (c) green only.

## 2.4.3 Reversibly Bound Gradients

An alternative to covalent bonding is to use heparin to promote electrostatic binding of heparin-binding proteins (Nie et al., 2007; Sakiyama-Elbert & Hubbell, 2000; Tae et al., 2006). Heparin-binding proteins potentially could be bound after microsphere formation, allowing microsphere formation at high temperatures, but eliminating the risk of protein denaturation. Non-covalent coupling would also prevent the reduction in activity that covalent binding might cause. To attach heparin to the microspheres, we activated carboxyl groups on heparin with EDC and NHS and reacted this with PEG8-amine, similar to the chemistry used by Tae et al. (Tae et al., 2006). The microspheres were formed as before using the PEG8-amine with covalently coupled heparin at 70 °C

or 95 °C, allowing the use of the most versatile gradient formation protocols. A 3-tier gradient of heparin-decorated microspheres with sharp interfaces is shown (Fig. 2.10).

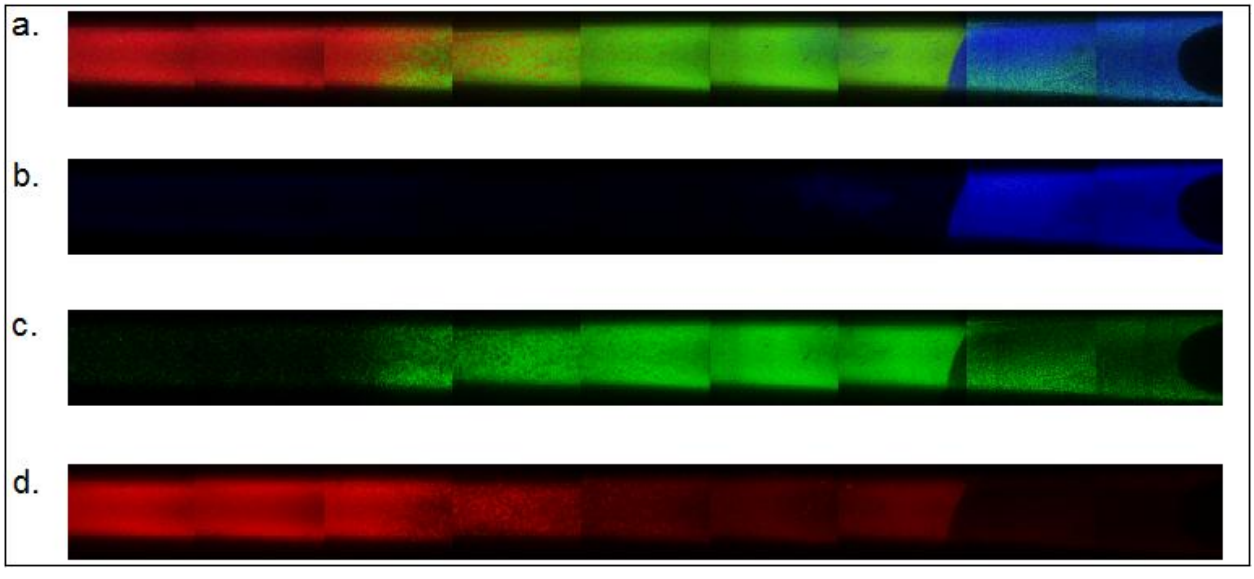


**Figure 2.10. Three-tier gradient with PEG/heparin microspheres.** Microspheres were formed above the cloud point at 70˚C using heparin-coupled $PEG_8$-amine. Dylight-488 (green) labeled microspheres were incubated above the cloud point for 45 minutes. Dylight-549 (red) labeled microspheres were incubated above the cloud point for 17 minutes. Dylight-633 (blue) labeled microspheres were incubated above the cloud point for 11 minutes. (a) combined channels, (b) blue only, (c) green only, (d) red only.

To demonstrate that the microspheres were indeed decorated with heparin, we performed a number of controls using Dylight-488 labeled protamine (a protein with very high affinity for heparin). Protamine bound to the formed PEG/heparin microspheres was shown to be non-covalently bound by eluting the protamine at elevated NaCl concentrations (Fig. 2.11). The denser PEG/heparin microspheres were incubated overnight with Dylight-488 labeled protamine and then spun down with lighter Dylight-633 labeled, PEG/heparin microspheres. A gradient of protamine was formed using the sharp, 2-tier gradient scheme (Fig. 2.12).

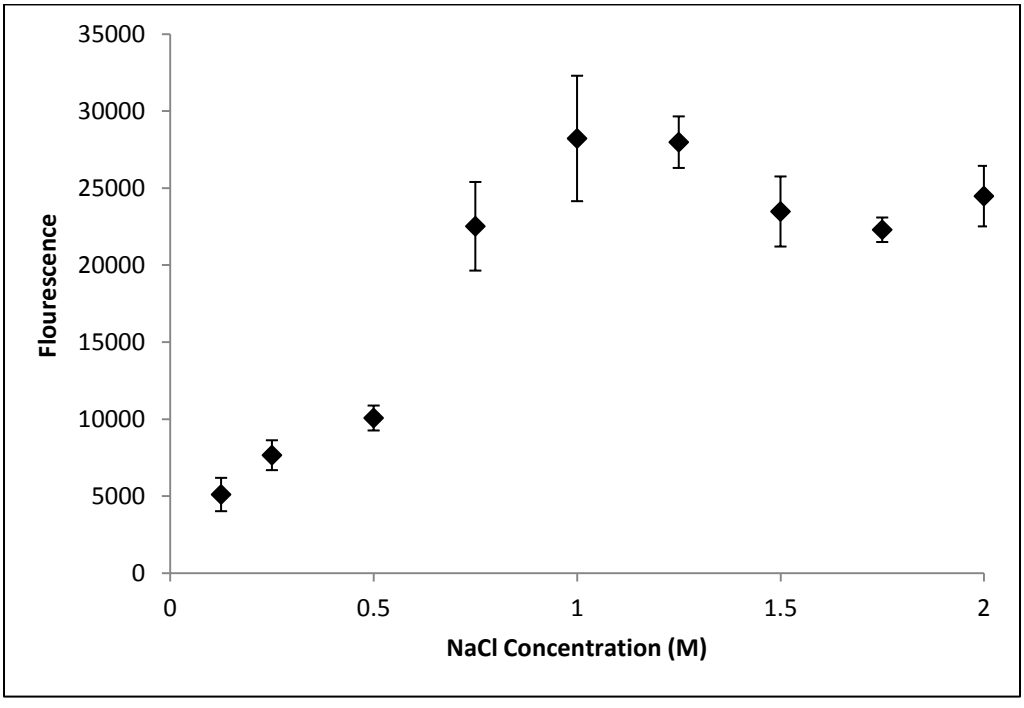


**Figure 2.11. High salt release of protamine.** NaCl was added in various concentrations (0-2 M) to heparin decorated microspheres with Dylight-488 labeled protamine attached. After 40 hours the flourescence of the supernatant was measured to track the release of protamine compared to salt concentration (n=2 for each data point, mean and standard deviation reported for each).

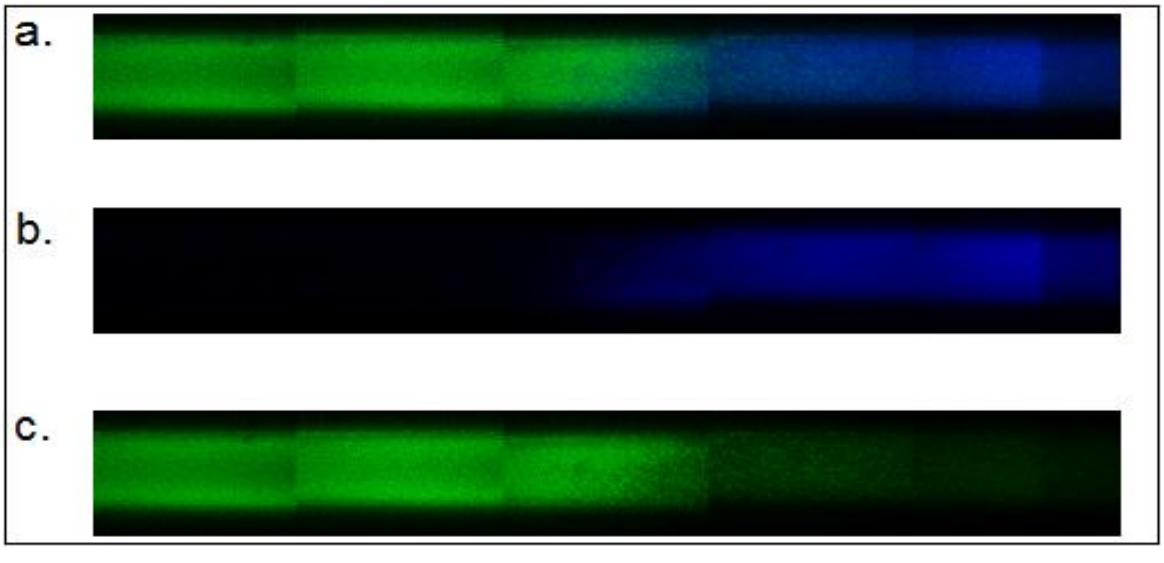


**Figure 2.12. Two-tier gradient with electrostatically bound protamine.** PEG-heparin microspheres were formed above the cloud point at 70˚C. PEG-heparin microspheres were incubated above the cloud point for 45 minutes. Following buffer exchange into PBS, microspheres were incubated with Dylight-488 (green) labeled protamine. Dylight-633 (blue) labeled PEG-heparin microspheres were incubated above the cloud point for 11 minutes. (a) combined channels, (b) blue only, (c) green only.

## 2.5 Discussion

Using differences in microsphere density, multiple-tier scaffolds were constructed with sharp or gradual transitions between levels. The 2-tiered scaffold with a gradual transition suggested the possibility to produce linear gradients in concentration of cell adhesion peptides/proteins, mechanical stiffness, growth factor/drugs, degradability, etc. Up to 5-tier gradients were possible. The degree to which a particular property is added to each tier could be controlled independently, such that exponential, parabolic, impulse, and many other gradient profiles may be imagined. In particular, a gradient might be chosen that balances the diffusion out of one or both ends of the scaffolds, producing zero order release (D. C. Scott & Hollenbeck, 1991).

The microsphere gradients were easily produced; however, several challenges remain to translate these properties into a functioning growth factor delivery system. The best results were obtained with microspheres formed at 70 °C and 95 °C. At 37 °C, the widest possible range of incubation times above the cloud point resulted in density differences that could only produce a 2-tiered gradient with a gradual transition. The mechanism for this was not determined, but we may speculate based on previous results. We previously demonstrated that following phase separation, the PEG-rich phases coarsen, or increase in size over time due to coalescence. At the gel point, coalescence is halted. Longer gelation times result in larger microspheres. The time to reach the gel point may be decreased by pre-reacting the PEG macromers prior to phase separation or by increasing temperature or pH. After gelation, the microspheres remain in the phase-separated state until buffer exchanged into PBS. After buffer exchange, crosslinking may continue, but is likely quite slow due to the lower concentration of PEG in the swollen gel. These are second order reactions, with the reaction rate scaling with the PEG concentration squared (note that the PEG8-vinylsulfone and PEG8-amine are not present at equal concentrations but the same scaling applies). Thus, the number of crosslinks

formed in the phase-separated state will be critical in determining the degree of swelling following buffer exchange. The relationship between crosslink density and swelling is described by the well-known Flory–Rehner equation (Flory, 1953). However, we previously found that the decrease in swelling with increasing crosslinking time was not readily described in the Flory–Rehner framework other than qualitatively (Nichols et al., 2009). Intuitively, one would expect that soon after gelation, the number of crosslinks should increase rapidly. A large number of multiarm-PEGs with two arms attached to the network should be present at the gel point, which soon become crosslink sites after only one more arm attaches to the network (assuming all three arms are elastically active). Later on, however, the formation of crosslink sites will be slowed by steric hindrance. The general shape of the curve provides guidelines for selecting time points to achieve gradual transitions between tiers. Close to the gel point, the incubation times must be closely spaced because the density is changing rapidly. At longer times, the incubation times must be spaced further apart. If the incubation times are too close, no separation into layers will be observed, while if they are too far apart, a sharp interface will develop. We found that the production of a gradual transition between 2 tiers was most successful if the microspheres were formed at 95 °C. Gradual transitions may be observed in the 5-tier scaffold made from microspheres formed at 70 °C. However, 2-tiered gradients formed from these microspheres had a transition zone that did not extend throughout the scaffold (data not shown). Due to the shape of the curve that describes swelling as a function of incubation time, finding times that led to a near linear gradient in a 2-tiered scaffold may simply have required more trial-and-error, and we most likely were just fortunate to find appropriate times in the 95 °C case. We examined the size and polydispersity of microspheres qualitatively and did not observe a striking difference between those formed at 70 °C and 95 °C, eliminating this as a possible source for the observed difference in gradient formation.

Covalent immobilization at 37 °C will be necessary to prevent protein denaturation, but the range of densities that could be generated at this temperature was quite limited. Close examination of the confocal images revealed what appear to be large aggregates of microspheres. According to Stoke's law, terminal velocity scales with radius squared, providing a mechanism for the aggregates to sediment more rapidly. The presence of aggregates may be related to the long incubation times. However, the aggregates appear to be present in the 37 °C microspheres that were incubated above the cloud point for only 20 min. Due to the slower reaction kinetics at 37 °C, the microspheres formed at this temperature were larger, likely due to a longer time to reach the gel point, despite the fact that the solutions were pre-reacted prior to phase separation. Aggregation may be related to microsphere size, as Stoke's law also applies to the rising of the larger microspheres in the dense sodium sulfate solutions ('creaming'). Aggregation thus may have been enhanced as microspheres concentrated near the top of the solution. Microsphere formation is performed in unstirred solutions to minimize coarsening prior to gelation, but this may also enhance aggregation of the formed microspheres that rise to the top of the solution.

The current results suggest that microsphere formation at 70 °C or higher has distinct advantages. Notably, it appears that aggregation was minimized due to a combination of small microsphere size and shorter incubation times. For the delivery of growth factors and other proteins, post-loading of the proteins would be necessary. Yet, the small size of the microspheres may make post-loading somewhat difficult. The effective diffusion coefficient of heparin-binding proteins in the presence of immobilized heparin is simply,

$$D_{AB}^{eff} = \frac{D_{AB}}{[B]/[P]+1}$$

where [P] is the concentration of free protein and [B] is the concentration of bound protein (Crank J., 1975). In the presence of an excess of heparin-binding sites, this ratio is simply:

$$\frac{[B]}{[P]} = \frac{[H]}{K_D}$$

where [H] is the concentration of bound heparin. To decrease the effective diffusion coefficient, high affinity interactions or high concentrations of heparin are required. This becomes important due to the small size of the microspheres produced (less than 5 microns in diameter). With microspheres of this size, the time for equilibration with the surrounding solution is quite short (order of seconds). To reach a Fick number (mass transfer Fourier number) of $\tau = 0.5$, representing about 99% equilibration between the microsphere and the surrounding medium, requires a time of $t = \tau R2/DAB$. A typical DAB for a heparin-binding growth factor (mol. wt. 20,000 Da) is $1.01 \times 10{-}4$ cm2/min (Maxwell, Hicks, Parsons, & Sakiyama-Elbert, 2005). With a KD of $3 \times 10{-}7$ m (Wacker et al., 2006) and a heparin concentration of $4.6 \times 10{-}5$ m calculated for these microspheres, the time to reach a Fick number of 0.5 is less than 3 s. After the microspheres are assembled into a scaffold, the appropriate length scale for diffusion is that of the scaffold and controlled release will occur of over much longer time periods. However, the rapid equilibration presents a challenge for forming gradients by centrifugation, which requires about 10 min. To overcome this limitation, the PEG/heparin microspheres were incubated with protamine, which has an extremely high binding affinity for heparin (Jaques, 1943; Jones, Hashim, & Power, 1986). However, the equations presented above provide a guidepost for engineering the system for growth factor delivery by non-covalent interactions. Another solution may be to incorporate high densities of positive or negative charges into the microspheres, such as are found in gelatin microspheres that are used for growth factor delivery (Morimoto et al., 2000; H. Park, Temenoff, Holland, Tabata, & Mikos, 2005). This may allow the attachment and controlled release of a variety of charged biological molecules.

## 2.6 Conclusions

We have shown that various gradients can be fabricated by manipulating the densities of PEG microspheres. In particular, the 5-tier gradient could be used to make a wide variety of complex profiles, while the gradual 2-tier gradient provided a fast and simple way of forming a linear gradient. Using these techniques, a 2-tier sharp gradient in GDNF was produced. A somewhat linear gradient in GDNF/BSA was formed with microspheres fabricated at a physiological temperature. Heparin was bound to the microspheres to promote attachment of heparin-binding molecules post-microsphere formation. The heparin microspheres formed gradients as before, and a 2-tiered gradient in protamine was produced. With further engineering, this system may be useful for the development of a variety of gradients in PEG-based scaffolds.

# Chapter 3*

# Controlled release and gradient formation of human glial-cell derived neurotrophic factor from heparinated poly(ethylene glycol) microsphere-based scaffolds

## 3.1 Abstract

Introduction of spatial patterning of proteins, while retaining activity and releasability, is critical for the field of regenerative medicine. Reversible binding to heparin, which many biological molecules exhibit, is one potential pathway to achieve this goal. We have covalently bound heparin to poly(ethylene glycol) (PEG) microspheres to create useful spatial patterns of glial-cell derived human neurotrophic factor (GDNF) in scaffolds to promote peripheral nerve regeneration. Labeled GDNF was incubated with heparinated microspheres that were subsequently centrifuged into cylindrical scaffolds in distinct layers containing different concentrations of GDNF. The GDNF was then allowed to diffuse out of the scaffold, and release was tracked via fluorescent scanning confocal microscopy. The measured release profile was compared to predicted Fickian models. Solutions of reaction–diffusion equations suggested the concentrations of GDNF in each discrete layer that would result in a nearly linear concentration gradient over much of the length of the scaffold. The agreement between the predicted and measured GDNF concentration gradients was high. Multilayer scaffolds

* Chapter 3 has been adapted from the following manuscript:
J. Roam, P. Nguyen, D. Elbert. Controlled release and gradient formation of human glial-cell derived neurotrophic factor from heparinated poly(ethylene glycol) microsphere-based scaffolds. Biomaterials, 35 (2014), pp. 6473–6481.

with different amounts of heparin and GDNF and different crosslinking densities allow the design of a wide variety of gradients and release kinetics. Additionally, fabrication is much simpler and more robust than typical gradient-forming systems due to the low viscosity of the microsphere solutions compared to gelating solutions, which can easily result in premature gelation or the trapping of air bubbles with a nerve guidance conduit. The microsphere-based method provides a framework for producing specific growth factor gradients in conduits designed to enhance nerve regeneration.

## 3.2 Introduction

The importance of gradients in biological molecules is well recognized. Processes such as nerve regeneration, wound healing, embryogenesis, angiogenesis, and immunity have been found to depend significantly on biological gradients (X. Cao & Shoichet, 2001; DeLong et al., 2005; Fisher et al., 1989; Kapur & Shoichet, 2004; Knapp et al., 1999; K. Moore et al., 2006; Parent & Devreotes, 1999; Rosoff et al., 2004; Singh et al., 2008; H. Song & Poo , 2001; H. J. Song et al., 1997; X. Wang et al., 2009). In chemotaxis cells follow concentration gradients in signaling molecules, with the steepness of the gradients greatly influencing cell movement more than the average concentration (Knapp et al., 1999; K. Moore et al., 2006; Parent & Devreotes, 1999). To replicate and improve upon developmental and repair processes to engineer tissues and organs, production of bioactive gradients along with spatial patterning will be essential.

In recent years an increasing number of researchers have proposed many methods to this end (Campbell et al., 2005; Chung et al., 2009; Cosson et al., 2009; Dodla & Bellamkonda, 2008, 2006; Dormer et al., 2010; J. He et al., 2010; Kipper et al., 2007; Lühmann et al., 2009; Mapili et al., 2005; Oh et al., 2011; Roam et al., 2010; Stefonek & Masters, 2007; Vepari & Kaplan, 2006; X Yu et al., 1999; Zaari et al., 2004). For example, Khademhosseini and colleagues have created gradients in adhesion peptides using inverse flows and photopolymerization in microfluidic channels to influence

and study endothelial cell migration (J. He et al., 2010). Shoichet, et al. have immobilized nerve growth factor in concentration gradients and observed enhanced directionality of extending dendrites (Kapur & Shoichet, 2004; Luo & Shoichet, 2004; K. Moore et al., 2006). Bellamkonda, et al. found increasing concentration gradients in laminin-1 could alter the direction of growing dorsal root ganglia and enhanced regeneration of sciatic nerves in rats with nerve growth factor (Dodla & Bellamkonda, 2008, 2006; Vepari & Kaplan, 2006).

Many of the current methods for the patterning and delivery of bioactive molecules use various forms of covalent attachment (Campbell et al., 2005; Cosson et al., 2009; Kipper et al., 2007; Lühmann et al., 2009; X Yu et al., 1999; Zaari et al., 2004). Irreversible coupling, however, may not be the optimal approach. Covalent attachment can potentially hinder the ability of cells to access the molecules, and chemical modification may result in a loss of activity. An alternative that our lab has explored recently is the use of heparin-decorated synthetic materials that can bind electrostatically (reversibly) many useful proteins, including proteins that promote nerve regeneration (Jaques, 1943; Jones et al., 1986; Maxwell et al., 2005; Nie et al., 2007; Oh et al., 2011; Roam et al., 2010; Sakiyama-Elbert & Hubbell, 2000; Stefonek & Masters, 2007; Tae et al., 2006). GDNF, a heparin binding protein, has been shown to enhance motor and sensory nerve regeneration (Barras et al., 2002; Fine et al., 2002). Synthetic polymer hydrogels have been extensively explored to create scaffolds for regenerative medicine, and have seen some promising results (Drury & Mooney, 2003; Nichols et al., 2009; Tessmar & Göpferich, 2007). Functional peptides, proteins, or other biological molecules like heparin may be incorporated into these hydrogels imparting biological functions, such as cell adhesion or cell-initiated degradability (Almany & Seliktar, 2005; DeLong et al., 2005; M P Lutolf & Hubbell, 2005; E. a. Scott et al., 2010; Zhang et al., 2006). However, bulk hydrogel scaffolds generally lack macroporosity or spatial anisotropy. To address these limitations we and others are seeking to produce heterogeneous scaffolds using modular assembly of hydrogel

microparticles (Boland et al., 2006; Khademhosseini & Langer, 2007; Liu Tsang & Bhatia, 2004; Rivest et al., 2007; Roam et al., 2010; E. a. Scott et al., 2010; Um et al., 2008; Yeh et al., 2006).

Gradient producing systems such as pulsatile application of picoliters of growth factor solutions, simple diffusion of molecules into a gel, gradient makers using two polymerizing solutions, and microfluidic devices have been used extensively (X. Cao & Shoichet, 2001; Chung et al., 2009; J. He et al., 2010; Kapur & Shoichet, 2004; Knapp et al., 1999; H. J. Song et al., 1997; Stefonek & Masters, 2007). However scaling issues and difficulties in pumping polymerizing solutions are only a few of the challenges faced by these methods due to the low volumes involved (e.g. about 70 µL of fluid per centimeter of conduit). The formation of gradients of growth factors, as well as addition of adhesion factors and degradibility in bioactive scaffolds, is proposed to be improved by assembling microparticles in a modular manner (Du et al., 2008; Rivest et al., 2007; Roam et al., 2010; E. a. Scott et al., 2010; Serban & Prestwich, 2008; Yeh et al., 2006). To this end our lab has developed PEG hydrogel microspheres fabricated from multi-arm PEG derivatives in aqueous solution with kosmotropic salts via a thermally induced phase separation (Roam et al., 2010; E. a. Scott et al., 2010). This is a novel strategy in that solutions are not mixed during microsphere formation, with size controlled by the length of time required for gelation (D. Elbert, Nichols, & Scott, 2013). We have already successfully imparted different functionalities, such as cell adhesion, degradability, heparination, and protein and drug delivery to these microspheres (Roam et al., 2010; E. a. Scott et al., 2010).

In a recent study we engineered gradients into scaffolds made from these PEG microspheres, most notably decorating the microspheres with heparin and creating a gradient of covalently coupled GDNF (Roam et al., 2010). However, we had not demonstrated the release of electrostatically (i.e.

reversibly) bound GDNF from these scaffolds. The challenges in the previous publication that did not allow release of GDNF were overcome and the results are presented here.

# 3.3 Materials and Methods

Unless otherwise noted, all reagents were purchased from Sigma–Aldrich.

## 3.3.1 PEG Synthesis

PEG8-vinylsulfone (PEG8-VS) and PEG8-amine was synthesized from eight-arm PEG-OH (PEG8-OH; mol. Wt. 10,000; Shearwater Polymers, Huntsville, AL) as previously described (Wacker et al., 2006). PEG macromonomers were dissolved separately at 200 mg/mL in Dulbecco's phosphate buffered saline (PBS; 8 mM sodium phosphate, 2 mM potassium phosphate, 140 mM sodium chloride, 10 mM potassium chloride, pH 7.4) and sterile filtered with 0.22 μm syringe filters (Millipore).

## 3.3.2 Heparin Attachment

A solution of 500 mM N-(3-Dimethylaminopropyl)-N'-ethylcarbodiimide hydrochloride (EDC), 12.5 mM N-Hydroxy-succinimide (NHS), and 50 mg/mL heparin sodium salt (mol. wt. ~18,000, ~2.78 mM) in MES buffer (10 mM, pH 6.0) was incubated at room temperature for 30 min. The activated heparin solution was then added to a 200 mg/mL solution of PEG8-amine at a 20:1, or 160:1 PEG8-amine to heparin molar ratio and incubated at room temperature for another 30 min before refrigeration. For microsphere formation, heparin-conjugated PEG8-amine was mixed with PEG8-VS in a 1:2 ratio of the two PEG types (see Figure 3.1).

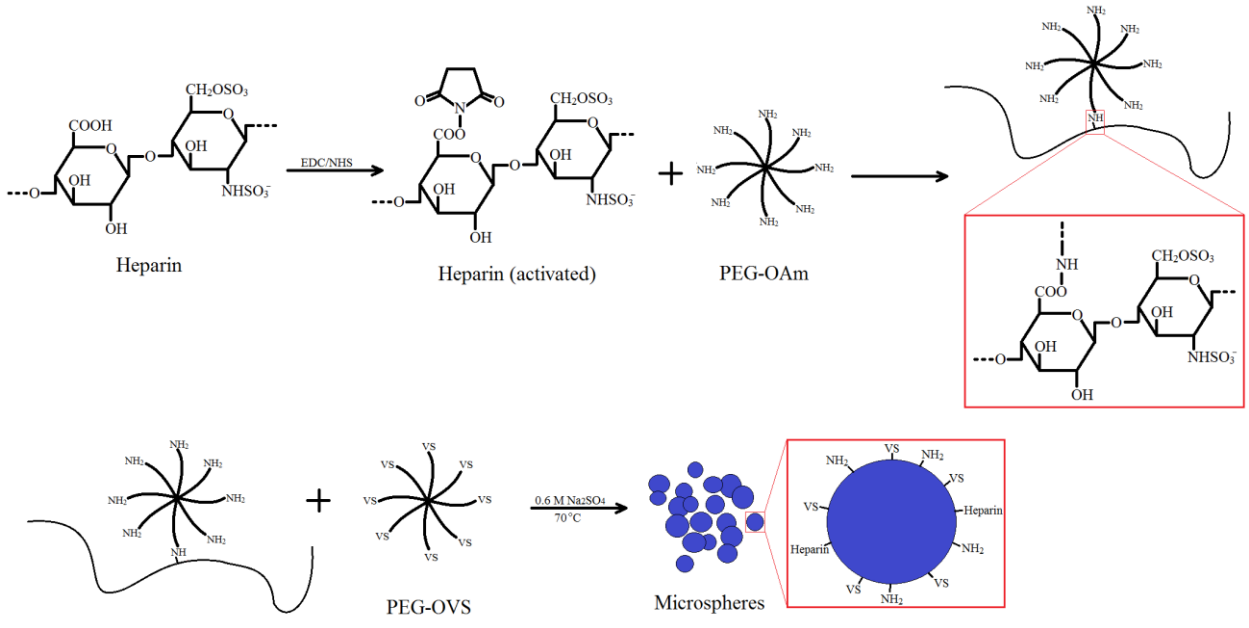


**Figure 3.1. Heparin Attachment**

## 3.3.3 Microsphere Formation

PEG8-amine (with or without bound heparin) solutions were combined with PEG8-VS solutions at a 1:2 ratio. The PEG solutions were diluted to 20 mg/mL PEG with PBS and 1.5 M sodium sulfate (in PBS) to a final sodium sulfate concentration of 0.6 M. The PEG8-VS/PEG8-amine solutions were then incubated above the cloud point at 70˚C for various times. Suspensions of microspheres were subsequently buffer exchanged into 8 mM sodium phosphate twice to remove the sodium sulfate by: (1) diluting the microsphere solution 3:1 with PBS and titurating, (2) centrifuging at 14,100g for 2 min, and (3) removing the supernatant.

## 3.3.4 GDNF Labeling

Dylight-488 NHS-ester (Pierce) was dissolved in dimethyl formamide at 10 mg/mL. Recombinant human GDNF (Peprotech, Rocky Hill, NJ) was dissolved in 8 mM sodium phosphate

buffer (pH 7.4). Dylight-488 was added to the solution for a final GDNF concentration of 10 μg/mL and a final Dylight-488 concentration of 50 ng/mL and incubated overnight at 2˚C. The solution was then dialyzed using Slide-A-Lyzer MINI Dialysis Units (Thermo Scientific, Rockford, IL, 3500 MWCO) in 8 mM sodium phosphate buffer (pH 7.4) to remove unbound Dylight-488.

### 3.3.5 Heparin labeling

For some experiments, heparin was labeled with Dylight-488. A solution of heparin (100 mg/mL) and Dylight-488 (560 □g/mL) in PBS was incubated overnight at room temperature. The labeled heparin solution was dialyzed using Slide-A-Lyzer MINI Dialysis Units in MES buffer (10 mM, pH 6.0) to remove any unbound Dylight-488. The heparin solution was then used in the microsphere formation protocol as described above.

### 3.3.6 GDNF Loading of Heparin Microspheres

Labeled or unlabeled GDNF solutions were added to buffer washed microspheres such that the GDNF concentration within the supernatant was 250 ng/mL. The microsphere/GDNF solution was well mixed, by tituration and incubated overnight to allow diffusion of the GDNF into the microspheres. Immediately before scaffold formation, the microspheres were centrifuged at 14,100 g, supernatant was removed, and microspheres were resuspended in 8 mM sodium phosphate.

### 3.3.7 Gradient Formation

The glass walls of Pasteur pipettes were passivated with PLL(375)-g[7]-PEG(5) (D. L. Elbert & Hubbell, 1998; Kenausis et al., 2000). The pipettes were filled with a 20 mg/mL PLL-g-PEG solution, incubated for 30 seconds, and washed with DI water. After sufficient drying time, the tips of the pipettes were sealed with silicone aquarium sealant (DAP Inc., Baltimore, MD). To form scaffolds, microsphere solutions loaded or unloaded with GDNF were sequentially added to the

pipettes that were placed in 15 mL conical vials. The microsphere solutions were centrifuged at 1000 g for 5 min before the next layer of microspheres was added (Figure 3.2). The supernatant was then removed once more and replaced with either 8 mM Sodium Phosphate or PBS.

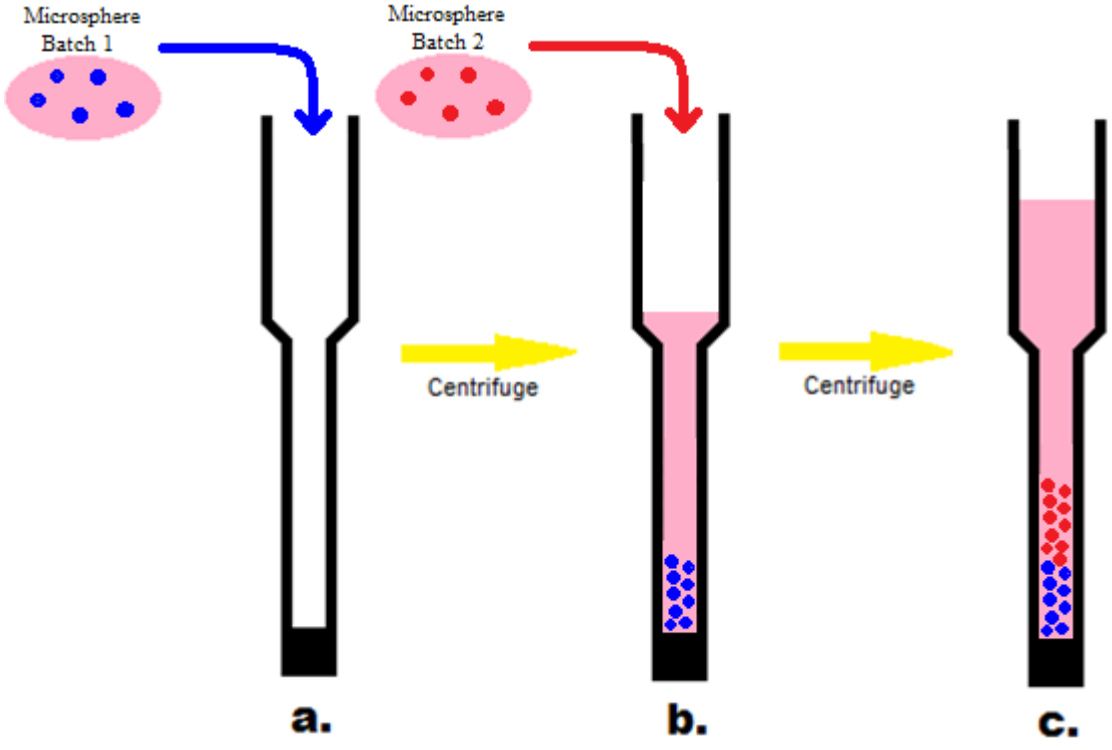


**Figure 3.2. Gradient formation.** (a) Batches of microspheres with similar chemical structures but varying amount of GDNF and/or heparin were created separately. One batch of microspheres were buffer exchanged to 8mM sodium phosphate buffer (pH 7.4) and immediately added to a PLL-*g*-PEG treated Pasteur pipette. (b) After centrifugation for 5 min at 1000 g, a second batch of different microspheres were added , and (c) Upon a second centrifugation, the microspheres formed two distinct layers.

## 3.3.8 Confocal Microscopy

Fluorescence microscopy was performed with a Nikon Eclipse C1/80i confocal microscope. Microsphere gradients were imaged while still in the Pasteur pipettes with a 10X objective (NA=0.30, DIC L/N1, WD= 16.0mm). Multiple images were taken along the length of the pipette and processed using EZ-C1 3.70 FreeViewer software (Nikon Instruments Inc.) and then combined. Fluorescence in the composite photographs was analyzed with ImageJ software.

## 3.4 Results and Discussion

### 3.4.1 Conformation of Heparin Attachment

To confirm attachment of heparin to PEG-OAm and subsequent incorporation into microspheres, heparin was labeled with Dylight-488. The mechanism to couple the NHS ester dye to heparin was conceived because of an observation that NHS-activated heparin alone will form a gel if the reaction is allowed to proceed overnight. Crosslinking was most likely due to reactions between the NHS-esters on heparin and secondary amines on heparin, although the concentration of this chemical linkage was too low to measure by NMR or IR. Though Dylight-488 normally reacts with primary amines, adequate incubation time allowed for reaction with heparin. Unreacted Dylight-488 was removed by dialysis as well as by the washing steps after microsphere formation (by which time the NHS-esters on Dylight-488 would be hydrolyzed and unreactive). After the washes, the microspheres were photographed with a fluorescence microscope (Figure 3.3A). The total fluorescence was also compared to unlabeled heparin microspheres on a fluorescence plate reader to confirm the fluorescence was originating from the labeled heparin (Figure 3.3B). Fluorescence readings were also taken on the labeled heparin microspheres before and after the washing steps. The washed microspheres contained 46% of the fluorescence of the unwashed microspheres. This indicated that at most 46% of the heparin was successfully integrated into the microspheres.

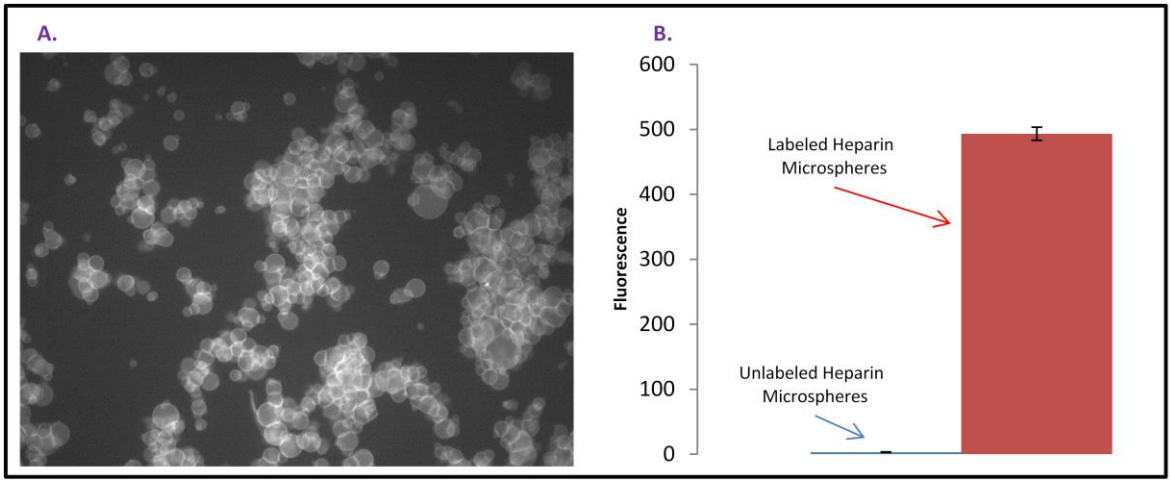


**Figure 3.3. Confirmation of Heparin Attachment** (A) Photomicrograph of PEG microspheres decorated with Dylight-488 labeled heparin. (20X) (B) Fluorescence of microspheres with labeled and unlabeled heparin. Excitation 488nm, Emission 530nm. (n=3, error bars shown)

## 3.4.2 Step Gradients

We previously presented a method of gradient formation in one step, using density (buoyancy) differences in microspheres to form distinct layers during centrifugation (Roam et al., 2010). However, we suspected that differences in crosslink density that resulted in differences in buoyancy may affect rates of growth factor diffusion within the microspheres. To test this, scaffolds were made from microspheres crosslinked for 11 minutes or 45 minutes. We had shown that these crosslinking times resulted in the full range of practically achievable buoyancies (less crosslinking time did not result in microsphere formation and more resulted in substantial microsphere aggregation) (Roam et al., 2010). Single-layer scaffolds were prepared from each microsphere type in the presence of 250 ng/mL Dylight-labeled GDNF. The interface between the microsphere layer and the supernatant was imaged immediately after scaffold formation (i.e. before removing the supernatant and washing the scaffold). Representative fluorescent images are shown in Figure 3.4, which suggest that the scaffold made from microspheres incubated in the phase separated state for only 11 minutes had higher GDNF concentrations than the adjacent supernatant. The opposite was true for a scaffold made from

microspheres incubated in the phase separated state for 45 minutes (the highest crosslinking density possible without substantial microsphere aggregation) (Roam et al., 2010). This indicated that the more densely crosslinked microsphere had a restricted ability to absorb GDNF. Although a one-step process for gradient formation is attractive, the non-uniformity in growth factor diffusion rates for the different layers makes prediction of release kinetics extremely challenging. Thus, we subsequently used the lowest crosslinking time (11 minutes) for all microspheres to ensure high loading of growth factor in the scaffolds and predictability of release kinetics. Gradient scaffolds were thus formed by sequentially centrifuging microspheres in distinct layers, with gradients formed by incubating microspheres with different concentrations of GDNF prior to and during centrifugation. The layer-by-layer scaffold formation method served to eliminate the high sensitivity of the microsphere structure to the length of incubation time in the phase separated state during microsphere formation. Although the layer-by-layer method initially produces step gradients in GDNF, continuous gradients of soluble GDNF are rapidly generated by diffusion and dynamic interactions with heparin in the scaffold.

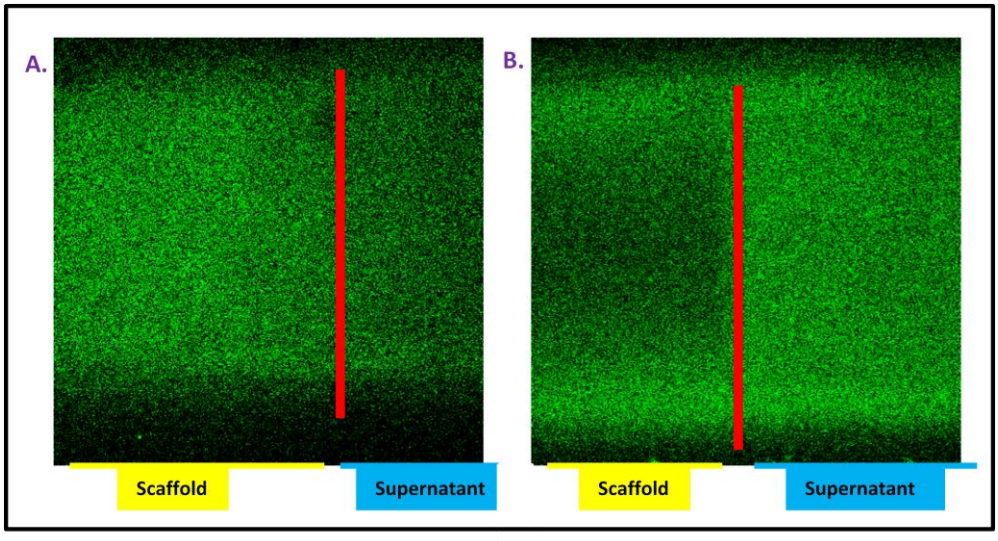


**Figure 3.4. Microsphere Displacement of GDNF.** Photomicrographs of Dylight-488 labeled GDNF on the boundaries of scaffolds made from PEG microspheres (A) incubated 11 minutes and (B) incubated 45 minutes. Scaffolds are located to the left of the red line while the supernatant lies to the right.

## 3.4.3 Linear Gradient Formation from Initial Step Gradients

Figures 3.5 and 3.6 show release for single tiered scaffolds made of heparin-containing microspheres incubated in 250 ng/mLGDNF during scaffold formation. Figures 3.7 and 3.8 show scaffolds with two tiers - a lower tier with scaffold made of heparin-containing microspheres incubated in 250 nM GDNFduring centrifugation, and an upper level with no GDNF present during centrifugation of heparin-containing microspheres. Figures 3.5A, 3.6A, 3.7A, and 3.8A demonstrate GDNF gradient formation within one or two tier scaffolds, with release into either physiological (Figures 3.5 and 3.7) and low salt conditions (Figures 3.6 and 3.8). The affinity of GDNF for heparin in the microspheres will be influenced by the concentration of salt in the surrounding buffer (Roam et al., 2010). Low salt (8mM sodium phosphate) should result in slower release than physiological salt concentrations (i.e. PBS). More rapid release of GDNF into buffer at physiological salt concentration was observed, as expected, which was quantified in Figures 3.5B, 3.6B, 3.7B and 3.8B.

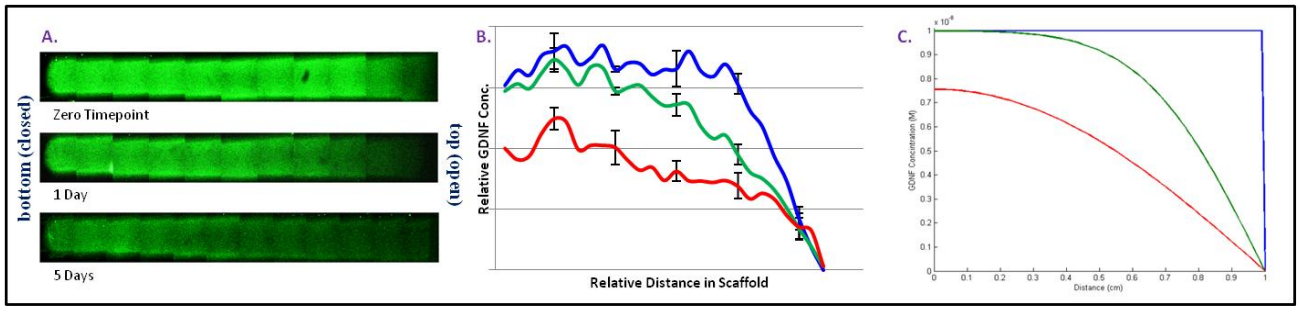


**Figure 3.5. Release from 1-Tier Scaffold in Physiological Salt.** Physiological salt (PBS) release of Dylight-488 labeled GDNF (constant initial profile) from Heparin decorated PEG microsphere (11 minute incubation) scaffold. (A) Composite photograph of fluorescence (GDNF) in scaffold at the zero time point, one day, and 5 days. (B) Graphical depiction of fluorescence (GDNF concentration) vs. the distance in the scaffold for the three time points: zero (blue), 1 day (green), and 5 days (red). n=3 sample error bars shown. (C) Plot of predicted release (GDNF Concentration vs. distance in the scaffold) based on Fick's 2nd law. Zero time point (blue), 1 day (green), and 5 days (red).

Each of these figures also contains mathematical predictions for the GDNF concentration profile within the scaffold based on Fick's 2nd Law (Figures 3.5C, 6C, 3.7C and 3.8C). The prediction was obtained using a model that utilized an effective diffusion constant for GDNF within the scaffold:

$$D_{eff} = \frac{D_{AB}}{[H]/K_D + 1}$$

where Deff = effective diffusion constant, DAB =diffusion constant of GDNF in PEG scaffolds without heparin, [H] = heparin concentration, KD = equilibrium dissociation constant for the interaction of heparin with GDNF (Crank J., 1975). Use of an effective diffusion coefficient is justified when binding equilibrium is rapidly achieved compared to the rate of diffusion. The constants used for the predictions (DAB, KD) were initially estimated using literature values for diffusion of proteins of similar size through collagen gels (DAB = 7x10-7 cm2 s-1) and interaction of GDNF with heparin at physiological salt concentration (KD = 1x10-7 M). (Saltzman, Radomsky, Whaley, & Cone, 1994; Wood, Borschel, et al., 2009). From these values, Deff was predicted to be

1.52x10-7 cm2 s-1. However, the rate of diffusion through these PEG hydrogels may be much slower than in a collagen gel. Thus, the release data in Figures 3.5 through 3.8 were fit to solutions of Fick's second law to determine best fit effective diffusion coefficients. In physiological salt we observed a Deff = 4.84x10-8 cm2 s-1, while in low salt we observed Deff = 2.52x10-8 cm2 s-1. The differences may be explained by the higher affinity of GDNF for heparin in low salt conditions. All predicted curves in Figures 3.5 through 3.8 use these values for the effective diffusion coefficients.

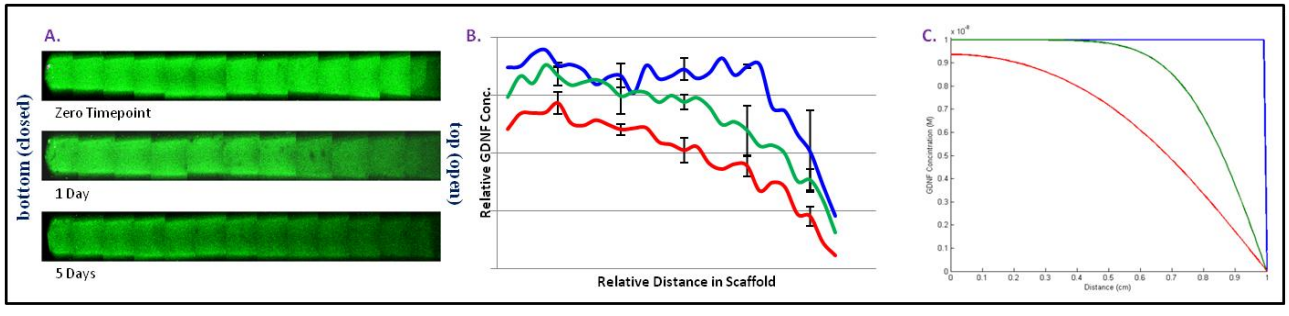


**Figure 3.6. Release from 1-Tier Scaffold in Low Salt.** "Low salt" (8 mM Sodium phosphate) release of Dylight-488 labeled GDNF (constant initial profile) from Heparin decorated PEG microsphere (11 minute incubation) scaffold. (A) Composite photograph of fluorescence (GDNF) in scaffold at the zero time point, one day, and 5 days. (B) Graphical depiction of fluorescence (GDNF concentration) vs. the distance in the scaffold for the three time points: zero (blue), 1 day (green), and 5 days (red). n=3 sample error bars shown. (C) Plot of predicted release (GDNF Concentration vs. distance in the scaffold) based on Fick's 2$^{nd}$ law. Zero time point (blue), 1 day (green), and 5 days (red).

Figure 3.5 shows the high salt release for a single tiered scaffold made of microspheres incubated in 250 ng/mLGDNF during scaffold formation. Reasonable agreement was observed between the predicted release profile and the measured release profile. The low salt release for the same initial single-tiered profile (Figure 3.6) also was markedly similar to the predicted release profile. Although the predicted release profile used an effective diffusion coefficient that was partially determined from this data, subsequent results will show that these same effective diffusion coefficients are able to describe release from a variety of scaffolds. As expected, release was much slower into low salt buffer than high salt buffer.

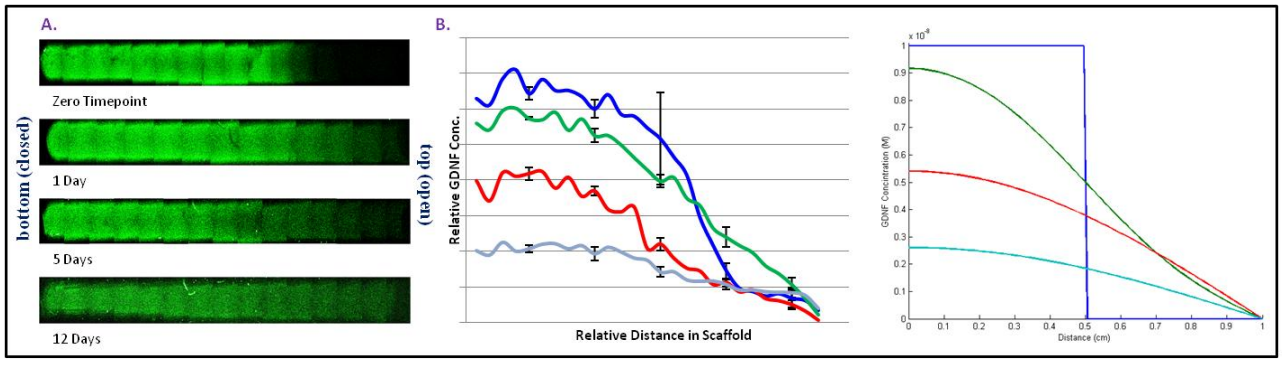


**Figure 3.7. Release from 2-Tier Scaffold in Physiological Salt.** 2-tier initial profile, physiological salt (PBS) release of Dylight-488 labeled GDNF from Heparin decorated PEG microsphere (11 minute incubation) scaffold. (A) Composite photograph of fluorescence (GDNF) in scaffold at the zero time point, one day, 5 days, and 12 days. (B) Graphical depiction of fluorescence (GDNF concentration) vs. the distance in the scaffold for the four time points: zero (blue), 1 day (green), 5 days (red), and 12 days (light blue). n=3 sample error bars shown. (C) Plot of predicted release (GDNF Concentration vs. distance in the scaffold) based on Fick's 2nd law. Zero time point (blue), 1 day (green), 5 days (red), and 12 days (light blue).

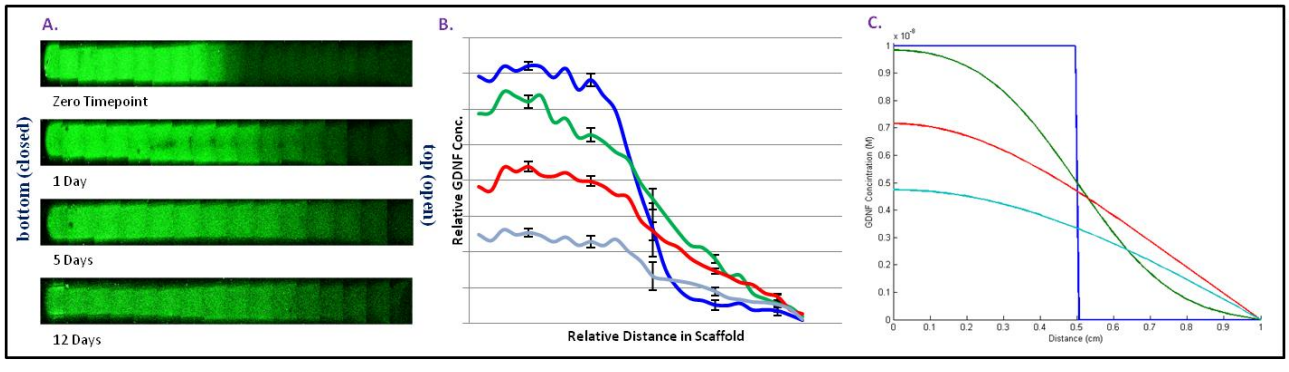


**Figure 3.8. Release from 2-Tier Scaffold in Low Salt.** 2-tier initial profile, "low salt" (8 mM sodium phosphate) release of Dylight-488 labeled GDNF from Heparin decorated PEG microsphere (11 minute incubation) scaffold. (A) Composite photograph of fluorescence (GDNF) in scaffold at the zero time point, one day, 5 days, and 12 days. (B) Graphical depiction of fluorescence (GDNF concentration) vs. the distance in the scaffold for the four time points: zero (blue), 1 day (green), 5 days (red), and 12 days (light blue). n=3 sample error bars shown. (C) Plot of predicted release (GDNF Concentration vs. distance in the scaffold) based on Fick's 2nd law. Zero time point (blue), 1 day (green), 5 days (red), and 12 days (light blue).

## 3.4.4 Analysis of Gradients

Table 3.1 presents an analysis of linearity of the graphs in Figures 3.5 through 3.8. Linear regressions were performed on both experimental and predicted curves (excluding zero time points),

requiring that points at (or near) the open end(right end) be included in the regression (for examples, see Figure 3.9). This would correspond to the growth factor gradient that extending axons would sense. The percentage of the length of the scaffold that produced a regression with an r2 value above a particular value is reported. For the predicted curves, we set a constraint of r2≥0.995 for the linear regression. Because the experimental curves contained experimental error, we set a constraint of r2≥0.95 for those regressions. It should be clear that the purpose of the linear regression is to characterize the morphology of the curve and not to explain the relationship between the measured and predicted curves. These values for the coefficient of determination produced similar percentages of the scaffolds with 'linear' GDNF concentration gradients (mostly below 50%) for the 1 tier scaffolds. Scaffolds with two tiers had consistently larger percentages of the scaffold with 'linear' gradients, in both the experimental and predicted curves.

| Table 1 - Linearity Comparison | | | |
|---|---|---|---|
| | 1 Day | 5 Days | 12 Days |
| 1 tier, Phys Salt (Exp) | 62% | 0% | - |
| 1 tier, Phys Salt (Pred) | 29% | 60% | - |
| 1 tier, Low Salt (Exp) | 11% | 19% | - |
| 1 tier, Low Salt (Pred) | 21% | 48% | - |
| 2 tier, Phys Salt (Exp) | 92% | 92% | 81% |
| 2 tier, Phys Salt (Pred) | 24% | 65% | 63% |
| 2 tiers, Low Salt (Exp) | 100% | 92% | 92% |
| 2 tiers, Low Salt (Pred) | 10% | 80% | 62% |

**Table 3.1. Linearity Comparisons.** Linearity comparisons between experimental and predicted models. Shown are the percentages of the length of the scaffolds with a linear regression which yielded a coefficient of determination above a particular threshold are shown (exp: $R^2 \geq 0.95$, pred: $R^2 \geq 0.995$), corresponding to correlation coefficients of 0.975 and 0.9975, respectively. Experimental (Exp) and predicted data (Pred) are shown for comparison. The line was required to include points at (or near) the open (right) end of the scaffolds. It should be understood that the coefficients of determination are used here to describe the morphology of the curve and not to explain the underlying relationships between the measured concentration profile and the predicted values. Sample linear regions are shown in Figure 3.9.

For the 1 tier scaffold, the linearity varied greatly from 1 to 5 days in both experimental and both experimental and predicted cases, though the experiments have the surprising distinction of producing larger linear regions earlier and losing them over time as opposed to the model slowly growing more linear.

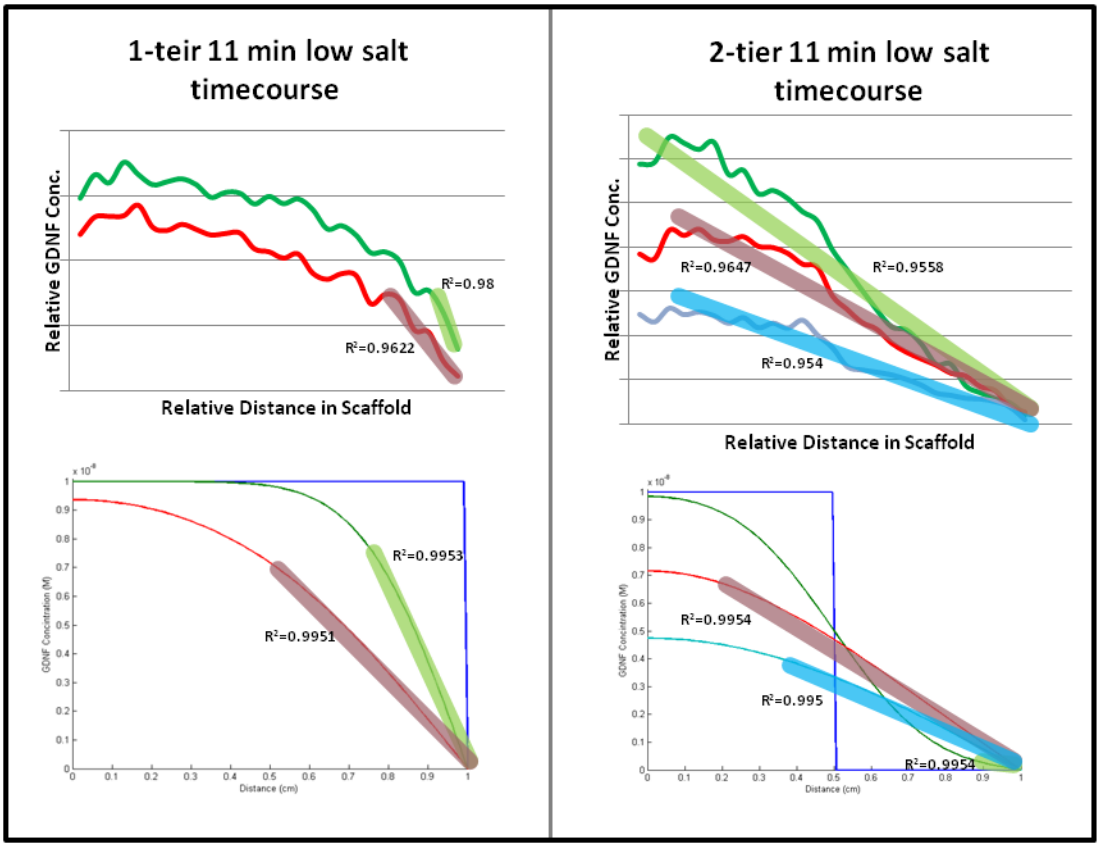


**Figure 3.9. Sample Linear Regions for Table 3.1.** Shown are linear regressions over the portion of each concentration profile which yielded a coefficient of determination above a particular threshold (exp: $R^2 \geq 0.95$, pred: $R^2 \geq 0.995$), corresponding to correlation coefficients of 0.975 and 0.9975, respectively. The percentage of length of the scaffold (x axis) that each section spanned is reported in Table 3.1. As in previous figures green, red, and blue lines correspond to 1, 5, and 12 days post-scaffold formation, respectively.

For the 2 tier scaffolds, the experimental profiles show larger linear regions that their predicted counterparts for all time points, though the 1 day profiles show the greatest disparity, with all or nearly all of the experimental profiles showing high linearity while the model predicts less than

25%. The presence of a linear gradient in GDNF concentration that emerges in just one day and is maintained for 12 days with only two tiers suggests that this strategy is highly promising for generating growth factor gradients within scaffolds. Furthermore, because of the high degree of predictability, more complex layer-by-layer arrangements may allow for the engineering of not only release kinetics but also gradient shape.

### 3.4.5 Multi-Tier Scaffolds

To demonstrate the robustness of this technique, multiple tiered scaffolds were fabricated with different amounts of GDNF in the tiers. Figure 3.10 shows three and four-tiered scaffolds with GDNF initially in alternating tiers. These scaffolds are the same length of their simpler counterparts and thus the tiers are smaller becoming much more homogenous in GDNF concentration after only a day. However, the intial GDNF concentration profile still strongly affects the resulting concentration profile at 1 day. These examples display the ability of this method to create more complex GDNF concentration profiles and release kinetics. The multiple tiers could also potentially be incubated with distinct concentrations of different growth factors, allowing release of multiple growth factors with different concentration profiles and release kinetics.

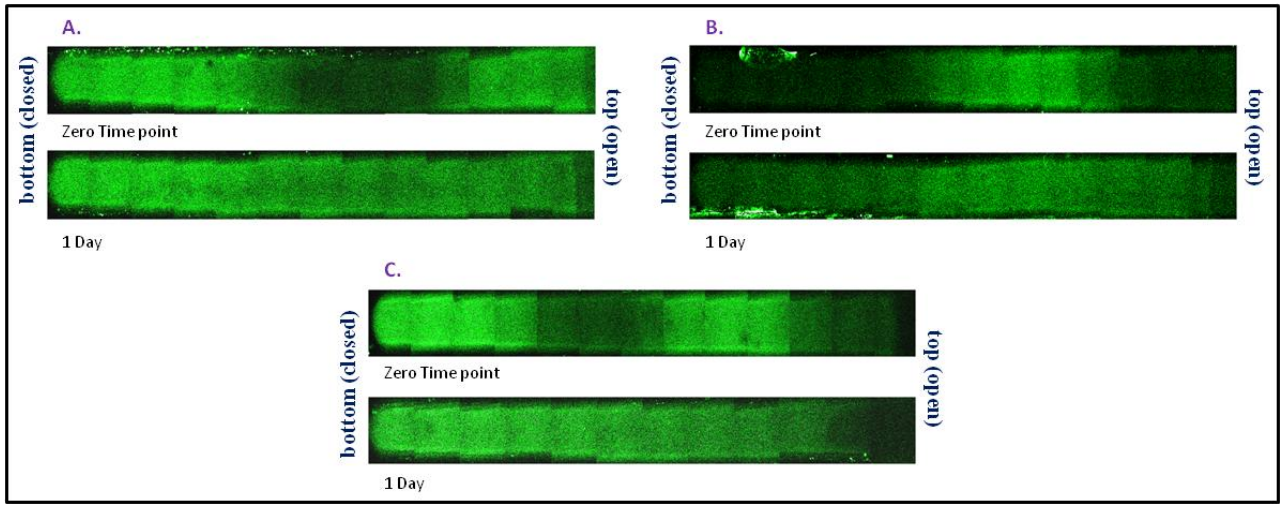


**Figure 3.10. Multi-Tier Formations.** The versatility of this gradient formation technique is displayed by three scaffolds with more complex patterns of GDNF. Composite photographs of fluorescence (GDNF) in the scaffolds taken at the zero time point and after one day. (A) 3-tier initial pattern: GDNF-Empty-GDNF. (B) 3-tier initial pattern: Empty-GDNF-Empty. (C) 4-tier initial pattern: GDNF-Empty-GDNF-Empty.

## 3.4.6 Heparin Variations within Scaffolds

The heparin content in the different tiers can also be varied to affect the release kinetics and gradient-forming capabilities of the scaffolds. Figures 3.11 and 3.12 show two cases where the top tier had a lower concentration of heparin than the bottom tier. The bottom tier for both experiments had the original amount of heparin (20:1 PEG-OAm to heparin) while the second tier contained either no heparin (Figure 3.11) or 1/8 of the original heparin concentration (160:1 PEG-OAm to heparin; Figure 3.12). In both cases, the microspheres were incubated overnight with 250 ng/mL GDNF. A major caveat is that the microspheres with less heparin were considerably less dense than their fully heparinated counterparts, and the photomicrographs clearly indicate that the microspheres with less heparin absorbed more GDNF during incubation. Thus, the top tier is initially much brighter than the bottom tier, so much so that the gain on the photodetector had to be greatly reduced below typical values. By one day, the brightness of the top tier was dramatically decreased, allowing the gain to be returned to normal values. The model predicted that with a higher initial GDNF concentration in the

top layer, rapid release of GDNF from the top of the scaffold would be combined with diffusion into the bottom layer, creating a maximum in the GDNF concentration profile at one day. Although not as dramatic as predicted, this maximum in GDNF concentration was observed for both cases (Figures 3.11 and 3.12). These experiments illustrated that heparin concentration and microsphere crosslink density are both variables that can be adjusted to control the rate of release and the shape of the growth factor gradient over time. Ideally, methods would be developed in the future such that the heparin concentration did not affect the crosslink density.

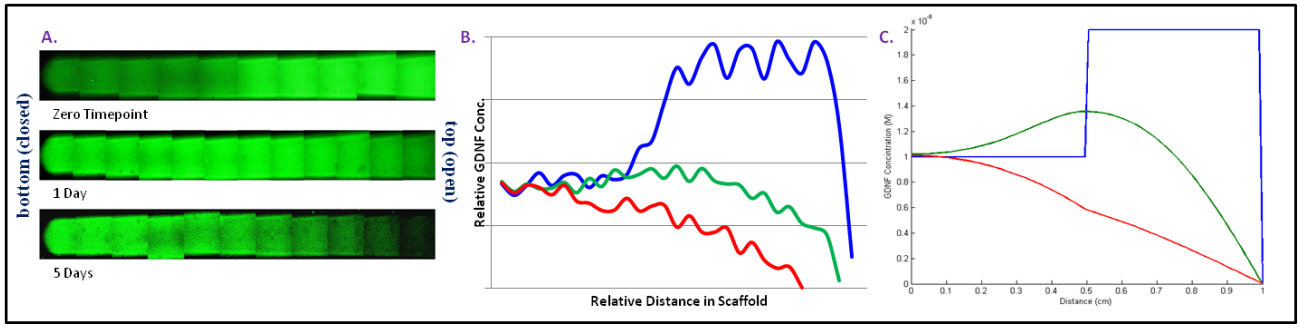


**Figure 3.11. Release from 2-Tier Heparin/No Heparin Scaffold.** PEG microsphere (11 minute incubation) scaffold with first half (d<0.5 cm) made with 20:1 PEG-Oam to Heparin and the second half (d>0.5 cm) made without heparin, releases Dylight-488 labeled GDNF (constant initial profile) under "low salt" (8 mM Sodium phosphate) conditions. (A) Composite photograph of fluorescence (GDNF) in scaffold at the zero time point, one day, and 5 days. (B) Graphical depiction of fluorescence (GDNF concentration) vs. the distance in the scaffold for the three time points: zero (blue), 1 day (green), and 5 days (red). (C) Plot of predicted release (GDNF Concentration vs. distance in the scaffold) based on Fick's 2$^{nd}$ law. Zero time point (blue), 1 day (green), and 5 days (red).

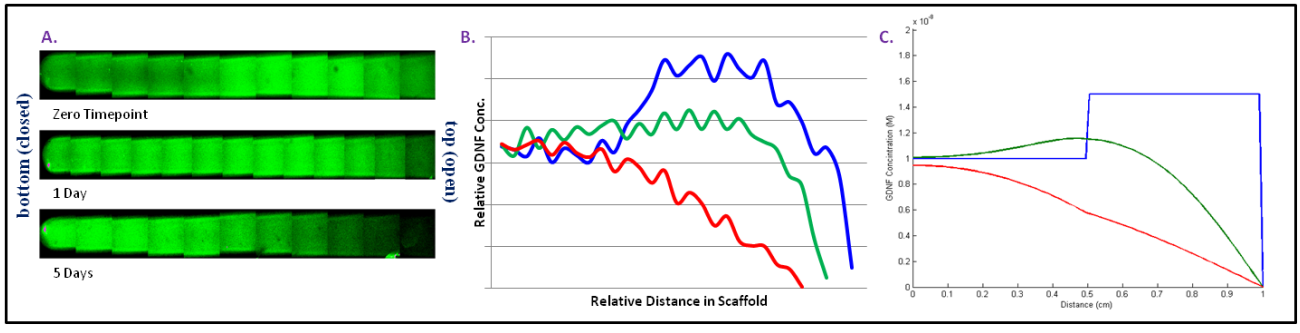


**Figure 3.11. Release from 2-Tier Heparin/Heparin (1/8) Scaffold.** PEG microsphere (11 minute incubation) scaffold with first half (d<0.5 cm) made with 20:1 PEG-Oam to Heparin and the second half (d>0.5 cm) made with 160:1 PEG-Oam to Heparin, releases Dylight-488 labeled GDNF (constant initial profile) under "low salt" (8 mM Sodium phosphate) conditions. (A) Composite photograph of fluorescence (GDNF) in scaffold at the zero time point, one day, and 5 days. (B) Graphical depiction of fluorescence (GDNF concentration) vs. the distance in the scaffold for the three time points: zero (blue), 1 day (green), and 5 days (red). (C) Plot of predicted release (GDNF Concentration vs. distance in the scaffold) based on Fick's 2nd law. Zero time point (blue), 1 day (green), and 5 days (red).

## 3.4.7 GDNF Preservation

A key consideration that must be addressed is whether or not the GDNF loses activity through this extensive incubation, scaffold formation, and subsequent release process. Due to significant dilution into the release medium, the concentration of GDNF was too low to test with cells, although subsequent studies will test the response of chick dorsal root ganglion cells within the scaffolds. For the current study, we asked if human GDNF retained its immuno-reactivity via ELISA measurements on the release solution. Results showed, approximately 8% of the initial activity introduced into the microspheres was released from a microsphere pellet after one day. A Matlab simulation of this process predicts a 55% release after 1 day. Adsorption to the various surfaces and the loss of activity overnight loading and one day of release may account for the difference between the model prediction and the measured activity. Further testing is required, but the retention of some GDNF immune-reactivity suggests the possibility for the retention of some biological activity in the released GDNF.

## 3.5 Conclusions

We devised robust methods for the creation of concentration gradients in GDNF. Through the sequential centrifugation of heparinated PEG microspheres loaded with varying amounts of GDNF, we quickly formed gradients in GDNF concentration. With relatively uncomplicated two-tiered scaffolds, linear gradients were produced and maintained for 12 days. The gradient shapes and kinetics agreed with mathematical predictions. We showed that the production of more complex gradients is possible and that microsphere characteristics, such as crosslink density and heparin content, can be tuned to alter release kinetics. This method of scaffold formation may be useful to improve nerve regeneration through engineered nerve guidance conduits.

# Chapter 4

# A Modular, Plasmin-Sensitive, Clickable Poly(ethylene glycol)-Heparin-Laminin Microsphere System for Establishing Growth Factor Gradients in Nerve Guidance Conduits

## 4.1 Abstract

Peripheral nerve regeneration is a complex problem that, despite many advancements and innovations, still has sub-optimal outcomes. Though biological techniques using nerve grafts and autographs are promising, completely synthetic nerve guidance conduits (NGC), which allow for precise engineering of their properties, are a far more intriguing proposition. One such property we have focused on is the introduction of spatial patterning of proteins, specifically glial-cell derived human neurotrophic factor (GDNF), which promotes nerve growth. We have created scaffolds made up of poly(ethylene glycol) (PEG) microspheres which form concentration gradients in reversibly bound GDNF. To facilitate nerve extension, we have engineered microspheres with tunable plasmin degradability, CLICK cross-linking chemistries, cell adhesion via laminin, and heparin binding. GDNF released from these microspheres was confirmed to have retained its activity. Methods for fabricating these scaffolds inside silicone conduits were developed using 3D printed molds. The fully formed NGC's contained degradable polymer scaffolding with linear gradients in reversibly bound GDNF. These NGC's were implanted into rats with severed sciatic nerves to confirm *in vivo* degradability and demonstrate that they do not elicit any negative biological responses.

## 4.2 Introduction

The treatment of peripheral nerve injury has advanced greatly in recent years. However, complete functional recovery continues to be difficult to achieve, suggesting it is critical that alternatives to the current standard of care (nerve autografts) be developed (Beazley, Milek, & Reiss, 1984; Dellon & Mackinnon, 1988; Wood et al., 2010). A promising strategy involves the use of nerve guidance conduits (NGCs), which can be filled with synthetic and/or biological matrices along with growth factors, to span nerve gaps and enhance axonal regeneration (Schmidt & Leach, 2003). Glial-derived neurotrophic factor (GDNF) has been reported by several studies to be the most potent motor neuron trophic and survival factor, showing great promise in the treatment of peripheral nerve injuries (Henderson et al., 1993; a Höke et al., 2002; L. Li et al., 1995; Oppenheim et al., 2000; Wood, Moore, et al., 2009; Yan, Matheson, & Lopez, 1995). NGC's delivering growth factors such as GDNF have been shown to shown to promote axonal regeneration better than isograft controls (Wood et al., 2010).

Gradients of biological molecules are known to significantly affect nerve regeneration, as well as other biological processes such as, wound healing, embryogenesis, angiogenesis, and immunity (X. Cao & Shoichet, 2001; DeLong et al., 2005; Fisher et al., 1989; Kapur & Shoichet, 2004; K. Moore et al., 2006; Singh et al., 2008; X. Wang et al., 2009). Our laboratory has created linear gradients in reversibly-bound GDNF within heparinated poly(ethylene glycol) (PEG) microsphere scaffolds (Roam et al., 2014, 2010). These gradients persist for more than a week and might enhance nerve regeneration within an NGC. However, before these microsphere scaffolds can be useful for *in vivo* nerve regeneration, several functionalities, including cell-initiated degradability, inter-microsphere cross-linking, and cell adhesion, must be incorporated into the microspheres.

Recent biomaterials approaches to tissue regeneration have sought to replicate the native degradability of natural biomaterials, such as fibrin, thereby stimulating the regeneration process (Ehrbar et al., 2007; M P Lutolf & Hubbell, 2005). Peptide sequences sensitive to enzymatic cleavage have been integrated into hydrogels to this end. Matrix metalloproteinase sensitive sequences have been used in a number of biomaterial systems (M P Lutolf et al., 2003; Matthias P Lutolf et al., 2003; Miller et al., 2010; Moon et al., 2010; Patterson & Hubbell, 2010; Raeber et al., 2005; Seliktar, Zisch, Lutolf, Wrana, & Hubbell, 2004; West & Hubbell, 1999). Plasmin is a second enzyme that plays a key role in cell migration, especially during wound healing (West & Hubbell, 1999). Plasmin sensitive sequences have also been used to extensively (Gobin & West, 2002; Halstenberg, Panitch, Rizzi, Hall, & Hubbell, 2002; Jo et al., 2010; Patterson & Hubbell, 2011; Van Dijk, Van Nostrum, Hennink, Rijkers, & Liskamp, 2010; West & Hubbell, 1999). For this system, the sequence must not contain any internal lysines or cysteines in order to prevent unwanted crosslinking. The sequence GGVRNGGK is one previously used plasmin-degradable sequence that fits these constraints (Gobin & West, 2002). This sequence, modified by adding a GC to N-terminus to make it reactive to vinyl-sulfone groups, could impart plasmin degradability to these PEG microspheres.

To promote scaffold stability, it was necessary for the microspheres to cross-link to one another. To accomplish this under physiological conditions without using agents that might interact with the GDNF, other ambient proteins, or the extending nerves themselves, we sought to utilize a Click reaction (Nwe & Brechbiel, 2009). Click reactions are bioorthogonal reactions such as the Huisgen 1,3-dipolar cycloaddition between azides and alkynes, thiol-ene/yne photoadditions, and Staudinger ligation(Brummelhuis, Diehl, & Schlaad, 2008; Hoyle, Lowe, & Bowman, 2010; Iha et al., 2009; Nwe & Brechbiel, 2009; H. Y. Park, Kloxin, Scott, & Bowman, 2010). Our lab has already utilized click reactions for both microsphere formation and inter-microsphere cross-linking for

scaffold stability (Nguyen et al., 2013). Because copper, a common catalyst for these reactions, can be toxic to cells, we have focused on copper-free azide–alkyne cycloadditions, which have high conversions, fast kinetics, insensitivity to oxygen and water, stereospecificity, regiospecificity, and mild reaction conditions (Clark & Kiser, 2009; DeForest, Polizzotti, & Anseth, 2009; Deforest et al., 2010; Johnson, Baskin, Bertozzi, Koberstein, & Turro, 2008).

To allow extending nerves to attach to and subsequently grow through the scaffold, it was necessary to affix a cell adhesion protein, such as laminin, to the microspheres. Laminin, a basement membrane protein, has been shown to be important to neural system development (Swindle-Reilly et al., 2012). Laminin not only influences cell adhesion, but also neurite outgrowth and growth cone movement, and acts as a neuronal cue (Culley et al., 2001; Evans et al., 2007; Swindle-Reilly et al., 2012). Many studies have already utilized laminin in their biomaterial systems to enhance neurite outgrowth (Dodla & Bellamkonda, 2008; Jurga et al., 2011; Neal et al., 2012; Swindle-Reilly et al., 2012; X Yu et al., 1999; Xiaojun Yu, Dillon, Bellamkonda, & Ph, 1999). The cell adhesion molecules fibronectin and an RGD peptide have previously been attached to the PEG microspheres via reaction of cysteines in the molecule with vinyl-sulfone groups on the PEG, and the same chemistry was used for conjugating laminin to the microspheres herein (E. a. Scott et al., 2010).

This study seeks to combine these various functionalities into these gradient-producing PEG microsphere scaffolds for use in NGC's. As an important step towards testing this system *in vivo*, NGC's containing these scaffolds were implanted into rats, traversing a severed sciatic nerve, to assess the degradability as well as any safety issues.

# 4.3 Materials and Methods

Unless otherwise noted, all reagents were purchased from Sigma–Aldrich.

## 4.3.1 PEG Synthesis

$PEG_8$-vinylsulfone ($PEG_8$-VS) and $PEG_8$-amine were synthesized from eight-arm PEG-OH ($PEG_8$-OH; mol. Wt. 10,000; Shearwater Polymers, Huntsville, AL) as previously described (Wacker et al., 2006). PEG macromonomers were dissolved separately at 200 mg/mL in Dulbecco's phosphate buffered saline (PBS; 8 mM sodium phosphate, 2 mM potassium phosphate, 140 mM sodium chloride, 10 mM potassium chloride, pH 7.4) and sterile filtered with 0.22 μm syringe filters (Millipore).

## 4.3.2 Heparin Attachment Pre-Microsphere Formation (for high heparin microspheres)

A solution 244 mg/mL Heparin sodium salt (mol. wt. ~18,000, ~2.78 mM), 0.081 mM N-(3-Dimethylaminopropyl)-N'-ethylcarbodiimide hydrochloride (EDC), and 0.203 mM N-Hydroxy-succinimide (NHS) in MES buffer (10 mM, pH 6.0) was incubated at room temperature for 30 min. L-Cysteine (free base) was added to the activated heparin solution to make a 6:1 cysteine:heparin molar ratio and allowed to react overnight. The solution was dialyzed in 10X PBS (pH 7.4) to remove unreacted cysteine. Ellman's assays were performed to determine substitution of cysteine on heparin (44% of heparin molecules determined to have cysteine). $PEG_8$-VS was added at a 10:3 $PEG_8$-VS:cysteinated-heparin molar ratio and incubated at room temperature overnight. For microsphere formation, heparin-conjugated $PEG_8$-VS was mixed with $PEG_8$-amine in a 1:1 ratio of the two PEG types (see Figure 4.1A).

### 4.3.3 Ellman's Assay

Ellman's reagent was dissolved in 0.1 M phosphate buffer (pH 8.0) at 40 mg/mL. 0.05-0.15 μmol of cysteinated heparin was added to 3 mL of 0.1 M phosphate buffer (pH 8.0) along with 100 μL Ellman's solution. The solution was mixed and incubated at room temperature for 15 minutes. Absorbance at 412nm was measured and compared to standard to determine cysteine content.

### 4.3.4 High Heparin Microsphere Formation

Heparinated $PEG_8$-VS solutions were combined with $PEG_8$-amine solutions at a 1:1 ratio. The PEG solutions were diluted to 20 mg/mL PEG with PBS and 1.5 M sodium sulfate (in PBS) to a final sodium sulfate concentration of 0.6 M. The $PEG_8$-VS/$PEG_8$-amine solutions were then incubated above the cloud point at 70˚C for 11 minutes. Suspensions of microspheres were subsequently buffer exchanged into 8 mM sodium phosphate twice to remove the sodium sulfate by: (1) diluting the microsphere solution 3:1 with PBS and titurating, (2) centrifuging at 14,100g for 2 min, and (3) removing the supernatant. Fluorescent and phase contrast images were captured using a MICROfire (Olympus, Center Valley, PA) camera attached to an Olympus IX70 inverted microscope.

### 4.3.5 Heparin Attachment Post-Microsphere Formation

A solution of 515 mg/mL Heparin sodium salt (mol. wt. ~18,000, ~2.78 mM), 0.101 mM N-(3-Dimethylaminopropyl)-N'-ethylcarbodiimide hydrochloride (EDC), and 0.042 mM N-Hydroxy-succinimide (NHS) in MES buffer (10 mM, pH 6.0) was incubated at room temperature for 30 min. L-Cysteine (free base) was added to the activated heparin solution to make a 8.82:1 cysteine:heparin molar ratio and allowed to react overnight. The solution was dialyzed in 10X PBS (pH 7.4) to remove unreacted cysteine. Ellman's assays were performed to determine substitution of cysteine on heparin (109% of heparin molecules determined to have cysteine). The solution was diluted to 130

mg/ml heparin and stored at -20˚C. For heparination of microspheres, cysteine-conjugated heparin was added to PEG microspheres at 2.6 mg/mL and incubated overnight (see Figure 4.1B).

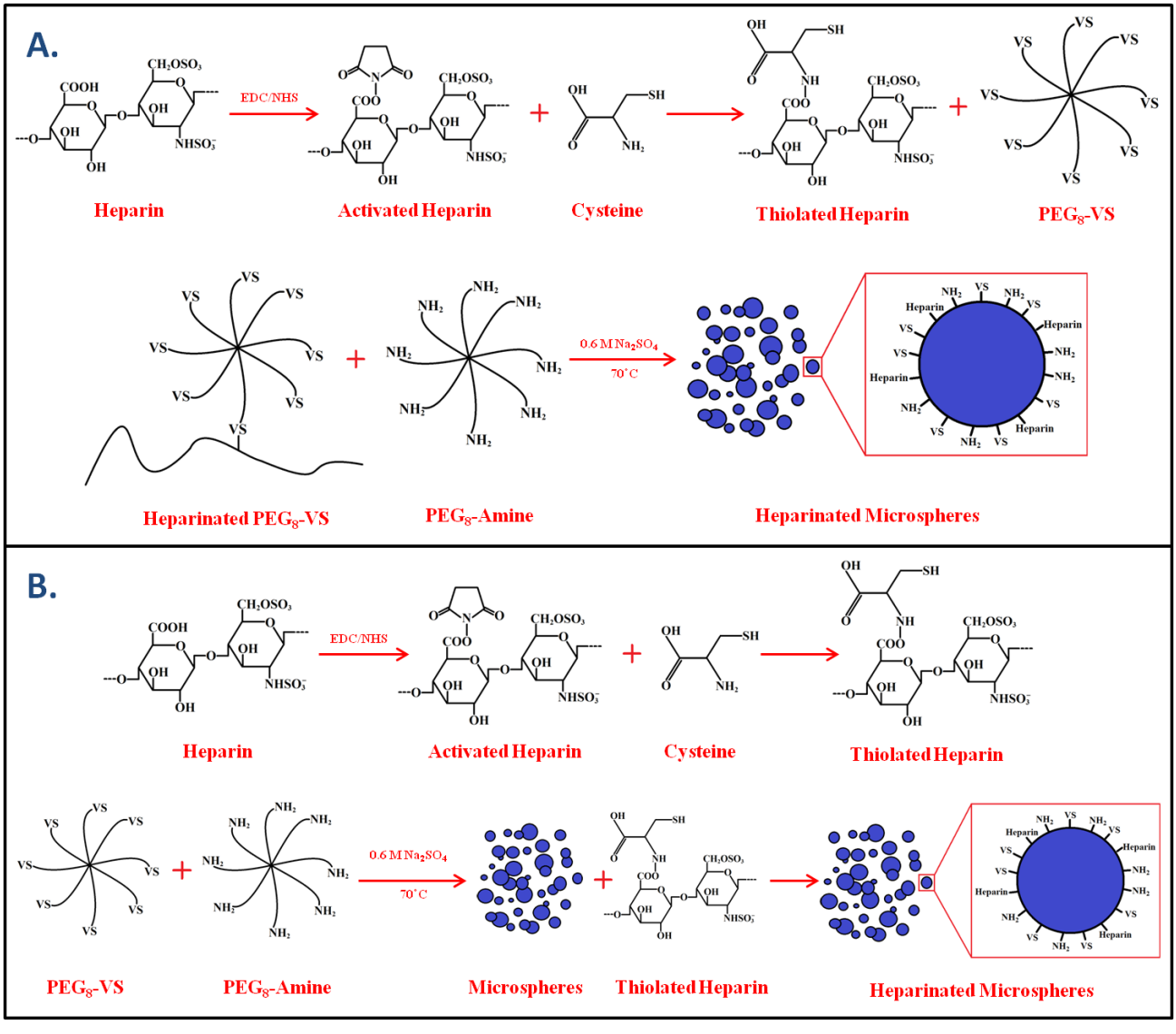


**Figure 4.1. Heparin Addition Chemistry.** A. Heparin addition chemistry for high heparin microspheres utilizing a "thiolated heparin" intermediate (maximum microsphere heparin content, 21% by weight). B. Post-microsphere formation heparin addition chemistry (maximum microsphere heparin content, 4% by weight).

## 4.3.6 Heparin Labeling

To confirm post-microsphere formation attachment, cysteinated heparin was labeled with Dylight-488 NHS-ester (Pierce). Cysteinated heparin (130 mg/mL) and Dylight-488 (560 μg/mL) in

PBS was incubated overnight at room temperature. The labeled heparin solution was dialyzed using Slide-A-Lyzer MINI Dialysis Units (Thermo Scientific, Rockford, IL, 3500 MWCO) in PBS (pH 7.4) to remove any unbound Dylight-488. The heparin solution was then used in the heparination post-microsphere formation protocol as described above. Fluorescence of suspended microsphere solution was measured and compared to a standard curve to determine heparin content (3.97% heparin by weight).

## 4.3.7 Plasmin-Degradable PEG Synthesis

Peptide sequence GCGGVRNGGK (N-Terminal Acetylation, C-Terminal Amidation, Purity >95%, GenScript USA Inc., Piscataway, NJ) was dissolved in 0.1 M phosphate buffer at 117.9 mg/mL with $PEG_8$-VS (200 mg/mL, 78% substitution) and brought to a pH of 7.4. The solution was incubated overnight at room temperature before storage at 4˚C.

## 4.3.8 Plasmin-Degradable Microsphere Formation

$PEG_8$-VS solutions were combined with degradable $PEG_8$-VS (PEG-$(VRN)_8$) solutions at a 1:1 molar ratio and incubated at 37˚C for 1 hour. The PEG solutions were diluted to 20 mg/mL PEG with PBS and 1.5 M sodium sulfate (in PBS) to a final sodium sulfate concentration of 0.6 M. $PEG_8$-Azide/Amine or $PEG_8$-CO/Amine were added to the regular PEG solutions at a 50:1 $PEG_8$-VS/PEG-$(VRN)_8$ to Clickable PEG ratio. The $PEG_8$-VS/PEG-$(VRN)_8$ solutions were then incubated above the cloud point at 70˚C for various times. Suspensions of microspheres were subsequently buffer exchanged into 8 mM sodium phosphate twice to remove the sodium sulfate by: (1) diluting the microsphere solution 3:1 with PBS and titurating, (2) centrifuging at 14,100g for 2 min, and (3)

removing the supernatant (see Figure 4.2).

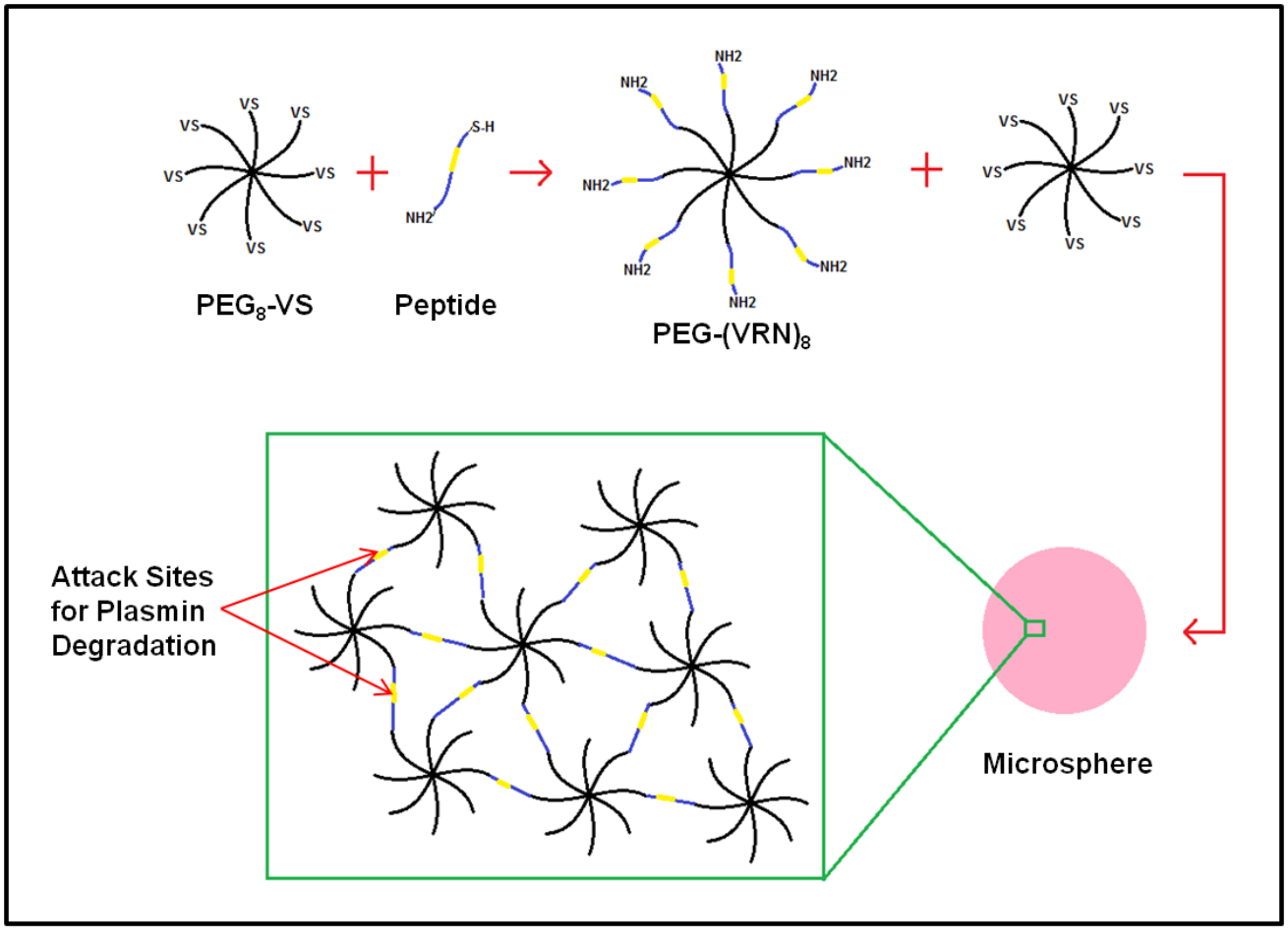


**Figure 4.2. Addition of Plasmin Degradability to Microspheres.**

## 4.3.9 $PEG_8$-Azide/Amine Synthesis

Eight arm PEG-mesylate ($PEG_8$-mesylate; mol wt 10,000) was first synthesized from four arm PEG-OH ($PEG_8$-OH; mol wt 10,000; Creative PEGWorks) by mesylating the alcohol group on $PEG_8$-OH with mesyl chloride. This was done by dissolving $PEG_8$-OH in dichloromethane (DCM), adding four equivalents of triethylamine and four equivalents of methanesulfonyl chloride while on ice, and letting it react overnight under constant stirring and nitrogen flow. After removing the salt byproduct, excess DCM was removed by using the rotovap, and the $PEG_8$-mesylate was precipitated out using cold diethyl ether. The product was dried under vacuum overnight to remove

any remaining diethyl ether. The next step was the nucleophilic azidation of the mesylate group with sodium azide. Three equivalents of sodium azide were dissolved in dimethylformamide (DMF). $PEG_8$-mesylate was then dissolved in the DMF mixture and put under nitrogen and constant stirring in a hot water bath at 60°C. The reaction was run overnight. The following day required the filtration of excess salt followed by rotovapping, diethyl ether precipitation, and drying as was done for the $PEG_8$-mesylate. The product was dissolved in a basic water solution with a pH between 9 and 12, and then extracted with DCM over anhydrous sodium sulfate ($Na_2SO_4$). A standard extraction procedure was done to extract the product into DCM. After three extractions, the Na2SO4 was filtered out and the process of rotovapping, diethyl ether precipitation, and drying was done as before. 1H NMR (300 MHz, CDCl3, δ): (s, 902.55H, PEG), 3.0 (s, 3H, -SO2CH3), 4.3 (t, 2H, -CH2OSO2-). NMR of the product confirmed that no mesylate features remained at 3.0 ppm and 4.3 ppm.

$PEG_8$-azide was dissolved in tetrahydrofuran (THF) and 1.15 equivalents of triphenylphosphine (TPP) and 30 equivalents of ultrapure H2O were added while on ice, and the reaction was allowed to go overnight under constant stirring and nitrogen flow. A large excess of H2O to TPP was needed for amine formation. Excess THF and H2O were removed by rotovapping, and $PEG_8$-Azide/Amine and triphenylphosphine oxide (TPPO) were precipitated out using cold diethyl ether. The product and byproduct were dried under vacuum overnight to remove any remaining diethyl ether. Once dry, the $PEG_8$-Azide/Amine and TPPO have cold toluene added, since TPPO is soluble in cold toluene and PEG is insoluble. The $PEG_8$-Azide/Amine was then vacuum filtered to remove the TPPO. The product then underwent the same extraction procedure with DCM that was done in the $PEG_8$-Azide synthesis. 1H NMR (300 MHz, CDCl3, δ): (s, 902.55H, PEG), 2.9 (t, 2H, -CH2CH2NH2). NMR of the product confirmed the reduction of 50 percent of azides to amines with the amine feature at 2.9 ppm.

## 4.3.10 $PEG_8$-CO/Amine Synthesis

Amines on $PEG_8$-Amine (prepared as previously described) were partially converted to cyclooctynes to form $PEG_8$-CO/Amine. $PEG_8$-Amine was dissolved in DCM in a beaker, and 0.5 equivalents of diisopropylcarbodiimide (DIPCDI) were added to a separate spherical flask with DCM while on ice and under nitrogen flow and constant stirring. Next, 0.5 equivalents of hydroxybenzotriazole (HOBt) and 0.5 equivalents of aza-dibenzocyclooctyne with a pendant carboxylic acid (DBCO-acid; Click Chemistry Tools) were added to the mixture in the flask and allowed to stir for 10 minutes. While waiting, one equivalent of N,N-diisopropylethylamine (DIPEA) was added to the dissolved $PEG_8$-Amine. Finally, this mixture was slowly added to the spherical flask, and the reaction was allowed to go for 24 hours in the ice bath, under constant stirring and nitrogen gas. Following that process, the urea precipitate was filtered out, and rotovapping, diethyl ether precipitation, and drying was performed. The product was then dissolved in distilled $H_2O$ and underwent the same extraction procedure that was done for the $PEG_8$-Amine. Further rotovapping, diethyl ether precipitation, and drying were done. 1H NMR (300 MHz, CDCl3, δ): (s, 902.55H, PEG), 5.1 (d, 2H, -CH2-). NMR of the product confirmed the conversion of 50 percent of amines to cyclooctynes ($PEG_8$-CO/Amine) with the presence of a doublet at 5.1 ppm.

## 4.3.11 Clickable Microsphere Formation

$PEG_8$- Azide/Amine and $PEG_8$-CO/Amine were separately dissolved in 0.1 M phosphate buffer (pH 7.4) at 40 mg/mL. Dylight-633 NHS-ester (Pierce) was dissolved in dimethyl formamide at 10 mg/mL and added to the clickable PEG's such that final concentrations were 33.33 mg/mL clickable PEG and 1.67 mg/mL Dylight. Solutions were incubated overnight at 25˚C to allow near complete reaction. The same methods for degradable microsphere formation were followed, except

that just prior to dilution in 0.6 M sodium sulfate, $PEG_8$-Azide/Amine and $PEG_8$-CO/Amine were added to separate batches of the degradable microsphere precursor solution at a 1:50 clickable PEG to other PEG molar ratio. The methods for degradable microsphere formation continued to be followed from this point, making sure to keep batches containing $PEG_8$-Azide/Amine and $PEG_8$-CO/Amine separate until just prior to scaffold formation. (see Figure 4.4)

## 4.3.12 Laminin Attachment

Laminin Mouse Protein, Natural (Life Technologies, Grand Island, NY) was added to microspheres at 20 μg/mL or 2-D gel 0.8 μg/mL and incubated at 37˚C overnight.

## 4.3.13 Cysteine capping of Vinyl-Sulfones

After all other functionalities were added to the microspheres (the last step being incubation with thiolated heparin and laminin) the microspheres were washed 2X and resupended in 2.5 mg/mL L-cysteine and incubated for 30 minutes at room temperature. The microspheres were then washed 3X before use.

## 4.3.14 GDNF Loading of Microspheres

Recombinant human GDNF (Peprotech, Rocky Hill, NJ) was dissolved in 8 mM sodium phosphate buffer (pH 7.4) and added to washed microspheres such that the GDNF concentration within the supernatant was 250 ng/mL (higher concentrations used for DRG experiments). The microsphere/GDNF solution was well mixed, by tituration and incubated 2 hours at 4˚C to allow diffusion of the GDNF into the microspheres. Immediately before scaffold formation, the microspheres were centrifuged at 14,100 *g*, supernatant was removed, and microspheres were resuspended in 8 mM sodium phosphate.

## 4.3.15 GDNF Labeling

Dylight-488 NHS-ester (Pierce) was dissolved in dimethyl formamide at 10 mg/mL. Recombinant human GDNF (Peprotech, Rocky Hill, NJ) was dissolved in 8 mM sodium phosphate buffer (pH 7.4). Dylight-488 was added to the solution for a final GDNF concentration of 10 μg/mL and a final Dylight-488 concentration of 50 ng/mL and incubated overnight at 2˚C. The solution was then dialyzed using Slide-A-Lyzer MINI Dialysis Units (Thermo Scientific, Rockford, IL, 3500 MWCO) in 8 mM sodium phosphate buffer (pH 7.4) to remove unbound Dylight-488.

## 4.3.16 Confirmation of Gradient Formation

The glass walls of Pasteur pipettes were passivated with PLL(375)-*g*[7]-PEG(5) (D. L. Elbert & Hubbell, 1998; Kenausis et al., 2000). The pipettes were filled with a 20 mg/mL PLL-*g*-PEG solution, incubated for 30 seconds, and washed with DI water. After sufficient drying time, the tips of the pipettes were sealed with silicone aquarium sealant (DAP Inc., Baltimore, MD). To form scaffolds, microsphere solutions loaded or unloaded with labeled GDNF were sequentially added to the pipettes that were placed in 15 mL conical vials. The microsphere solutions were centrifuged at 1000 *g* for 5 min before the next layer of microspheres (not loaded with GDNF) was added. The supernatant was then removed once more and replaced with 8 mM Sodium Phosphate.

## 4.3.17 Confocal microscopy

Fluorescence microscopy was performed with a Nikon Eclipse C1/80i confocal microscope. Microsphere gradients were imaged while still in the Pasteur pipettes with a 10X objective (NA=0.30, DIC L/N1, WD= 16.0mm). Multiple images were taken along the length of the pipette and processed using EZ-C1 3.70 FreeViewer software (Nikon Instruments Inc.) and then combined. Fluorescence in the composite photographs was analyzed with ImageJ software.

## 4.3.18 Analysis of GDNF Activity Retention

$PEG_8$-VS and $PEG_8$-Amine solutions were combined at a 1:1 ratio and diluted to 66.66 mg/mL PEG in PBS. 0.6 mL of the PEG solution was added to each well of a 24 well plate (BD Falcon, Franklin Lakes, NJ) and incubated at 37˚C for 3 days. Wells were washed 2X with 1 mL PBS before adding 0.6 mL of Laminin (0.8 μg/mL) in PBS and incubated at 37˚C overnight. GDNF (833 ng/mL 8 mM sodium phosphate buffer) was loaded into microspheres as decribed above. After incubation, microspheres were centrifuged and supernatant was removed. Microspheres were resuspended in modified neurobasal (MNB) media (Invitrogen, Carlsbad, CA) containing 0.1% BSA, 0.5 mMl-glutamine, 2.5 μMl-glutamate, 1% N2 supplement, and 1% antibiotic/antimycotic solution (ABAM) (all from Invitrogen) and quickly centrifuged again to remove free GDNF. Supernatant was removed and the microspheres were resuspended in MNB media (1 mL of media for about 0.5 mL of loaded microspheres) and incubated 2 hours at 4˚C. The microspheres were centrifuged once again and the supernatant was transferred to the 24 well plate with PEG gels (1 mL per well). Dorsal root ganglions (DRGs) were dissected from day 10 White Leghorn chicken embryos (Sunrise Farms, Catskill, NY) and placed into wells containing either microsphere MNB media or fresh MNB media (no GDNF). At 24, 48, and 72 hours, phase contrast images of the neurite extension from the DRGs were taken with the 4x objective.

## 4.3.19 Conduit Assembly

Sections of standard silicone tubing (Helix Medical, Carpinteria, CA) (1.47 mm inside diameter × 0.39 mm wall thickness) were stretched over the ends of a 1mL pipette tips (Rainin Instrument LLC, Oakland, CA) until secure with ~2 cm protruding from the ends. After autoclaving, a small amount (~3mm once inside tube) of hot glue was drawn into the tube to form a plug. Plugged tips were stored under UV to enhance sterility in a sterile cabinet. Fibrinogen solutions were prepared by

dissolving human plasminogen-free fibrinogen in deionized water at 8 mg/mL for 1 h and dialyzing vs. 4 L of Tris-buffered saline (TBS) (33 mM Tris, 8 g/L NaCl, 0.2 g/L KCl) at pH 7.4 overnight to exchange salts present in the protein solution. The resulting solution was sterilized by filtration through 5.0 and 0.22 μm syringe filters, and the final fibrinogen concentration was determined by measuring absorbance at 280 nm. Components were mixed to obtain the following final solution concentrations: 8 mg/mL fibrinogen, 2.5 mM Ca2+, and 1 NIH U/mL of thrombin. Using a 30 gauge syringe (Exel International Medical Products, St. Petersburg, FL), this solution was added inside the tube on top of the glue plug such that a 1-2 mm plug of fibrin was formed. The conduits were then incubated for 1 hour at 37˚C. The pipette tip and conduit were them placed inside a 3-D printed mold designed to allow for centrifugation of the conduit (Figure 4.12). Microspheres were then added to the pipette tip and centrifuged to form a scaffold within the tube as previously described. The conduit was then cut away from the tip. The supernatant was removed from the microspheres, and another small fibrin plug was added on top of the microspheres. The glue plug was then excised by cutting the silicone tube around the plug 1 mm from the top of the plug and pulling the plug free (Figure 4.12 A and B).

## 4.3.20 Experimental Animals

Adult male Lewis rats (Charles River Laboratories, Wilmington, MA), each weighing 250-300 g, were used in this study. All surgical procedures and perioperative care was performed in accordance with the National Institutes of Health guidelines, where NIH guidelines (or for non-U.S. residents similar national regulations) for the care and use of laboratory animals (NIH Publication #85-23 Rev. 1985) have been observed.

## 4.3.21 Operative Procedure

All surgical procedures were performed using aseptic technique and microsurgical dissection and repairs. Under subcutaneous anesthesia with ketamine (75 mg kg−1) and medetomidine (0.5 mg kg−1), the hind leg of the rat was prepped with betadine and alcohol and the sciatic nerve was exposed through a dorsolateral gluteal muscle splitting incision. A 5 mm nerve segment was excised proximal to the trifurcation of the sciatic nerve and a nerve guidance conduit was sutured to the transected proximal and distal stumps, incorporating 1 mm of nerve on either end. Two 9-0 nylon interrupted microepineurial sutures were used to secure the conduit at each end, resulting in a 13mm, tension-free gap between the proximal and distal stumps. Wounds were irrigated with saline, dried and closed with a running 5-0 vicryl suture in muscle fascia, and then interrupted 4-0 nylon skin sutures.

Anesthesia in experimental animals was then reversed with a subcutaneous injection of atipamezole HCl (1 mg kg−1) (Pfizer Animal Health, Exton, PA), and the animals recovered in a warm environment. After recovery, the animals were returned to the housing facility.

At 1, 2, 4, 6, and 8 weeks postoperatively, all animals were re-anesthetized and the conduits/nerves were exposed by reopening the prior muscle splitting incision. At this time, light and fluorescence photomicrographs were taken, and the wounds were re-closed as before. At 8 weeks, the nerve conduit and a 5 mm portion of native nerve both proximally and distally were harvested. The specimens were marked with a proximal suture and stored in 3% glutaraldehyde in 0.1 M phosphate buffer (pH 7.2) at 4 °C until immunohistochemical analysis was performed (Hunter et al., 2007). Following the tissue harvest, the animals were then euthanized with intraperitoneal injection of Euthasol (150 mg kg−1) (Delmarva Laboratories, Des Moines, IA).

### 4.3.22 Immunohistochemistry

Cross-sections of the delivery system and nerve were cut at 10 μm on a cryostat and stained with S100: 1:500, rabbit anti S100 (Dako) primary antibody followed by S100: goat anti rabbit 555 secondary antibody and NF-160 mouse polyclonal primary antibody followed by NF-160: 488 goat anti mouse secondary antibody using standard immunohistochemistry techniques.

## 4.4 Results and Discussion

### 4.4.1 New Heparin Binding Strategies

For this system we devised a new heparin attachment chemistry that would alleviate limits (controllability, maximum amount of heparin) of the previous method of incorporating heparin into the microspheres. In this new chemistry, seen in Figure 4.1A, an intermediate step of bonding cysteine to the heparin through a previously used EDC/NHS activation of carboxyl groups was added to the previous method (Roam et al., 2014). The amount of cysteine conjugated to the heparin was evaluated by an Elman's assay for the thiols on the cysteines. This "thiolated heparin" could then be reacted with $PEG_8$-VS in a much more controlled manner than the previous reaction of activated carboxyl groups with $PEG_8$-Amine. This allowed for the creation of microspheres with as much as 21 percent by weight heparin content. However, these higher amounts of heparin inhibited, and sometimes even prevented, the formation of microspheres. Microspheres that were successfully formed in these high heparin conditions were much smaller (less than 1 micron in diameter, Figure 4.3) than the previously fabricated microspheres (5-20 microns). Upon introduction of further functionalities such as plasmin degradability, microspheres no longer formed at all unless the heparin content was dropped to levels below that which the previous chemistry afforded (less than 3 percent by weight). Thus, we altered this method, creating the thiolated heparin as before, but only bonding

the thiolated heparin to $PEG_8$-VS after the microspheres had been formed (see Figure 4.1B). To assess the heparin content of these microspheres, we labeled the heparin with Dylight-488. By comparing the fluorescence of a solution of suspended heparinated microspheres to standard curve of fluorescent thiolated heparin, the heparin content of the microspheres was determined to be at least 4 percent by weight. This heparin content was greater than the previous system yielded, while having the added benefit of not interfering with the microsphere formation process.

## 4.4.2 Addition of Degradable Peptide

To allow nerves extending axons to degrade the scaffold as they move through, a plasmin sensitive peptide sequence, GCGGVRNGGK, was incorporated into the microspheres (see Figure 4.2). The cysteine contains a thiol group that will react quickly with vinyl sulfone groups on the $PEG_8$-VS. By combining the peptide with $PEG_8$-VS such that there was one peptide chain for every vinyl sulfone group and giving ample time for complete reaction (overnight, room temperature), we created an eight arm PEG with arms vulnerable to attack by plasmin. We refer to this as PEG-$(VRN)_8$. The lysine the C-terminal end of the peptide causes each arm to end in an amine group, effectively producing a plasmin-degradable $PEG_8$-Amine. Regular $PEG_8$-Amine could now be substituted with this PEG-$(VRN)_8$ in the microsphere formation process. The N-terminus and C-terminus of the peptide were acetylated and amidated, respectively, to prevent any unwanted cross-linking during microsphere formation. To form microspheres, PEG-$(VRN)_8$ and $PEG_8$-VS was added at a 1:1 molar ratio and reacted as the previous $PEG_8$-Amine/ $PEG_8$-VS constituents were. The production of microspheres was hindered somewhat by the introduction of the PEG-$(VRN)_8$, however, due possibly to electrostatic interactions of the peptide. In order for microspheres to form, a pre-incubation step had to be added, in which the undiluted PEG-$(VRN)_8$/$PEG_8$-VS mixture (200 mg/mL PEG) was incubated for at least 30 minutes (1 hour in final protocol) at 37˚C before dilution

in 0.6 M sodium sulfate and subsequent incubation at 70˚C. All cross-linkages between PEG molecules in the microspheres that were formed were vulnerable to attack by plasmin.

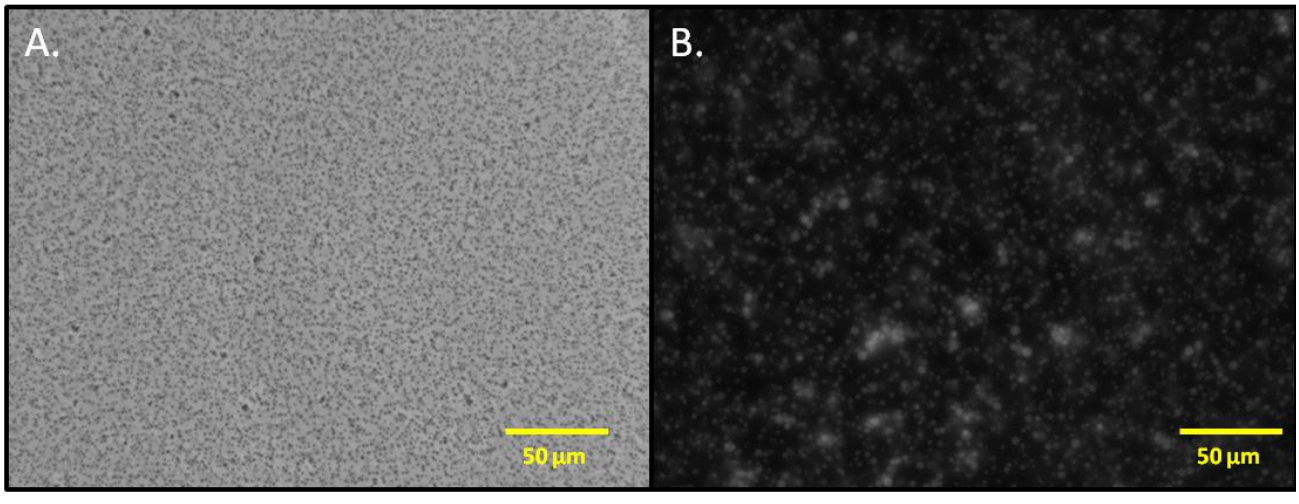


**Figure 4.3. High Heparin Microspheres.** A. Phase-contrast image of high heparin microspheres (400X). B. Flourescent image of Dylight-488 Labeled heparin in high heparin micropheres (400X).

## 4.4.3 Addition of Click Crosslink

PEG microspheres with click cross-linking functionality have already been developed by our laboratory (Nguyen et al., 2013). $PEG_8$-Amine fifty percent substituted with either azide or cyclooctyne groups ($PEG_8$-Azide/Amine and $PEG_8$-CO/Amine) was added to the microspheres during formation producing batches of microspheres decorated with either azide or cyclooctyne groups. Upon the mixing of these two types of microspheres together, the click agents reacted to one another, covalently coupling the microspheres together into a scaffold (see Figure 4.4). However, with the addition of the clickable PEG agents (more specifically, the non-degradable PEG-Amine arms within the clickable PEG agents), the individual microspheres became so thoroughly cross-linked that they lost their ability to be degraded. By lowering the amount of clickable-PEG added to the microspheres we were able to recover plasmin degradability, but only once the clickable PEG content was lowered to a 50:1 non-clickable PEG:clickable PEG molar ratio. At this level, enhanced

scaffold stability due to click cross-linking was not observed until after the scaffold had sat for a considerable amount of time (more than a few days). When implanted *in vivo* these scaffold will be in place for weeks, so the click cross-linking functionality will still be advantageous for the system.

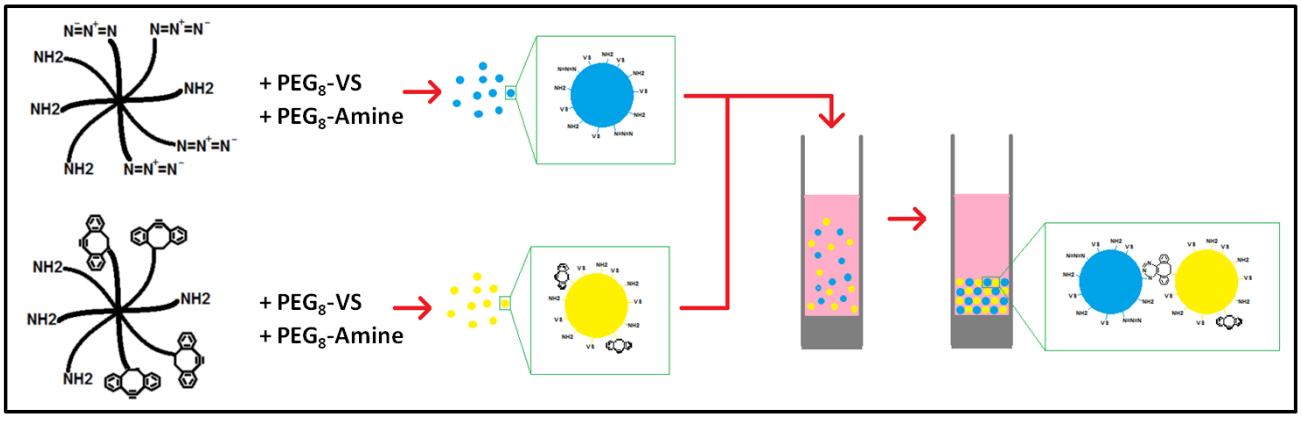


**Figure 4.4. Scaffold formation by Click Cross-Linking.** $PEG_8$-Azide/Amine and $PEG_8$-CO/Amine were added to the microspheres during formation producing batches of microspheres decorated with either azide or cyclooctyne groups. Upon mixing and centrifugation, the click agents will react to one another, covalently coupling the microspheres into a scaffold.

## 4.4.4 Addition of Laminin

The final functionality added to the microspheres was cell adhesion, via laminin. To confirm laminin would encourage neuronal growth on the microspheres, 2D gels made from $PEG_8$-Amine/ $PEG_8$-VS (6.66% in PBS) were incubated overnight with laminin (20 µg/mL) at 37˚C, allowing the cysteines on laminin to react with free vinyl-sulfones, covalently coupling the laminin to the gels. DRG's were cultured on the gels with laminin and compared to those without (Figure 4.5). DRG's cultured on PEG gels without laminin showed no growth at all. DRG's cultured on PEG gels with laminin extended neurites. This confirmed that laminin did attach to the gel and subsequently encouraged neurite growth. To attach laminin to the microspheres, laminin (20 µg/mL) was added to

previously formed and washed microspheres and incubated overnight at room temperature.

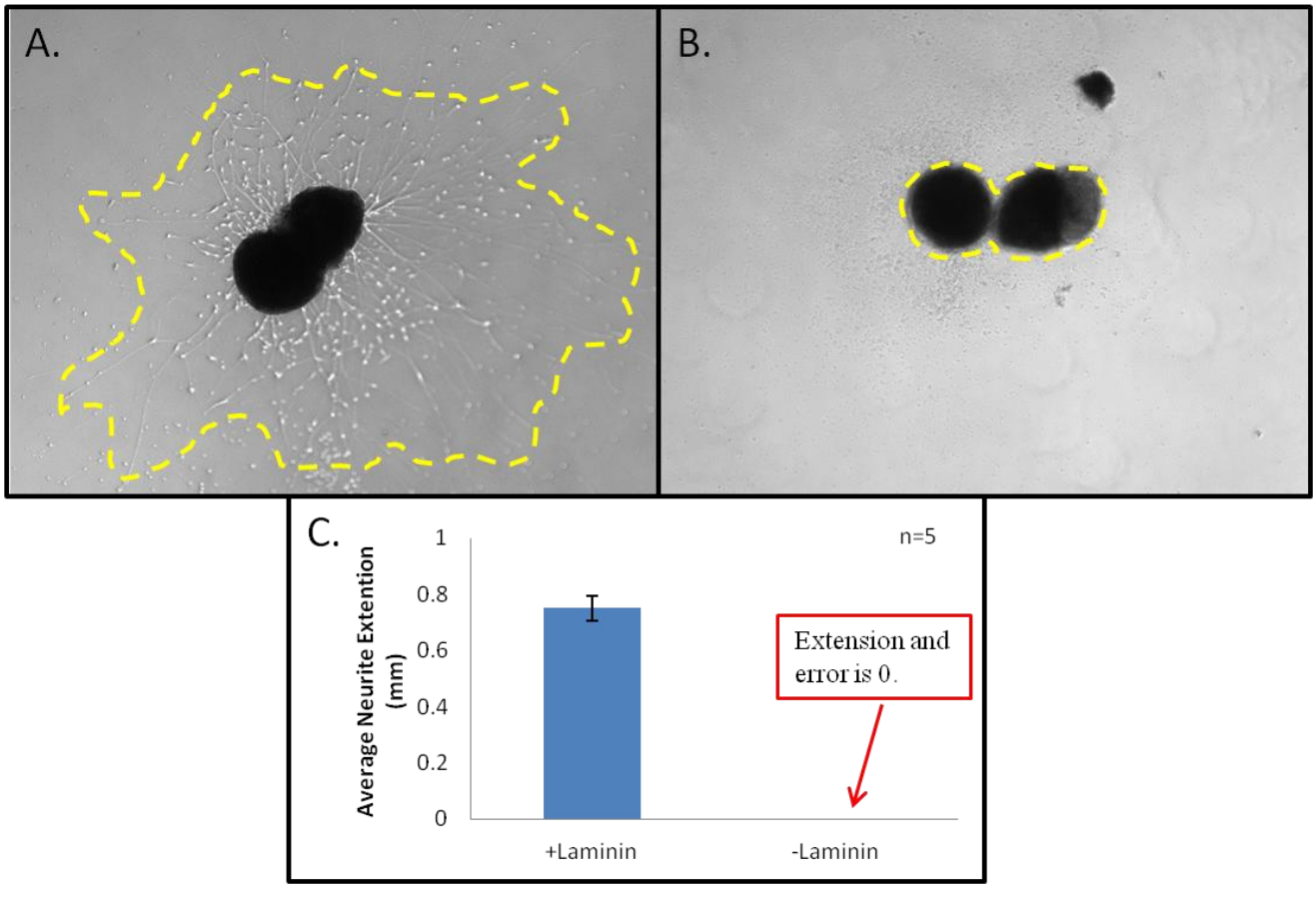


**Figure 4.5. Laminin Promoted Growth of DRG's.** A. Sample DRG growth on $PEG_8$-VS/$PEG_8$-Amine gels decorated with Laminin at 20 µg/mL. (2 days after seeding, dashes show border of growth). B. DRG growth on $PEG_8$-VS/$PEG_8$-Amine gel without Laminin. (2 days after seeding, dashes show border of growth). C. Average neurite extension in mm for DRG's cultured on PEG gel with and without laminin (n=5). No growth was observed in DRG's without Laminin present. Error bars shown but equal to 0 for the –Laminin condition.

## 4.4.5 Combining Functionalities

Once the addition of each functionality (heparin binding, plasmin degradability, click cross-linking, and cell adhesion) was demonstrated, they needed to be combined into one material. The final method for fabricating these fully functionalized microspheres is shown in Figure 4.6. This protocol is the combination of all the processes discussed above ending in a 30 minute incubation in 2.5 mg/mL cysteine to cap any remaining free vinyl-sulfone groups. This prevented any unwanted

covalent binding of the microspheres to GDNF (or any other proteins) as demonstrated in our previous work (Roam et al., 2014).

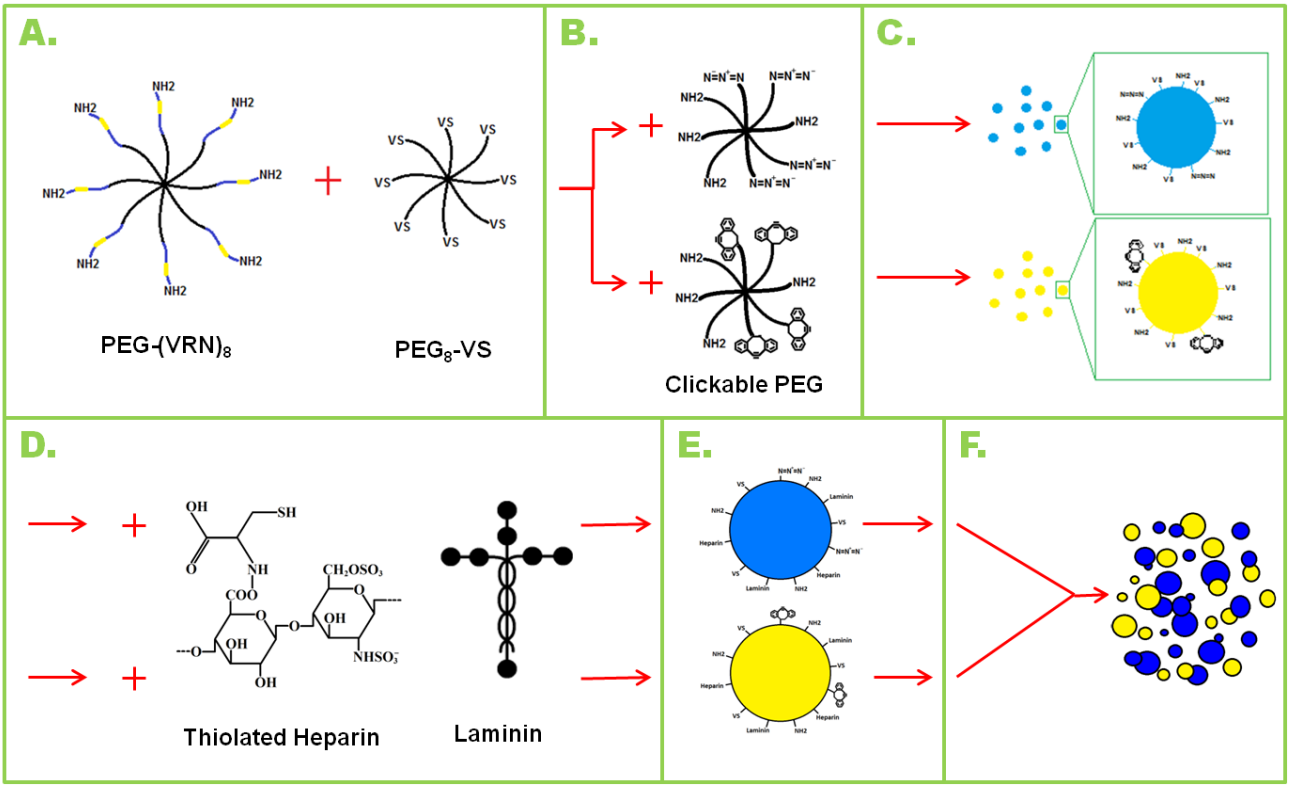


**Figure 4.6. Final Functionalized Microsphere Procedure.** A. PEG-$(VRN)_8$ and $PEG_8$-VS (200 mg/mL) were combined at 1:1 molar ratio and incubated at 37˚C for 1 hour. B. $PEG_8$-Azide/Amine and $PEG_8$-CO/Amine were added at 1:50 (Click:Regular) ratio. C. PEG was diluted to 20 mg/mL in 0.6 M $Na_2SO_4$ and incubated 8 min at 70˚C. D. Microspheres were washed 3X in PBS and Thiolated Heparin (2.6 mg/mL) and Laminin (20 µg/mL) was added to suspended µspheres and incubated at 25˚C overnight. Microspheres were washed 2X in low salt buffer. E. Cysteine (2.5 mg/mL) was added and incubated 25˚C for 30 minutes to cap remaining vinyl-sulfones. Microspheres were washed 2X in low salt buffer. F. The two microsphere types were combined prior to growth factor loading and/or scaffold formation.

While the lowered amount of click agents (50:1 Non-clickable PEG to clickable PEG) allowed for the retention of plasmin degradability, this is only with a particular range of microsphere formation incubation times. For less than 8 minutes at 70˚C, no microspheres formed. For more than 10 minutes, the microspheres cross-linked to a degree that eliminated their ability to be degraded by plasmin. Within this range, 8-10 minutes incubation at 70˚C, the rate of degradation was tunable. To

test the rate of degradability, microspheres were suspended in 1 unit/mL of plasmin and incubated at 37˚C, with samples taken periodically to be viewed by phase-contrast microscopy. Microspheres incubated less than 10 minutes degraded in a matter of hours while 10 minute incubated microspheres degraded over the course of days or not at all. A graph and representative samples of this process are shown in Figure 4.7. Those microspheres with above a 10 minute incubation time did not degrade completely and are not shown. In this experiment, each of the suspended microspheres was attacked from all directions by the plasmin in which they were suspended. *In vivo*, however, nerves releasing plasmin must eat away at the microsphere scaffold from one direction, which will take a considerably greater amount of time. Thus, this should represent an accelerated model compared to *in vivo*.

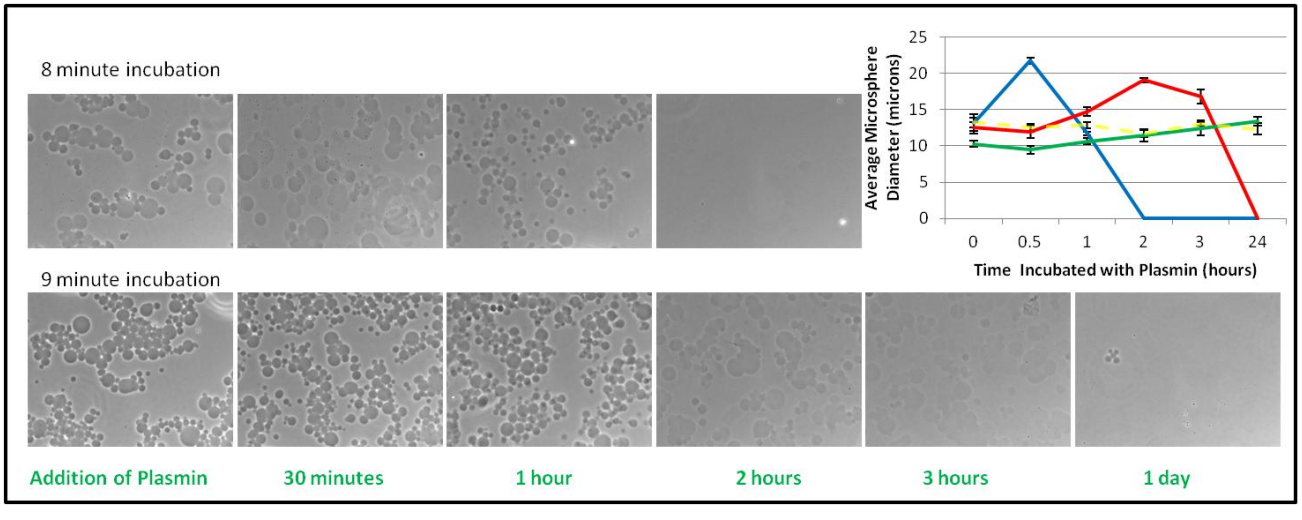


**Figure 4.7. Degradation of Microspheres Suspended in Plasmin.** Microspheres formed by incubation at 70˚C for 8 and 9 minutes were suspended in 1 unit/mL of plasmin and incubated at 37˚C to view the rate of degradation. Graph shows average microsphere diameter over time for 8 (blue), 9 (red), and 10 minute (green) formation times. Yellow dashes indicate 9 minute microspheres in control conditions (no plasmin). (n=4)

With the protocol for the fabrication of these microspheres finalized, we needed to confirm that the linear concentration gradient making capability discussed in the previous study was retained (Roam et al., 2014). A two-tier initial step gradient in GDNF was created as before, using these fully

functionalized microspheres. The release profile of the GDNF visualized by confocal microscopy is shown in Figure 4.8. The initial step gradient formed a very linear shape after one day. This shows that the fully functionalized microspheres form linear concentration gradients in GDNF just as the previous microspheres did.

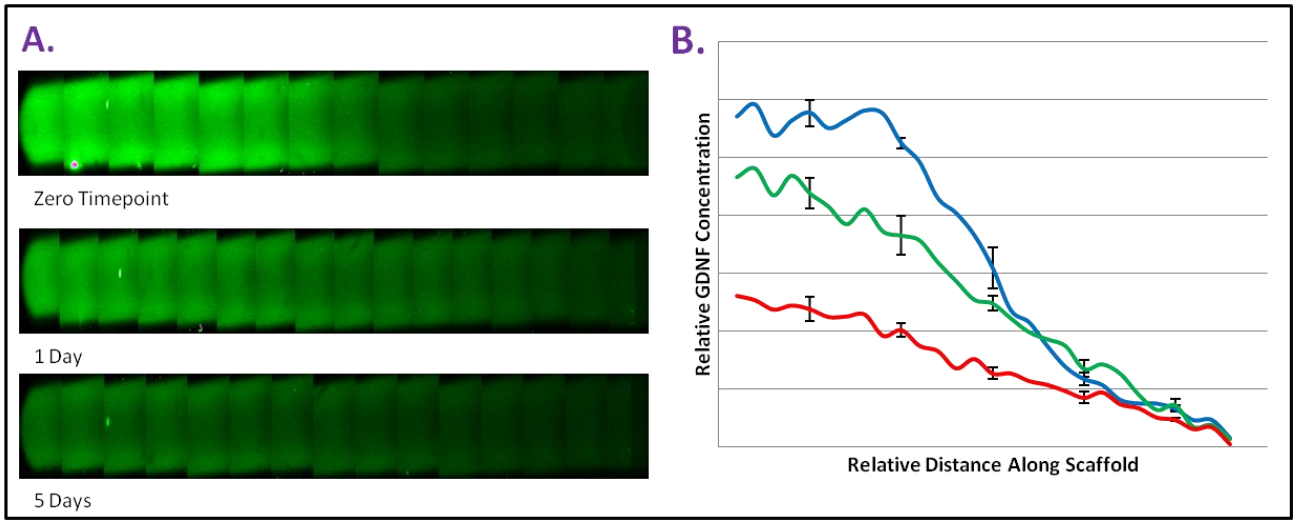


**Figure 4.8. Confirmation of GDNF Gradients.** 2-tier initial profile, "low salt" (8 mM sodium phosphate) release of Dylight-488 labeled GDNF from fully functionalized microsphere scaffold. (A) Composite photograph of fluorescence (GDNF) in scaffold at the zero time point, one day, and 5 days. (B) Graphical depiction of fluorescence (GDNF concentration) vs. the distance in the scaffold for the four time points: zero (blue), 1 day (green), and 5 days (red). n=4 sample error bars shown.

## 4.4.6 Confirmation of GDNF Activity Retention

The next important question to answer was whether or not GDNF loaded into the microspheres and subsequently released retains its biological activity. DRG's cultured on 2D $PEG_8$-Amine/ $PEG_8$-VS with laminin extended neurites regardless of inclusion of GDNF (100 ng/mL) in the media. Differences between DRG's given media with and without GDNF were only observed once the concentration of laminin incubated on the gel was drastically decreased. It was only within a range of 0.5-1.0 μg/mL laminin incubated on the PEG gel that a difference was observed. DRG's in both conditions (with and without GDNF) extended neurites on these gels initially. However, after 2-

3 days (length of time varied between experimental sets) there would come a point when DRG's without GDNF would lose their extensions or even detach from the gel completely while the DRG's given GDNF (100 ng/mL) in the media would stay attached and healthy looking. With this knowledge, an experiment was performed comparing the growth of DRG's given media without GDNF to those given media with GDNF released from the fully functionalized microspheres.

Fully functionalized microspheres were fabricated and washed thoroughly. Enough microspheres were made such that there would be approximately 0.5 mL of microspheres for every 1 mL of cell culture media needed. The microspheres were then suspended in low salt buffer (8 mM sodium phosphate, pH 7.4) with a high concentration of GDNF (833 ng/mL for the experiment shown in Figures 4.9 and 4.10) and incubated for 2 hours at 4˚C to give the GDNF plenty of time to thoroughly infiltrate the microspheres. The microspheres were then centrifuged and the supernatant was removed. The microspheres were next loaded with GDNF. However, some GDNF that had not interacted with the microspheres could be in the media between microspheres. To remove this GDNF as well as avoid dilution of the cell culture media, the microspheres were resuspended in MNB media and quickly (less than 10 seconds later) centrifuged again. The supernatant was removed and the microspheres were once again resuspended in fresh MNB media. The suspended microspheres were incubated for 2 hours at 4˚C to thoroughly release the loaded GDNF into the MNB media. The microspheres were then centrifuged and the supernatant (MNB media with released GDNF, no microspheres) was transferred to a 24 well plate containing the PEG gel (with 0.8 μg/mL incubated laminin) and DRG's. Phase-contrast photo micrographs were taken at 1, 2, and 3 days. The results are shown in Figures 4.9 and 4.10. In Figure 4.9, examples of DRG's cultured with microsphere released GDNF and without GDNF are shown. At day 3, DRG's without GDNF have lost their extensions and detached from the gel completely while the DRG's given GDNF from microspheres stayed attached and healthy looking. In fact, all DRG's not given GDNF had no extensions at this

time point. Figure 4.10 shows the average neurite extension of the two conditions. The conditions look similar for the first two days, but at day 3, the average extension of the DRG's given microsphere released GDNF was maintained from day 2 while the average extension of the DRG's without GDNF falls to zero. This drastic difference in the two cases shows that the GDNF loaded into and subsequently released from the microspheres retains its biological activity.

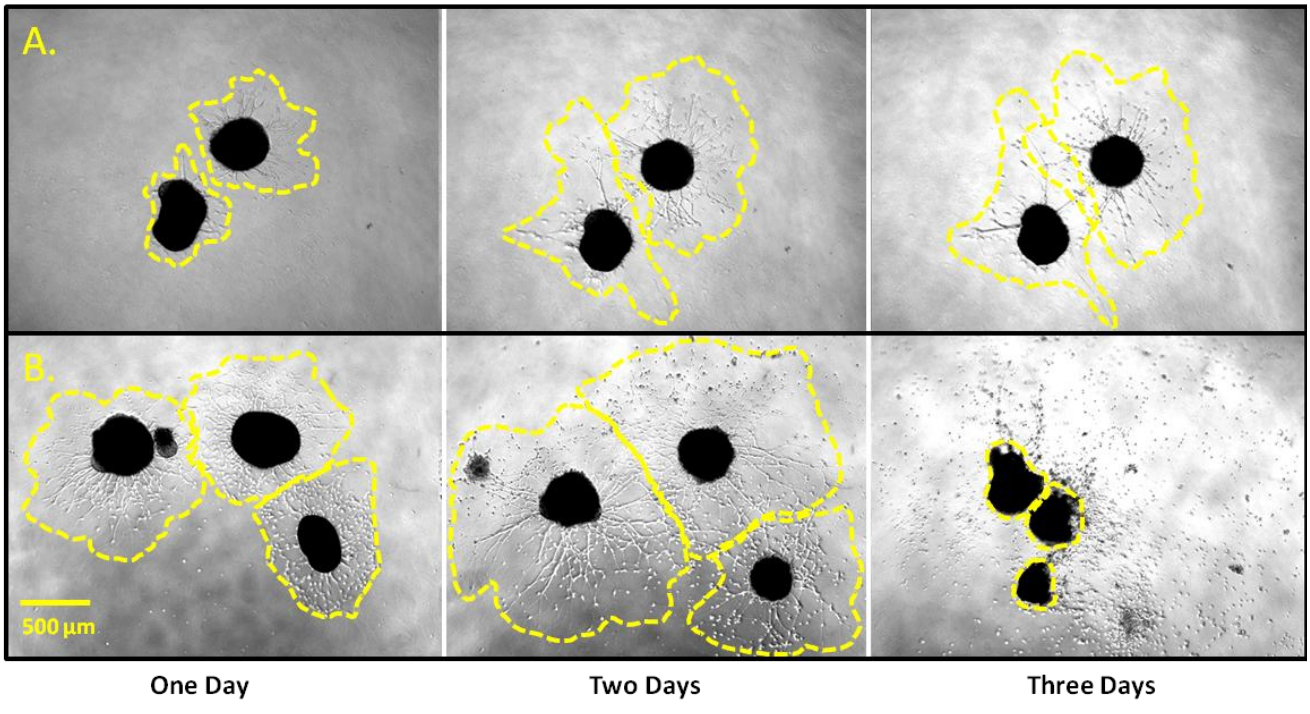


**Figure 4.9. GNDF Activity Retention - DRG growth.** DRG growth on PEG gels with 0.8 µg/mL incubated laminin for one, two, and three days under two media conditions: A. Microsphere released GDNF (833 ng/mL incubation) in MNB media, B. MNB media with no GDNF. Yellow dashes indicate boundary of neurite extension.

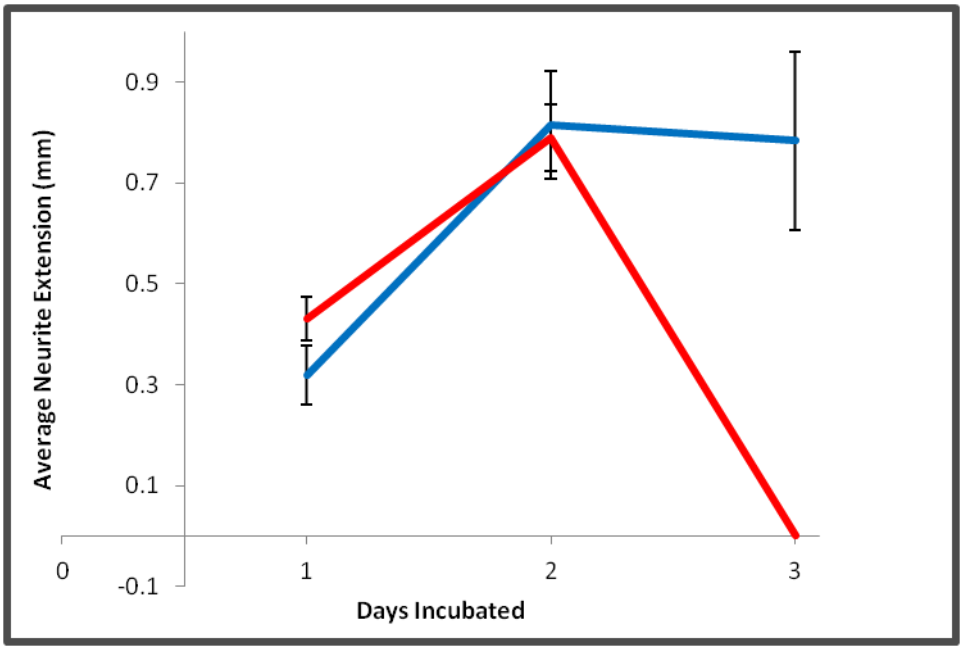


**Figure 4.10. GNDF Activity Retention – Neurite extension analysis.** Average neurite extension for DRG's grown on PEG gels with 0.8 µg/mL incubated with laminin for one, two, and three days under two media conditions: Microsphere released GDNF (833 ng/mL incubation) in MNB media (Blue line, n=8), MNB media with no GDNF (Red line, n=14).
*Note: All DRG's in the control condition (No GDNF) had no extensions at Day 3. Error bars shown, but error was zero due to uniformity of samples at this condition.

## 4.4.7 Conduit Formation and *In Vivo* Testing

Lastly we transferred our gradient containing scaffolds made up of fully functionalized microspheres to NGC's. Microspheres, incubated for various times to alter the degradation rate, were centrifuged into silicone tubes by stretching the tube securely over a 1 mL pipette tip and stopping up the end with hot glue (Figure 4.11A). This was enclosed within a custom made 3D printed mold, which could be inserted into a 15 mL conical vial for centrifugation (Figure 4.11 B-D). The NGC was then excised from the pipette tip, and the glue plug was removed (4.12 A and B). Though handling and implantation of the conduits was possible, it was also difficult, and the scaffold within was easily destabilized. Fibrin plugs were formed at either end of the scaffold to increase stabilization (fibrin plugs can be seen in Figure 4.12 A and B). Conduits were then ready for *in vivo* testing.

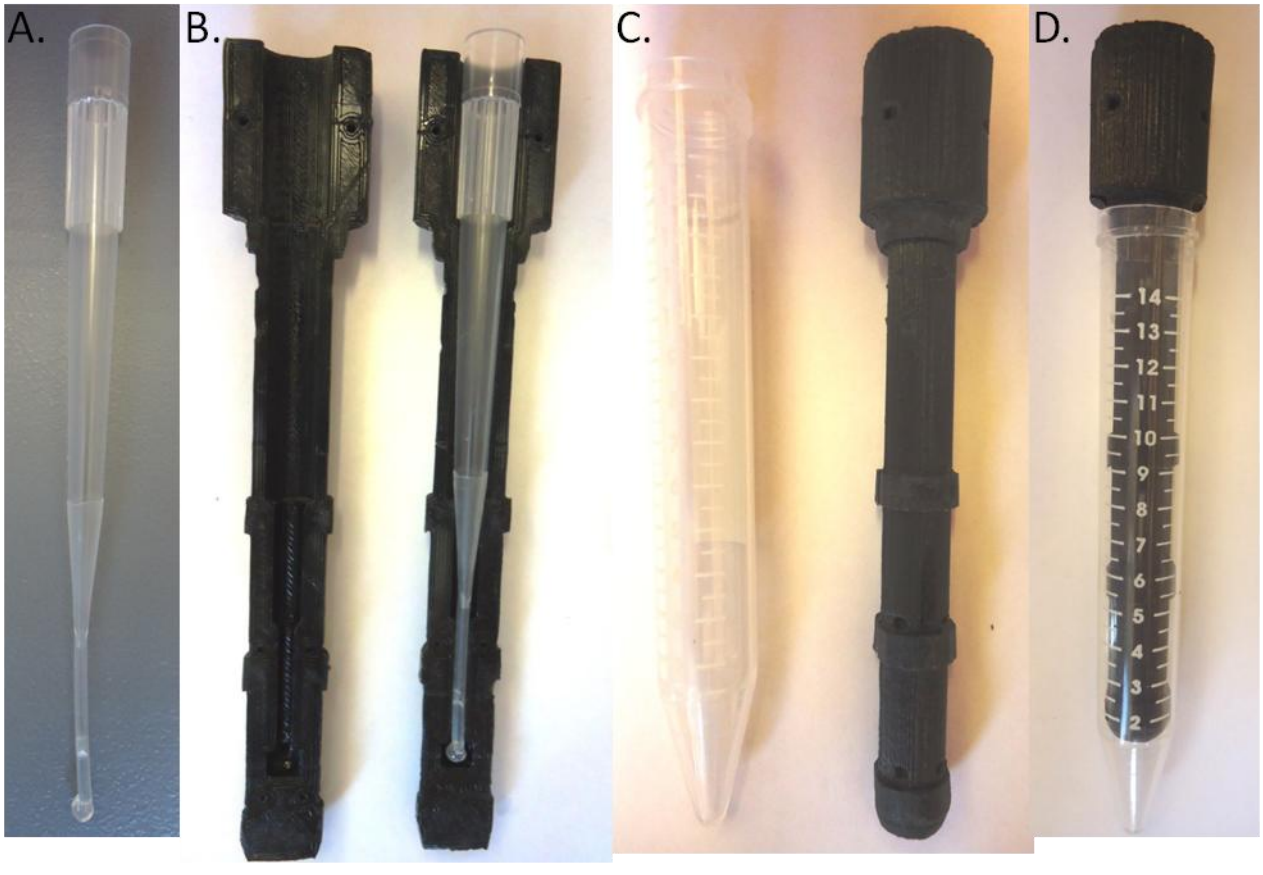


**Figure 4.11. Conduit Fabrication Apparatus.** A. 1 mL pipette tip inserted securely into silicone tube plugged with glue. B. and C. 3D printed mold fit tightly around pipette tip and silicone tube, holding the tube in shape during centrifugation. D. Apparatus is inserted into 15 mL conical vial and is ready for centrifugation of microspheres into a scaffold.

Conduits containing scaffolds labeled with Dylight-633 for easy visualization were implanted into rats traversing a severed sciatic nerve (Figure 4.12 C and D). Scaffolds were 10 mm in length, with some variation, and with the fibrin plugs the total length of nerve gap was ~13 mm. Fluorescence images indicating the presence of non-degraded scaffold were compared to light images of the conduit to determine the percentage of each scaffold's length that had degraded at each time point (Table 1).

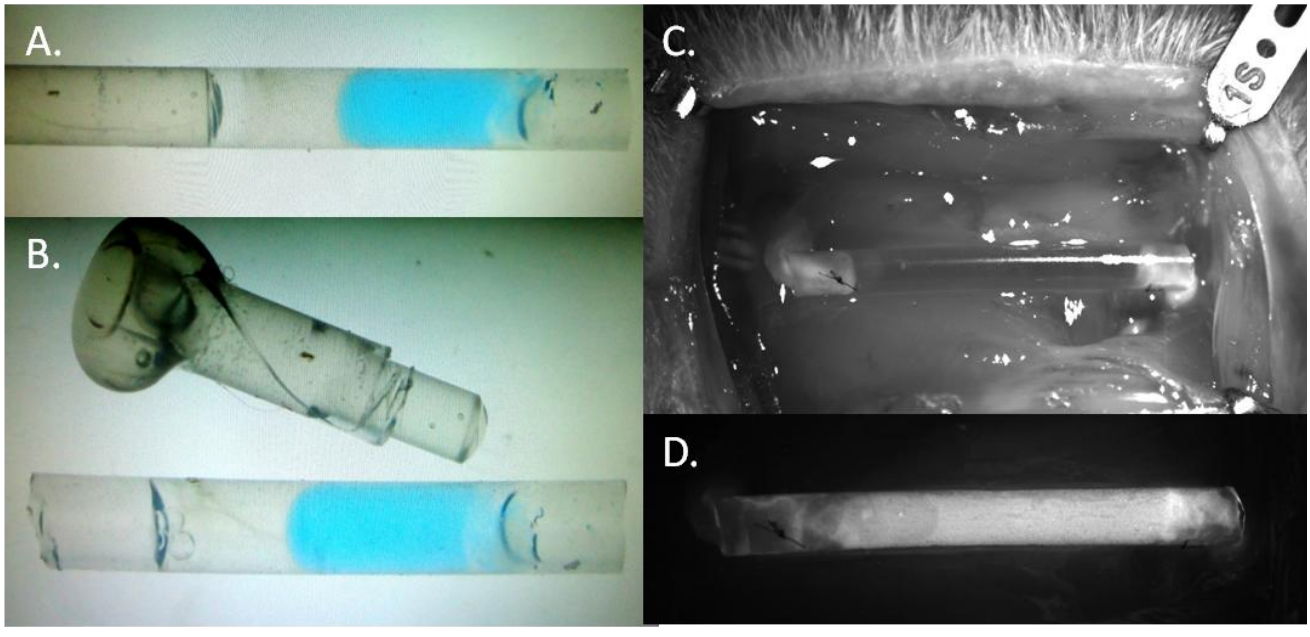


**Figure 4.12. Fully Formed Conduit Implantation.** A. Fully formed conduit: microsphere scaffold (blue) flanked by two fibrin plugs, glue plug still intact. B. Fully formed conduit, glue plug excised. Ready for implantation. C. Implanted conduit traversing the severed sciatic nerve in a rat . D. Fluorescent photograph of implanted conduit seen in C. (microspheres labeled with Dylight-633)

Most scaffolds composed of microspheres incubated less than 10 minutes were largely degraded after 1 week. There was no appreciable change in the length of the scaffolds composed of microspheres incubated 10 minutes, and were classified as 0% percent degraded, though small perturbations on the images would suggest that some degradation was occurring. This was also true for two of the conduits with microspheres incubated below 10 minutes, 9 minute #2 and 9.5 minute #3. What is most interesting about these two cases, in addition to their seeming inability to degrade like their counterparts created under the same conditions, is that it was these two conduits that resulted in tissue regeneration across the nerve gap. Immunohistochemistry for the 3 cases of regenerated tissue is shown in Figure 4.13. In the 9 and 9.5 minutes cases, a porous structure can be seen where the scaffold did not degrade. DAPI showed cell growth throughout the tissue in all cases and S100 staining indicates the strong presence of Schwann cells in the porous regions. Staining for neurofilaments (NF-160) was weak and did not indicate the presence of neurons. In the conduits that

did incur an appreciable amount of degradation over their length, some differences were observed in their rates of degradation. The conduits formed from 8 minute microspheres, especially, degraded faster than the other cases with longer incubation times. The conduits were also evaluated for any observed foreign body response, infection, or necrosis. None of the conduits were observed to elicit any of these negative biological reactions.

| µSphere Incubation Time | | % of Scaffold Degraded | | | | | Observed Foreign Body Response? | Observed Infection? | Observed Necrosis? | Regenerated Tissue? |
|---|---|---|---|---|---|---|---|---|---|---|
| | | 7 Days *in vivo* | 14 Days *in vivo* | 32 Days *in vivo* | 41 Days *in vivo* | 55 Days *in vivo* | | | | |
| 8 Minutes | #1 | 86% | 89% | 96% | 98% | 99% | No | No | No | No |
| | #2 | 89% | 91% | 96% | 99% | 99% | No | No | No | No |
| | #3 | 99% | 100% | 100% | 100% | 100% | No | No | No | Yes |
| 9 Minutes | #1 | 0% | 76% | 81% | 83% | 83% | No | No | No | No |
| | #2 | 0% | 0% | 0% | 2% | 4% | No | No | No | Yes |
| | #3 | 45% | 57% | 74% | 76% | 84% | No | No | No | No |
| 9.5 Minutes | #1 | 80% | 80% | 98% | 97% | 98% | No | No | No | No |
| | #2 | 77% | 89% | 91% | 92% | 99% | No | No | No | No |
| | #3 | 0% | 0% | 0% | 0% | 0% | No | No | No | Yes |
| 10 Minutes | #1 | 0% | 0% | 0% | 0% | 0% | No | No | No | No |
| | #2 | 0% | 0% | 0% | 0% | 0% | No | No | No | No |
| | #3 | 0% | 0% | 0% | 0% | 0% | No | No | No | No |

**Table 4.1. *In vivo* degradation of scaffolds.** Conduits containing fully-functionalized PEG microsphere scaffolds with gradients in GDNF were implanted in rats traversing a severed sciatic nerve. Degradation of the scaffolds was evaluated using fluorescence microscopy. Implants were evaluated for the presence of foreign body response, infection, and necrosis. The conduits were also evaluated for whether or not tissue regenerated across the gap.

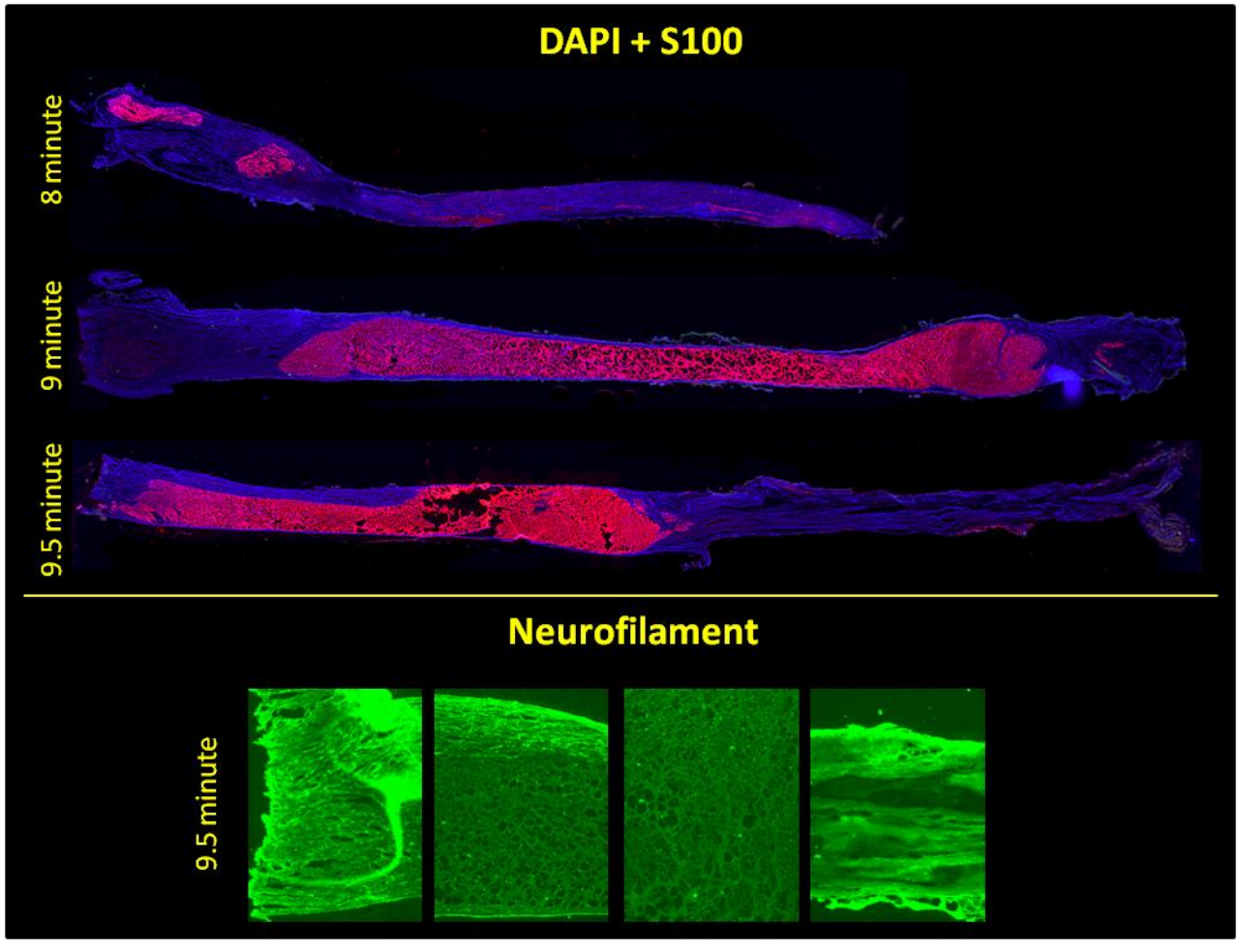


**Figure 4.13: IHC for Regenerated Tissue.** Fluorescent photomicrographs of sectioned tissue harvested from NGC's at 8 weeks. S100 (red) layered with DAPI (blue) staining over the whole length of the tissue is shown for the 3 instances of regeneration (occurring in different microsphere incubation time conditions). Sample fluorescent photomicrographs at higher magnification (100X) of tissue stained for neurofilaments (green) shown for the 9.5 minute condition.

# 4.5 Conclusions

We have developed a process for creating nerve guidance conduits containing multi-functionalized PEG microsphere scaffolds with concentration gradients in GDNF. These microspheres have been engineered with multiple functionalities. They were made capable of heparin binding, to slow and control the rate of GDNF release, using a post-microsphere formation chemistry. In order to allow nerves to invade the conduit and extend successfully to the distal stump, we made

the microspheres degradable by plasmin, with tunable rates of degradation. Click cross-linking chemistries were incorporated to add stability to the scaffold. The cell adhesion protein, laminin, was bound to the microspheres to encourage cell growth. The functionalities were combined and the GDNF concentration gradient making capability of these fully functionalized microspheres was confirmed. GDNF released from these microspheres was confirmed to be biologically active. Finally we developed methods for forming these scaffolds in silicone conduits using 3D printed plastic molds and added fibrin plugs to enhance scaffold stability. Finally, conduits were fabricated and implanted into rats traversing a severed sciatic nerve for a 55 day period to demonstrate that the conduit fabrication system was effective, that the scaffolds degrade *in vivo*, and that the conduits do not elicit any negative biological responses, such as infection or necrosis.

# Chapter 5

# Conclusions

## 5.1 Summary of Dissertation

Peripheral nerve injury is a critical area of healthcare in very real need of innovations to improve outcomes. Gradients in biological factors could prove very effective in treatments, but with current technologies creating and maintaining these gradients in biologically relevant system is problematic. This work has sought to develop a treatment for PNI using gradients in GDNF formed by modular means utilizing PEG microspheres. In the first study this end pursued the formation of scaffolds with gradients in different types of microspheres based on their relative densities (buoyancies) and attaching proteins to the microspheres, by various means, allowing them to form gradients along with the microspheres. While successful in some respects, disadvantages led to the adoption of a different method in the second study. Here, different batches of one type of microsphere (with one density) were loaded with GDNF or left empty. The different batches were used to form layers within scaffolds, creating step gradients in GDNF that, when allowed to diffuse over the course of days, produced useful linear concentration profiles in GDNF along the length of the scaffold. This method being very successful and robust, the third study sought to develop the system further by adding various biological functionalities to the microspheres, thereby making the resulting scaffolds applicable for nerve regeneration. These functionalized microspheres were used to create NGC's with linear concentration gradients in GNDF which were implanted into rats with severed sciatic nerves.

Chapter 2 presented the development of protein gradients created by harnessing density differences in batches of microspheres created under different conditions. The principle variable used to alter the density of the microspheres was the incubation time during microsphere formation. By manipulating this to the greatest degree, microspheres were fabricated with a range of densities adequate for producing scaffolds with up to three distinct (sharp transitioning) tiers or up to five tiers with smooth transitions upon centrifugation of a mixed microsphere suspension. By manipulating another variable, temperature of microsphere formation, a two tier gradient with a smooth transition from one end to the other was produced. Proteins, GDNF and BSA, were covalently bound to the microspheres such that the formation of gradients in microspheres resulted in the formation of a gradient in those proteins. Heparin, which electrostatically binds many growth factors, was conjugated to the PEG so that proteins could be reversibly bound within the microsphere scaffold, preventing possible deformation of the protein and providing any present cells easier access to it. Through the heparin decorated microspheres, gradients in protamine and GDNF were created.

Though the density mediated method of gradient making had many merits, difficulties led to the pursuit of a new method in Chapter 3. It was found that the higher density microspheres rejected the GDNF to some extent, most likely do the high amounts of intra-microsphere cross-linking, which prevented swelling and caused the microspheres to become impenetrable by the GDNF. Since the lowest density microspheres, having the lowest cross-linking, would allow the highest infusion of GDNF, it was decided that strategy sequentially centrifuging microspheres of the same density (the lowest density possible) but with various concentrations of GDNF would be employed. The downside of this strategy, implicitly, was that only sharp transition, step gradients could be made, allowing diffusion of the GDNF to produce more complex and useful gradients over time. The concentration profiles of GDNF in these scaffolds were monitored over time, in some cases 12 days. Surprisingly, a simple two tier initial step gradient produced a very linear profile after only 1 day and

maintained that profile out to twelve days. Models based on Fickian diffusion mechanics were used to produce predictions of these profiles. Again quite surprisingly, the experimental profiles proved much more linear than their predicted counterparts in many cases. Though the simple two tier model produced the best results, multi-tier formations were also fabricated to show the robustness of the technique. The heparin content of the microspheres was also altered to produce a step gradient in heparin, yielding various effects.

With the success of the two tier, sequentially made gradient in GDNF, it was decided to modify the system to enhance biological relevance, shown in chapter 4. Functionalities such as cell initiated degradability, inter-microsphere cross-linking, and cell adhesion would be needed if the scaffold was guide extending nerves. Before adding any new functionalities to the microspheres, issues with the heparin attachment method needed to be addressed. The chemistries used in chapters 2 and 3 did not allow for a very high rate of heparin incorporation. A new chemistry implementing an intermediate cysteine addition step was developed, yielding microspheres with up to 21 percent by weight heparin content, the highest of these being very small, even nano-scale. As with the previous chemistry, however, there was an issue with the heparin interfering with microsphere formation. Upon the addition of other functionalities, such as cell initiated degradability, the microspheres would not form unless the heparin content was lowered to around the same levels as the previous chemistry. Thus, the chemistry was further modified such that the heparin would be added post microsphere formation. Cell initiated degradability was added via the incorporation of a plasmin degradable peptide into the microspheres. Click chemistries were also integrated into the microspheres to enhance the stability of the scaffold, though with markedly less effect. Attachment of laminin allowed for cell adhesion. The functionalities were combined, the gradient making capability was confirmed, and GDNF released from the microsphere was established to have retained its biological activity. Scaffolds made up of the functionalized microspheres were formed in silicone tubes by using

custom printed 3D plastic molds. Fibrin plugs were used to stabilize the scaffolds containing gradients in GDNF before implantation into rats, traversing a severed sciatic nerve, showing that the scaffolds degrade in vivo, incur no negative biological effects, such as infection or necrosis, and in some cases regenerate nerve tissue.

## 5.2 Future Directions

The future for this method of fabricating NGC's with gradients in neurotrophic factors through modular formation of scaffolds with PEG microspheres is quite promising. In its current iteration, the method presented in chapter 4 should be tested in the rat sciatic nerve model more extensively. Studies seeking to bridge shorter, less aggressive nerve gaps (less than 10 mm) should be explored to get more consistent regeneration before moving on to longer gaps. After refinement and success in longer gaps, models with larger diameter nerves should also be considered, eventually scaling up to treatment defects applicable to humans. One could envision a future commercially available kit with which these NGC's containing gradients in GDNF can be produced by a hospital lab, ready for direct implantation into patients with peripheral nerve injury.

There are opportunities for improvement within the system that should be explored. Most notably, the Click cross-linking functionally could be drastically improved upon, possibly eliminating the need to stabilize the scaffold with fibrin plugs in the conduit. More of the Click agents will need to be incorporated into the microspheres or, at least, conjugated to them in a more efficient manner, decorating the outside of the microspheres rather than dispersing them throughout. The amount of Click agents was limited in this system mainly due to the intra-microsphere cross-linking it caused, hindering or even eliminating the plasmin degradability (which is crucial). One way to mitigate this

cross-linking is to change the clickable PEG molecule from an 8-arm structure to a 4-arm or linear structure. A linear PEG, especially, would completely eliminate the ability of the Click agents to coss-link the individual microspheres further, though they would provide fewer Clickable groups for inter-microsphere cross-linking. Currently, the Clickable PEG conjugates within the microspheres via reaction of amine groups on the Clickable PEG with vinyl sulfone groups on $PEG_8$-VS. This Micheal-type addition reaction will only occur efficiently under conditions found during microsphere fabrication. Clickable PEG with thiol groups rather than amine groups could be useful because thiols react much more readily with vinyl sulfone groups, allowing for incorporation of Click agents at any point in the process, even post-microsphere formation.

Adding the Click cross-linking functionality post microsphere formation would have a number of benefits. Because the Click agents would no longer be involved during microsphere formation, they would no longer affect plasmin degradability. This could yield added controllability to the kinetic of degradation as well as a wider range of degradation rates. Adding the Click cross-linking functionality post microsphere formation would also mean that the Click agents could be sequestered more on the outside of the microspheres, where they would be more available to react with their counterparts on other microspheres. This method could incur a problem, however. Since both heparin binding and cell adhesion already make use of this thiol/vinyl sulfone chemistry, the addition of yet another molecule attempting to bind in this way could very well cause interference. There are a set amount of free vinyl sulfones within the microsphere, and considering that many will be sterically unavailable for attack by these large molecules, it is possible that there would not be enough vinyl sulfones to support all 3 of these participants. As a result, the binding, and therefore the functionality, of one or more of these agents could be negatively affected. Small alterations and fine tuning could certainly resolve this, should it occur.

Other changes to improve the system could also be made. Adhesion molecules other than laminin could be employed to enhance the nerve cell adhesion. The plasmin degradable peptide used in this system could modified in a number of ways: making it longer or shorter to affect properties of the microspheres it forms, adding amino acids with different charges or specific functional groups capable some desirable reaction with the microspheres, or swapping it out for another degradable peptide entirely that has different kinetics or is sensitive to another enzyme. The initial gradient of GDNF can be changed to produce different profiles, or another neurotrophic factor such as NGF could be used in its stead. The makeup of the scaffold layers could be modified to affect how the nerve is allowed to extend through it. For instance, a thin layer of non-degradable microspheres could be placed at the distal end of conduit to slow the progress of Schwann cells that might degrade the scaffold faster than what would be desirable.

With regards to the density mediated gradient formation system discussed in Chapter 2, there are certainly opportunities to expand upon that method. While the method was not pursued further in this work due to the exclusion of GDNF in higher density microspheres as well as more general difficulties, the robustness of the system for creating seamless scaffolds with gradients in one step should not be discounted. As discussed in chapter 4, the addition of heparin to the microspheres did hinder their formation and limit controllability to some extent, which wasn't known at the time during the research conducted in chapter 2. The new post-microsphere formation addition of heparin could greatly enhance the efficacy of the density mediated system. There are also many possibilities for the creation of other types of gradients and concentration profiles. More combinations of incubation times and temperatures could be tested, and gradients in other factors such as porosity, adhesion molecules, degradability, structural stability, and heparin content could be engineered for a nearly limitless number of applications. One application discussed yet not pursued in this study was the use of the system for zero-order release of a drug or protein. An exponential initial concentration profile

could be created by the 5 tier gradient, shown in Figure 2.6, or another set-up devised in the future (or possibly through the sequential method of chapter 3), and the drug or protein allowed to release out one end of the scaffold could have a near constant flux out that end over an extended period of time. One can envision this scaffold formed inside a tube, much like the NGC's in chapter 4, and implanted subcutaneously to deliver a steady stream of drug to the patient's blood stream, or even implanted at the site of a tumor to deliver a constant, localized dose of a therapeutic agent.

Another technology developed but not explored much further in the course of this work were the small, nano-scale, high heparin microspheres seen in chapter 4. At their size, around 500 nm, they would be suitable for injection into the bloodstream without fear of them causing an obstruction. The very large content of heparin, around 21 percent by weight, would also allow these microspheres to tightly, but reversibly, bind many different heparin binding molecules, delivering them to the patient in a very controlled manner and maintaining them in the blood stream for extended periods of time. While this was not pursued in this study, due to its lack of focus in the area of nerve regeneration and gradients, these small, high heparin microspheres may have many applications in the pharmaceutical industry.

# References


Abuchowski, a., McCoy, J. R., Palczuk, N. C., van Es, T., & Davis, F. F. (1977). Effect of covalent attachment of polyethylene glycol on immunogenicity and circulating life of bovine liver catalase. *Journal of Biological Chemistry*, *252*(11), 3582–3586. Retrieved from http://www.jbc.org/content/252/11/3582.short

Abuchowski, A., van Es, T., Palczuk, N. C., & Davis, F. F. (1977). Alteration of Immunological Properties of Bovine Serum Albumin by Covalent Attachment of Polyethylene Glycol. *The Journal*, *252*(11), 3578–3581. Retrieved from http://www.jbc.org/content/252/11/3578.short

Airaksinen, M. S., & Saarma, M. (2002). The GDNF family: signalling, biological functions and therapeutic value. *Nature Reviews. Neuroscience*, *3*(5), 383–394. doi:10.1038/nrn812

Almany, L., & Seliktar, D. (2005). Biosynthetic hydrogel scaffolds made from fibrinogen and polyethylene glycol for 3D cell cultures. *Biomaterials*, *26*(15), 2467–2477. doi:10.1016/j.biomaterials.2004.06.047

Arce, V., Pollock, R. a, Philippe, J. M., Pennica, D., Henderson, C. E., & deLapeyrière, O. (1998). Synergistic effects of schwann- and muscle-derived factors on motoneuron survival involve GDNF and cardiotrophin-1 (CT-1). *The Journal of Neuroscience : The Official Journal of the Society for Neuroscience*, *18*(4), 1440–1448. Retrieved from http://www.jneurosci.org/content/18/4/1440.short

Archibald, S. J., Shefner, J., Krarup, C., & Madison, R. D. (1995). Monkey median nerve repaired by nerve graft or collagen nerve guide tube. *The Journal of Neuroscience : The Official Journal of the Society for Neuroscience*, *15*(5), 4109–4123. Retrieved from http://www.jneurosci.org/content/15/5/4109.short

Aubert-Pouëssel, A., Venier-Julienne, M. C., Clavreul, A., Sergent, M., Jollivet, C., Montero-Menei, C. N., … Benoit, J. P. (2004). In vitro study of GDNF release from biodegradable PLGA microspheres. *Journal of Controlled Release*, *95*(3), 463–475. doi:10.1016/j.jconrel.2003.12.012

Bailey, F., & Koleske, J. (1967). Configuration and hydrodynamic properties of the polyoxyethylene chain in solution. *Nonionic Surfactants*, 794–821.

Barras, F. M., Pasche, P., Bouche, N., Aebischer, P., & Zurn, A. D. (2002). Glial cell line-derived neurotrophic factor released by synthetic guidance channels promotes facial nerve regeneration in the rat. *Journal of Neuroscience Research*, *70*(6), 746–755. doi:10.1002/jnr.10434

Beazley, W. C., Milek, M. a, & Reiss, B. H. (1984). Results of nerve grafting in severe soft tissue injuries. *Clinical Orthopaedics and Related Research*, (188), 208–212. Retrieved from http://www.ncbi.nlm.nih.gov/pubmed/6467717

Bennett, D. L., Michael, G. J., Ramachandran, N., Munson, J. B., Averill, S., Yan, Q., … Priestley, J. V. (1998). A distinct subgroup of small DRG cells express GDNF receptor components and GDNF is protective for these neurons after nerve injury. *The Journal of Neuroscience : The Official Journal of the Society for Neuroscience*, *18*(8), 3059–3072. Retrieved from http://www.jneurosci.org/content/18/8/3059.short

Boland, T., Xu, T., Damon, B., & Cui, X. (2006). Application of inkjet printing to tissue engineering. *Biotechnology Journal*. doi:10.1002/biot.200600081

Borschel, G. H., Wood, M. D., Kim, H., Kemp, S. W. P., Szynkaruk, M., Phua, P., … Gordon, T. (2012). Glial-derived neurotrophic factor (GDNF) delivered from microspheres enhances peripheral nerve regeneration after delayed nerve repair. *Journal of the American College of Surgeons*, *215*(3), S90. doi:10.1016/j.jamcollsurg.2012.06.241

Boucher, T. J., Okuse, K., Bennett, D. L., Munson, J. B., Wood, J. N., & McMahon, S. B. (2000). Potent analgesic effects of GDNF in neuropathic pain states. *Science (New York, N.Y.)*, *290*(5489), 124–127. doi:10.1126/science.290.5489.124

Brash, J. L., & Uniyal, S. (1979). Dependence of albumin-fibrinogen simple and competitive adsorption on surface properties of biomaterials. *Journal of Polymer Science: Polymer Symposia*, *66*(1), 377–389. doi:10.1002/polc.5070660135

Brattain, K. (2012). *Analysis of the Peripheral Nerve Repair Market in The United States*. Minneapolis, MN.

Brenner, M. J., Dvali, L., Hunter, D. a, Myckatyn, T. M., & Mackinnon, S. E. (2007). Motor neuron regeneration through end-to-side repairs is a function of donor nerve axotomy. *Plastic and Reconstructive Surgery*, *120*(1), 215–223. doi:10.1097/01.prs.0000264094.06272.67

Brenner, M. J., Hess, J. R., Myckatyn, T. M., Hayashi, A., Hunter, D. a, & Mackinnon, S. E. (2006). Repair of motor nerve gaps with sensory nerve inhibits regeneration in rats. *The Laryngoscope*, *116*(9), 1685–1692. doi:10.1097/01.mlg.0000229469.31749.91

Bruder, J. M., Lee, A. P., & Hoffman-Kim, D. (2007). Biomimetic materials replicating Schwann cell topography enhance neuronal adhesion and neurite alignment in vitro. *Journal of Biomaterials Science. Polymer Edition*, *18*(8), 967–982. doi:10.1163/156856207781494412

Brummelhuis, N. Ten, Diehl, C., & Schlaad, H. (2008). Thiol-Ene modification of 1,2-polybutadiene using UV light or sunlight. *Macromolecules*, *41*(24), 9946–9947. doi:10.1021/ma802047w

Burchenal, J. E. B., Deible, C. R., Deglau, T. E., Russell, a. J., Beckman, E. J., & Wagner, W. R. (2002). Polyethylene glycol diisocyanate decreases platelet deposition after balloon injury of rabbit femoral arteries. *Journal of Thrombosis and Thrombolysis*, *13*(1), 27–33. doi:10.1023/A:1015364024487

Burnett, M. G., & Zager, E. L. (2004). Pathophysiology of peripheral nerve injury: a brief review. *Neurosurgical Focus*, *16*(5), E1. doi:10.3171/foc.2004.16.5.2

Cajal, S. R. (1995). *Histology of the Nervous System of Man and Vertebrates*. Oxford Univ. Press, New York.

Campbell, P. G., Miller, E. D., Fisher, G. W., Walker, L. M., & Weiss, L. E. (2005). Engineered spatial patterns of FGF-2 immobilized on fibrin direct cell organization. *Biomaterials*, *26*(33), 6762–6770. doi:10.1016/j.biomaterials.2005.04.032

Cao, J., Sun, C., Zhao, H., Xiao, Z., Chen, B., Gao, J., … Dai, J. (2011). The use of laminin modified linear ordered collagen scaffolds loaded with laminin-binding ciliary neurotrophic factor for sciatic nerve regeneration in rats. *Biomaterials*, *32*(16), 3939–3948. doi:10.1016/j.biomaterials.2011.02.020

Cao, J., Xiao, Z., Jin, W., Chen, B., Meng, D., Ding, W., … Dai, J. (2013). Induction of rat facial nerve regeneration by functional collagen scaffolds. *Biomaterials*, *34*(4), 1302–1310. doi:10.1016/j.biomaterials.2012.10.031

Cao, X., & Shoichet, M. S. (2001). Defining the concentration gradient of nerve growth factor for guided neurite outgrowth. *Neuroscience*, *103*(3), 831–840. doi:10.1016/S0306-4522(01)00029-X

Catrina, S., Gander, B., & Madduri, S. (2013). Nerve conduit scaffolds for discrete delivery of two neurotrophic factors. *European Journal of Pharmaceutics and Biopharmaceutics*, *85*(1), 139–142. doi:10.1016/j.ejpb.2013.03.030

Chen, J., Chu, Y. F., Chen, J. M., & Li, B. C. (2010). Synergistic effects of NGF, CNTF and GDNF on functional recovery following sciatic nerve injury in rats. *Advances in Medical Sciences*, *55*(1), 32–42. doi:10.2478/v10039-010-0020-9

Chew, S. Y., Mi, R., Hoke, A., & Leong, K. W. (2007). Aligned protein-polymer composite fibers enhance nerve regeneration: A potential tissue-engineering platform. *Advanced Functional Materials*, *17*(8), 1288–1296. doi:10.1002/adfm.200600441

Chiu, D. T., Janecka, I., Krizek, T. J., Wolff, M., & Lovelace, R. E. (1982). Autogenous vein graft as a conduit for nerve regeneration. *Surgery*, *91*(2), 226–233. doi:10.1097/00006534-198305000-00106

Chiu, D. T., & Strauch, B. (1990). A prospective clinical evaluation of autogenous vein grafts used as a nerve conduit for distal sensory nerve defects of 3 cm or less. *Plastic and Reconstructive Surgery*, *86*(5), 928–934. doi:10.1097/00006534-199011000-00015

Cho, Y. Il, Choi, J. S., Jeong, S. Y., & Yoo, H. S. (2010). Nerve growth factor (NGF)-conjugated electrospun nanostructures with topographical cues for neuronal differentiation of mesenchymal stem cells. *Acta Biomaterialia*, *6*(12), 4725–4733. doi:10.1016/j.actbio.2010.06.019

Chu, T. H., Wang, L., Guo, a., Chan, V. W. K., Wong, C. W. M., & Wu, W. (2012). GDNF-treated acellular nerve graft promotes motoneuron axon regeneration after implantation into cervical root avulsed spinal cord. *Neuropathology and Applied Neurobiology*, *38*(7), 681–695. doi:10.1111/j.1365-2990.2012.01253.x

Chung, S., Sudo, R., Mack, P. J., Wan, C.-R., Vickerman, V., & Kamm, R. D. (2009). Cell migration into scaffolds under co-culture conditions in a microfluidic platform. *Lab on a Chip*, *9*(2), 269–275. doi:10.1039/b807585a

Ciardelli, G., & Chiono, V. (2006). Materials for peripheral nerve regeneration. *Macromolecular Bioscience*, *6*(1), 13–26. doi:10.1002/mabi.200500151

Clark, M., & Kiser, P. (2009). In situ crosslinked hydrogels formed using Cu(I)-free Huisgen cycloaddition reaction. *Polymer International*, *58*(10), 1190–1195. doi:10.1002/pi.2650

Clavreul, A., Sindji, L., Aubert-Pouëssel, A., Benoît, J. P., Menei, P., & Montero-Menei, C. N. (2006). Effect of GDNF-releasing biodegradable microspheres on the function and the survival of intrastriatal fetal ventral mesencephalic cell grafts. *European Journal of Pharmaceutics and Biopharmaceutics*, *63*(2), 221–228. doi:10.1016/j.ejpb.2005.11.006

Cosson, S., Kobel, S. a., & Lutolf, M. P. (2009). Capturing complex protein gradients on biomimetic hydrogels for cell-based assays. *Advanced Functional Materials*, *19*(21), 3411–3419. doi:10.1002/adfm.200900968

Crank J. (1975). *The mathematics of diffusion* . Clarendon Press, Oxford .

Cullen, D. K., Tang-Schomer, M. D., Struzyna, L. a., Patel, A. R., Johnson, V. E., Wolf, J. a., & Smith, D. H. (2012). Microtissue Engineered Constructs with Living Axons for Targeted Nervous System Reconstruction. *Tissue Engineering Part A*, *18*(21-22), 120817094501006. doi:10.1089/ten.tea.2011.0534

Culley, B., Murphy, J., Babaie, J., Nguyen, D., Pagel, A., Rousselle, P., & Clegg, D. O. (2001). Laminin-5 promotes neurite outgrowth from central and peripheral chick embryonic neurons. *Neuroscience Letters*, *301*(2), 83–86. doi:10.1016/S0304-3940(01)01615-9

Daly, W. T., Yao, L., Abu-rub, M. T., O'Connell, C., Zeugolis, D. I., Windebank, A. J., & Pandit, A. S. (2012). The effect of intraluminal contact mediated guidance signals on axonal mismatch during peripheral nerve repair. *Biomaterials*, *33*(28), 6660–6671. doi:10.1016/j.biomaterials.2012.06.002

Davidenko, N., Gibb, T., Schuster, C., Best, S. M., Campbell, J. J., Watson, C. J., & Cameron, R. E. (2012). Biomimetic collagen scaffolds with anisotropic pore architecture. *Acta Biomaterialia*, *8*(2), 667–676. doi:10.1016/j.actbio.2011.09.033

De Winter, F., Hoyng, S., Tannemaat, M., Eggers, R., Mason, M., Malessy, M., & Verhaagen, J. (2013). Gene therapy approaches to enhance regeneration of the injured peripheral nerve. *European Journal of Pharmacology*, *719*(1-3), 145–152. doi:10.1016/j.ejphar.2013.04.057

DeForest, C. a, Polizzotti, B. D., & Anseth, K. S. (2009). Sequential click reactions for synthesizing and patterning three-dimensional cell microenvironments. *Nature Materials*, *8*(8), 659–664. doi:10.1038/nmat2473

Deforest, C. a., Sims, E. a., & Anseth, K. S. (2010). Peptide-functionalized click hydrogels with independently tunable mechanics and chemical functionality for 3D cell culture. *Chemistry of Materials*, *22*(16), 4783–4790. doi:10.1021/cm101391y

Dellon, a L., & Mackinnon, S. E. (1988). An alternative to the classical nerve graft for the management of the short nerve gap. *Plastic and Reconstructive Surgery*, *82*(5), 849–856. doi:10.1097/00006534-198811000-00020

DeLong, S. a., Moon, J. J., & West, J. L. (2005). Covalently immobilized gradients of bFGF on hydrogel scaffolds for directed cell migration. *Biomaterials*, *26*(16), 3227–3234. doi:10.1016/j.biomaterials.2004.09.021

Demir, A., Simsek, T., Acar, M., Aktaş, A., Vlamings, R., Ayyıldız, M., … Kaplan, S. (2014). Comparison between flexible collagen and vein conduits used for size-discrepant nerve repair: an experimental study in rats. *Journal of Reconstructive Microsurgery*, *30*(5), 329–34. doi:10.1055/s-0033-1356551

Dodla, M. C., & Bellamkonda, R. V. (2008). Differences between the effect of anisotropic and isotropic laminin and nerve growth factor presenting scaffolds on nerve regeneration across long peripheral nerve gaps. *Biomaterials*, *29*(1), 33–46. doi:10.1016/j.biomaterials.2007.08.045

Dodla, M. C., & Bellamkonda, R. V. (2006). Anisotropic scaffolds facilitate enhanced neurite extension in vitro. *Journal of Biomedical Materials Research - Part A*, *78*(2), 213–221. doi:10.1002/jbm.a.30747

Dormer, N. H., Singh, M., Wang, L., Berkland, C. J., & Detamore, M. S. (2010). Osteochondral interface tissue engineering using macroscopic gradients of bioactive signals. *Annals of Biomedical Engineering*, *38*(6), 2167–2182. doi:10.1007/s10439-010-0028-0

Drury, J. L., & Mooney, D. J. (2003). Hydrogels for tissue engineering: Scaffold design variables and applications. *Biomaterials*, *24*(24), 4337–4351. doi:10.1016/S0142-9612(03)00340-5

Du, Y., Lo, E., Ali, S., & Khademhosseini, A. (2008). Directed assembly of cell-laden microgels for fabrication of 3D tissue constructs. *Proceedings of the National Academy of Sciences of the United States of America*, *105*(28), 9522–9527. doi:10.1073/pnas.0801866105

Edalat, F., Sheu, I., Manoucheri, S., & Khademhosseini, A. (2012). Material strategies for creating artificial cell-instructive niches. *Current Opinion in Biotechnology*, *23*(5), 820–825. doi:10.1016/j.copbio.2012.05.007

Eggers, R., de Winter, F., Hoyng, S. a., Roet, K. C. D., Ehlert, E. M., Malessy, M. J. a, … Tannemaat, M. R. (2013). Lentiviral Vector-Mediated Gradients of GDNF in the Injured Peripheral Nerve: Effects on Nerve Coil Formation, Schwann Cell Maturation and Myelination. *PLoS ONE*, *8*(8), e71076. doi:10.1371/journal.pone.0071076

Eggers, R., Hendriks, W. T. J., Tannemaat, M. R., van Heerikhuize, J. J., Pool, C. W., Carlstedt, T. P., … Verhaagen, J. (2008). Neuroregenerative effects of lentiviral vector-mediated GDNF

expression in reimplanted ventral roots. *Molecular and Cellular Neuroscience*, *39*(1), 105–117. doi:10.1016/j.mcn.2008.05.018

Ehrbar, M., Rizzi, S. C., Hlushchuk, R., Djonov, V., Zisch, A. H., Hubbell, J. a., … Lutolf, M. P. (2007). Enzymatic formation of modular cell-instructive fibrin analogs for tissue engineering. *Biomaterials*, *28*(26), 3856–3866. doi:10.1016/j.biomaterials.2007.03.027

Elbert, D. L., & Hubbell, J. a. (1998). Self-assembly and steric stabilization at heterogeneous, biological surfaces using adsorbing block copolymers. *Chemistry & Biology*, *5*(3), 177–183. doi:10.1016/S1074-5521(98)90062-X

Elbert, D., Nichols, M., & Scott, E. (2013). Hydrogel microparticle formation in aqueous solvent for biomedical applications. . United States.

Eser, F., Aktekin, L., Bodur, H., & Atan, C. (2009). Etiological factors of traumatic peripheral nerve injuries. *Neurology India*, *57*(4), 434. doi:10.4103/0028-3886.55614

Evans, A. R., Euteneuer, S., Chavez, E., Mullen, L. M., Hui, E. E., Bhatia, S. N., & Ryan, A. F. (2007). Laminin and fibronectin modulate inner ear spiral ganglion neurite outgrowth in an in vitro alternate choice assay. *Developmental Neurobiology*, *67*(13), 1721–1730. doi:10.1002/dneu.20540

Fan, J., Zhang, H., He, J., Xiao, Z., Chen, B., Xiaodan, J., … Xu, R. (2011). Neural regrowth induced by PLGA nerve conduits and neurotrophin-3 in rats with complete spinal cord transection. *Journal of Biomedical Materials Research - Part B Applied Biomaterials*, *97 B*(2), 271–277. doi:10.1002/jbm.b.31810

Fine, E. G., Decosterd, I., Papaloïzos, M., Zurn, A. D., & Aebischer, P. (2002). GDNF and NGF released by synthetic guidance channels support sciatic nerve regeneration across a long gap. *European Journal of Neuroscience*, *15*(4), 589–601. doi:10.1046/j.1460-9568.2002.01892.x

Fisher, P. R., Merkl, R., & Gerisch, G. (1989). Quantitative analysis of cell motility and chemotaxis in Dictyostelium discoideum by using an image processing system and a novel chemotaxis chamber providing stationary chemical gradients. *Journal of Cell Biology*, *108*(3), 973–984. doi:10.1083/jcb.108.3.973

Flory, P. J. (1953). *Principles of Polymer Chemistry: Paul J. Flory*. Cornell University Press. Retrieved from http://books.google.com/books?hl=en&lr=&id=CQ0EbEkT5R0C&pgis=1

George, J. N. (1972). Direct assessment of platelet adhesion to glass: a study of the forces of interaction and the effects of plasma and serum factors, platelet function, and modification of the glass surface. *Blood*, *40*(6), 862–874. Retrieved from http://www.bloodjournal.org/content/40/6/862.abstract

Gobin, A. S., & West, J. L. (2002). Cell migration through defined, synthetic ECM analogs. *The FASEB Journal : Official Publication of the Federation of American Societies for Experimental Biology*, *16*(7), 751–753. doi:10.1096/fj.01-0759fje

Greiner, A., & Wendorff, J. H. (2007). Electrospinning: a fascinating method for the preparation of ultrathin fibers. *Angewandte Chemie (International Ed. in English)*, *46*(30), 5670–703. doi:10.1002/anie.200604646

Gundersen, R., & Barrett, J. (1979). Neuronal chemotaxis: chick dorsal-root axons turn toward high concentrations of nerve growth factor. *Science*, *206*(4422), 1079–1080. doi:10.1126/science.493992

Halstenberg, S., Panitch, A., Rizzi, S., Hall, H., & Hubbell, J. a. (2002). Biologically engineered protein-graft-poly(ethylene glycol) hydrogels: A cell adhesive and plasmin-degradable biosynthetic material for tissue repair. *Biomacromolecules*, *3*(4), 710–723. doi:10.1021/bm015629o

Harris, J. M., Struck, E. C., Case, M. G., Paley, M. S., Yalpani, M., Van Alstine, J. M., & Brooks, D. E. (1984). Synthesis and characterization of poly(ethylene glycol) derivatives. *Journal of Polymer Science: Polymer Chemistry Edition*, *22*(2), 341–352. doi:10.1002/pol.1984.170220207

Hase, A., Saito, F., Yamada, H., Arai, K., Shimizu, T., & Matsumura, K. (2005). Characterization of glial cell line-derived neurotrophic factor family receptor alpha-1 in peripheral nerve Schwann cells. *Journal of Neurochemistry*, *95*(2), 537–543. doi:10.1111/j.1471-4159.2005.03391.x

He, J., Du, Y., Villa-Uribe, J. L., Hwang, C., Li, D., & Khademhosseini, A. (2010). Rapid generation of biologically relevant hydrogels containing long-range chemical gradients. *Advanced Functional Materials*, *20*(1), 131–137. doi:10.1002/adfm.200901311

He, L., Zhang, Y., Zeng, C., Ngiam, M., Liao, S., Quan, D., … Ramakrishna, S. (2009). Manufacture of PLGA multiple-channel conduits with precise hierarchical pore architectures and in vitro/vivo evaluation for spinal cord injury. *Tissue Engineering. Part C, Methods*, *15*(2), 243–255. doi:10.1089/ten.tec.2008.0255

Hedstrom, K. L., Murtie, J. C., Albers, K., Calcutt, N. a, & Corfas, G. (2014). Treating small fiber neuropathy by topical application of a small molecule modulator of ligand-induced GFRα/RET receptor signaling. *Proceedings of the National Academy of Sciences of the United States of America*, *111*(6), 2325–30. doi:10.1073/pnas.1308889111

Hench, L. L., & Polak, J. M. (2002). Third-generation biomedical materials. *Science (New York, N.Y.)*, *295*(5557), 1014–1017. doi:10.1126/science.1067404

Henderson, C. E., Camu, W., Mettling, C., Gouin, a, Poulsen, K., Karihaloo, M., … Armanini, M. P. (1993). Neurotrophins promote motor neuron survival and are present in embryonic limb bud. *Nature*, *363*(6426), 266–270. doi:10.1038/363266a0

Herrán, E., Ruiz-Ortega, J. Á., Aristieta, A., Igartua, M., Requejo, C., Lafuente, J. V., … Hernández, R. M. (2013). In vivo administration of VEGF- and GDNF-releasing biodegradable polymeric microspheres in a severe lesion model of Parkinson's disease. *European Journal of Pharmaceutics and Biopharmaceutics*, *85*(3 Pt B), 1183–1190. doi:10.1016/j.ejpb.2013.03.034

Heuberger, M., Drobek, T., & Spencer, N. D. (2005). Interaction forces and morphology of a protein-resistant poly(ethylene glycol) layer. *Biophysical Journal*, *88*(1), 495–504. doi:10.1529/biophysj.104.045443

Hill-West, J. L., Chowdhury, S. M., Slepian, M. J., & Hubbell, J. a. (1994). Inhibition of thrombosis and intimal thickening by in situ photopolymerization of thin hydrogel barriers. *Proceedings of the National Academy of Sciences of the United States of America*, *91*(13), 5967–5971. doi:10.1073/pnas.91.13.5967

Hoke, a, Bell, R., & Zochodne, D. W. (1998). GDNF and its receptors are upregulated in the denervated distal stump of injured sciatic nerves. *Neurology*, *50*(4), A28–A28.

Höke, a, Gordon, T., Zochodne, D. W., & Sulaiman, O. a R. (2002). A decline in glial cell-line-derived neurotrophic factor expression is associated with impaired regeneration after long-term Schwann cell denervation. *Experimental Neurology*, *173*(1), 77–85. doi:10.1006/exnr.2001.7826

Höke, A. (2006). Neuroprotection in the peripheral nervous system: rationale for more effective therapies. *Archives of Neurology*, *63*(12), 1681–1685. doi:10.1001/archneur.63.12.1681

Höke, A. (2014). Augmenting glial cell-line derived neurotrophic factor signaling to treat painful neuropathies. *Proceedings of the National Academy of Sciences of the United States of America*, *111*(6), 10–11. doi:10.1073/pnas.1324047111

Höke, A., Cheng, C., & Zochodne, D. W. (2000). Expression of glial cell line-derived neurotrophic factor family of growth factors in peripheral nerve injury in rats. *NeuroReport*, *11*(8), 1651–1654. doi:10.1097/00001756-200006050-00011

Horne, R. a, Almeida, J. P., Day, a F., & Yu, N. T. (1971). Macromolecule hydration and the effect of solutes on the cloud point of aqueous solutions of polyvinyl methyl ether: a possible model for protein denaturation and temperature control in homeothermic animals. *Journal of Colloid and Interface Science*, *35*(1), 77–84. doi:10.1016/0021-9797(71)90187-1

Howell, W. H., & Holt, E. (1918). Two new factors in blood coagulation-heparin and pro-antithrombin. *Am J Physiol*, *47*(3), 41. Retrieved from http://ajplegacy.physiology.org/content/47/3/328.short

Hoyle, C. E., Lowe, A. B., & Bowman, C. N. (2010). Thiol-click chemistry: a multifaceted toolbox for small molecule and polymer synthesis. *Chemical Society Reviews*, *39*(4), 1355–1387. doi:10.1039/b901979k

Hoyng, S. A., De Winter, F., Gnavi, S., de Boer, R., Boon, L. I., Korvers, L. M., … Verhaagen, J. (2014). A comparative morphological, electrophysiological and functional analysis of axon regeneration through peripheral nerve autografts genetically modified to overexpress BDNF, CNTF, GDNF, NGF, NT3 or VEGF. *Experimental Neurology*, *261*, 578–93. doi:10.1016/j.expneurol.2014.08.002

Hsieh, S. C., Tang, C. M., Huang, W. T., Hsieh, L. L., Lu, C. M., Chang, C. J., & Hsu, S. H. (2011). Comparison between two different methods of immobilizing NGF in poly(DL -lactic acid-co-glycolic acid) conduit for peripheral nerve regeneration by EDC/NHS/MES and genipin. *Journal of Biomedical Materials Research - Part A*, *99 A*(4), 576–585. doi:10.1002/jbm.a.33157

Hunter, D. A., Moradzadeh, A., Whitlock, E. L., Brenner, M. J., Myckatyn, T. M., Wei, C. H., … Mackinnon, S. E. (2007). Binary imaging analysis for comprehensive quantitative histomorphometry of peripheral nerve. *Journal of Neuroscience Methods*, *166*(1), 116–124. doi:10.1016/j.jneumeth.2007.06.018

Iha, R. K., Wooley, K. L., Nyström, A. M., Burked, D. J., Kade, M. J., & Hawker, C. J. (2009). Applications of orthogonal "Click" Chemistries in the synthesis of functional soft materials. *Chemical Reviews*, *109*(11), 5620–5686. doi:10.1021/cr900138t

Iwase, T., Jung, C. G., Bae, H., Zhang, M., & Soliven, B. (2005). Glial cell line-derived neurotrophic factor-induced signaling in Schwann cells. *Journal of Neurochemistry*, *94*(6), 1488–1499. doi:10.1111/j.1471-4159.2005.03290.x

Jaques, L. B. (1943). The reaction of heparin with proteins and complex bases. *The Biochemical Journal*, *37*(2), 189–195.

Jeon, S. I., Lee, J. H., Andrade, J. D., & de Gennes, P. G. (1991). Protein Surface Interactions in the Presence of Polyethylene Oxide .1. Simplified Theory. *J Colloid Interface Sci*, *142*(1), 149–158. doi:10.1016/0021-9797(91)90043-8

Jo, Y. S., Rizzi, S. C., Ehrbar, M., Weber, F. E., Hubbell, J. a., & Lutolf, M. P. (2010). Biomimetic PEG hydrogels crosslinked with minimal plasmin-sensitive tri-amino acid peptides. *Journal of Biomedical Materials Research - Part A*, *93*(3), 870–877. doi:10.1002/jbm.a.32580

Johnson, J. a, Baskin, J. M., Bertozzi, C. R., Koberstein, J. T., & Turro, N. J. (2008). Copper-free click chemistry for the in situ crosslinking of photodegradable star polymers. *Chemical Communications (Cambridge, England)*, (26), 3064–3066. doi:10.1039/b803043j

Jones, G. R., Hashim, R., & Power, D. M. (1986). A comparison of the strength of binding of antithrombin III, protamine and poly(L-lysine) to heparin samples of different anticoagulant activities. *Biochimica et Biophysica Acta*, *883*(1), 69–76. doi:10.1016/0304-4165(86)90136-4

Joung, Y. K., Bae, J. W., & Park, K. D. (2008). Controlled release of heparin-binding growth factors using heparin-containing particulate systems for tissue regeneration. *Expert Opinion on Drug Delivery*, *5*(11), 1173–1184. doi:10.1517/17425240802431811

Jurga, M., Dainiak, M. B., Sarnowska, A., Jablonska, A., Tripathi, A., Plieva, F. M., … McGuckin, C. P. (2011). The performance of laminin-containing cryogel scaffolds in neural tissue regeneration. *Biomaterials*, *32*(13), 3423–3434. doi:10.1016/j.biomaterials.2011.01.049

K. Furasawa, Y. S. K. O. K. A. K. T. (1977). Blood compatibility of polyether-polyurethanes. . *Ronbushi Kobushu , 4*.

Kapur, T. A., & Shoichet, M. S. (2004). Immobilized concentration gradients of nerve growth factor guide neurite outgrowth. *Journal of Biomedical Materials Research. Part A*, *68*(2), 235–243. doi:10.1002/jbm.a.10168

Kehoe, S., Zhang, X. F., & Boyd, D. (2012). FDA approved guidance conduits and wraps for peripheral nerve injury: A review of materials and efficacy. *Injury*, *43*(5), 553–572. doi:10.1016/j.injury.2010.12.030

Kelsey, ed., & Praemer A., N. L. . F. A. . R. D. (1997). *Upper extremity disorders: frequency, impact, and cost.* Churchill Livingstone.

Kemp, S. W. P., Syed, S., Walsh, W., Zochodne, D. W., & Midha, R. (2009). Collagen nerve conduits promote enhanced axonal regeneration, schwann cell association, and neovascularization compared to silicone conduits. *Tissue Engineering. Part A*, *15*, 1975–1988. doi:10.1089/ten.tea.2008.0338

Kenausis, G. L., Vörös, J., Elbert, D. L., Huang, N., Hofer, R., Ruiz-Taylor, L., … Spencer, N. D. (2000). Poly( l -lysine)- g -Poly(ethylene glycol) Layers on Metal Oxide Surfaces: Attachment Mechanism and Effects of Polymer Architecture on Resistance to Protein Adsorption †. *The Journal of Physical Chemistry B*, *104*(14), 3298–3309. doi:10.1021/jp993359m

Khademhosseini, A., & Langer, R. (2007). Microengineered hydrogels for tissue engineering. *Biomaterials*, *28*(34), 5087–5092. doi:10.1016/j.biomaterials.2007.07.021

Kijeńska, E., Prabhakaran, M. P., Swieszkowski, W., Kurzydlowski, K. J., & Ramakrishna, S. (2012). Electrospun bio-composite P(LLA-CL)/collagen I/collagen III scaffolds for nerve tissue engineering. *Journal of Biomedical Materials Research - Part B Applied Biomaterials*, *100 B*(4), 1093–1102. doi:10.1002/jbm.b.32676

Kim, Y. T., Haftel, V. K., Kumar, S., & Bellamkonda, R. V. (2008). The role of aligned polymer fiber-based constructs in the bridging of long peripheral nerve gaps. *Biomaterials*, *29*(21), 3117–3127. doi:10.1016/j.biomaterials.2008.03.042

Kipper, M. J., Kleinman, H. K., & Wang, F. W. (2007). Covalent surface chemistry gradients for presenting bioactive peptides. *Analytical Biochemistry*, *363*(2), 175–184. doi:10.1016/j.ab.2007.01.036

Kjellander, R., & Florin, E. (1981). Water structure and changes in thermal stability of the system poly(ethylene oxide)?water. *Journal of the Chemical Society, Faraday Transactions 1*, *77*(9), 2053. doi:10.1039/f19817702053

Knapp, D. M., Helou, E. F., & Tranquillo, R. T. (1999). A fibrin or collagen gel assay for tissue cell chemotaxis: assessment of fibroblast chemotaxis to GRGDSP. *Experimental Cell Research*, *247*(2), 543–553. doi:10.1006/excr.1998.4364

Kokai, L. E., Bourbeau, D., Weber, D., McAtee, J., & Marra, K. G. (2011). Sustained growth factor delivery promotes axonal regeneration in long gap peripheral nerve repair. *Tissue Engineering. Part A*, *17*(9-10), 1263–1275. doi:10.1089/ten.tea.2010.0507

Kokai, L. E., Ghaznavi, A. M., & Marra, K. G. (2010). Incorporation of double-walled microspheres into polymer nerve guides for the sustained delivery of glial cell line-derived neurotrophic factor. *Biomaterials*, *31*(8), 2313–2322. doi:10.1016/j.biomaterials.2009.11.075

Kraus, A., Täger, J., Kohler, K., Haerle, M., Werdin, F., Schaller, H.-E., & Sinis, N. (2010). Non-viral genetic transfection of rat Schwann cells with FuGENE HD© lipofection and AMAXA© nucleofection is feasible but impairs cell viability. *Neuron Glia Biology*, *6*(4), 225–230. doi:10.1017/S1740925X11000056

Lampe, K. J., Antaris, A. L., & Heilshorn, S. C. (2013). Design of three-dimensional engineered protein hydrogels for tailored control of neurite growth. *Acta Biomaterialia*, *9*(3), 5590–5599. doi:10.1016/j.actbio.2012.10.033

Lee, B. K., Ju, Y. M., Cho, J. G., Jackson, J. D., Lee, S. J., Atala, A., & Yoo, J. J. (2012). End-to-side neurorrhaphy using an electrospun PCL/collagen nerve conduit for complex peripheral motor nerve regeneration. *Biomaterials*, *33*(35), 9027–9036. doi:10.1016/j.biomaterials.2012.09.008

Li, L., Wu, W., Lin, L. F., Lei, M., Oppenheim, R. W., & Houenou, L. J. (1995). Rescue of adult mouse motoneurons from injury-induced cell death by glial cell line-derived neurotrophic factor. *Proceedings of the National Academy of Sciences of the United States of America*, *92*(21), 9771–9775. doi:10.1073/pnas.92.21.9771

Li, Q., Ping, P., Jiang, H., & Liu, K. (2006). Nerve conduit filled with GDNF gene-modified Schwann cells enhances regeneration of the peripheral nerve. *Microsurgery*, *26*(2), 116–121. doi:10.1002/micr.20192

Lih, E., Yoon Ki Joung, Jin Woo Bae, & Ki Dong Park. (2008). An In Situ Gel-Forming Heparin-Conjugated PLGA-PEG-PLGA Copolymer. *Journal of Bioactive and Compatible Polymers*, *23*(5), 444–457. doi:10.1177/0883911508095245

Lin, Y.-C., Ramadan, M., Hronik-Tupaj, M., Kaplan, D. L., Philips, B. J., Sivak, W., … Marra, K. G. (2011). Spatially controlled delivery of neurotrophic factors in silk fibroin-based nerve conduits for peripheral nerve repair. *Annals of Plastic Surgery*, *67*(2), 147–155. doi:10.1097/SAP.0b013e3182240346

Liu, G.-S., Shi, J.-Y., Lai, C.-L., Hong, Y.-R., Shin, S.-J., Huang, H.-T., … Tai, M.-H. (2009). Peripheral gene transfer of glial cell-derived neurotrophic factor ameliorates neuropathic deficits in diabetic rats. *Human Gene Therapy*, *20*(7), 715–727. doi:10.1089/hum.2009.002

Liu, K. J., & Parsons, J. L. (1969). Solvent effects on the preferred conformation of poly (ethylene glycols). *Macromolecules*, *2*(5), 529–533. doi:10.1021/ma60011a015

Liu Tsang, V., & Bhatia, S. N. (2004). Three-dimensional tissue fabrication. *Advanced Drug Delivery Reviews*. doi:10.1016/j.addr.2004.05.001

Lokanathan, Y., Ng, M. H., Hasan, S., Ali, A., Mahmod, M., Htwe, O., … Naicker, A. S. (2014). Olfactory ensheathing cells seeded muscle-stuffed vein as nerve conduit for peripheral nerve repair: A nerve conduction study. *Journal of Bioscience and Bioengineering*, *118*(2), 231–234. doi:10.1016/j.jbiosc.2014.02.002

Lühmann, T., Hänseler, P., Grant, B., & Hall, H. (2009). The induction of cell alignment by covalently immobilized gradients of the 6th Ig-like domain of cell adhesion molecule L1 in 3D-fibrin matrices. *Biomaterials*, *30*(27), 4503–4512. doi:10.1016/j.biomaterials.2009.05.041

Lundborg, G. (2000). A 25-year perspective of peripheral nerve surgery: Evolving neuroscientific concepts and clinical significance. *Journal of Hand Surgery*, *25*(3), 391–414. doi:10.1053/jhsu.2000.4165

Lundborg, G., & Dahlin, L. B. (1992). The pathophysiology of nerve compression. *Hand Clinics*, *8*(2), 215–227. doi:10.1016/S0363-5023(87)80254-X

Lundborg, G., Gelberman, R. H., Longo, F. M., Powell, H. C., & Varon, S. (1982). In vivo regeneration of cut nerves encased in silicone tubes: growth across a six-millimeter gap. *Journal of Neuropathology and Experimental Neurology*, *41*(4), 412–422. doi:10.1097/00005072-198207000-00004

Lundborg, G., & Rydevik, B. (1973). Effects of stretching the tibial nerve of the rabbit. A preliminary study of the intraneural circulation and the barrier function of the perineurium. *The Journal of Bone and Joint Surgery. British Volume*, *55*(2), 390–401. doi:10.1002/bjs.5095

Luo, Y., & Shoichet, M. S. (2004). A photolabile hydrogel for guided three-dimensional cell growth and migration. *Nature Materials*, *3*(4), 249–253. doi:10.1038/nmat1092

Lutolf, M. P., & Hubbell, J. a. (2005). Synthetic biomaterials as instructive extracellular microenvironments for morphogenesis in tissue engineering. *Nature Biotechnology*, *23*(1), 47–55. doi:10.1038/nbt1055

Lutolf, M. P., Lauer-Fields, J. L., Schmoekel, H. G., Metters, a T., Weber, F. E., Fields, G. B., & Hubbell, J. a. (2003). Synthetic matrix metalloproteinase-sensitive hydrogels for the conduction of tissue regeneration: engineering cell-invasion characteristics. *Proceedings of the National Academy of Sciences of the United States of America*, *100*(9), 5413–5418. doi:10.1073/pnas.0737381100

Lutolf, M. P., Weber, F. E., Schmoekel, H. G., Schense, J. C., Kohler, T., Müller, R., & Hubbell, J. a. (2003). Repair of bone defects using synthetic mimetics of collagenous extracellular matrices. *Nature Biotechnology*, *21*(5), 513–518. doi:10.1038/nbt818

Ma, H. W., Hyun, J. H., Stiller, P., & Chilkoti, a. (2004). "Non-fouling" oligo(ethylene glycol)-functionalized polymer brushes synthesized by surface-initiated atom transfer radical polymerization. *Advanced Materials*, *16*(4), 338–+. doi:10.1002/adma.200305830

Mackinnon SE, & AL Dellon. (1988). Median nerve entrapment in the proximal forearm and brachium: results of surgery. . *Surgery of the Peripheral Nerves, New York: Thieme*, 192–194.

Madduri, S., di Summa, P., Papaloïzos, M., Kalbermatten, D., & Gander, B. (2010). Effect of controlled co-delivery of synergistic neurotrophic factors on early nerve regeneration in rats. *Biomaterials*, *31*(32), 8402–8409. doi:10.1016/j.biomaterials.2010.07.052

Madduri, S., Feldman, K., Tervoort, T., Papaloïzos, M., & Gander, B. (2010). Collagen nerve conduits releasing the neurotrophic factors GDNF and NGF. *Journal of Controlled Release*, *143*(2), 168–174. doi:10.1016/j.jconrel.2009.12.017

Madison, R. D., Archibald, S. J., & Krarup, C. (1992). Peripheral nerve injury. In I. K. Cohen, R. F. Diegelmann, & W. J. Lindblad (Eds.), *Wound Healing: Biochemical and Clinical Aspects* (pp. 450–487). Philadelphia, PA: W. B. Saunders.

Magill, C. K., Moore, A. M., Yan, Y., Tong, A. Y., MacEwan, M. R., Yee, A., … Mackinnon, S. E. (2010). The differential effects of pathway- versus target-derived glial cell line-derived neurotrophic factor on peripheral nerve regeneration. *Journal of Neurosurgery*, *113*(1), 102–109. doi:10.3171/2009.10.JNS091092

Malda, J., Woodfield, T. B. F., Van Der Vloodt, F., Kooy, F. K., Martens, D. E., Tramper, J., … Riesle, J. (2004). The effect of PEGT/PBT scaffold architecture on oxygen gradients in tissue engineered cartilaginous constructs. *Biomaterials*, *25*(26), 5773–5780. doi:10.1016/j.biomaterials.2004.01.028

Malda, J., Woodfield, T. B. F., Van Der Vloodt, F., Wilson, C., Martens, D. E., Tramper, J., … Riesle, J. (2005). The effect of PEGT/PBT scaffold architecture on the composition of tissue engineered cartilage. *Biomaterials*, *26*(1), 63–72. doi:10.1016/j.biomaterials.2004.02.046

Mapili, G., Lu, Y., Chen, S., & Roy, K. (2005). Laser-layered microfabrication of spatially patterned functionalized tissue-engineering scaffolds. *Journal of Biomedical Materials Research - Part B Applied Biomaterials*, *75*(2), 414–424. doi:10.1002/jbm.b.30325

Marquardt, L., & Willits, R. K. (2011). Neurite growth in PEG gels: Effect of mechanical stiffness and laminin concentration. *Journal of Biomedical Materials Research. Part A*, *98*(1), 1–6. doi:10.1002/jbm.a.33044

Mason, M. R. J., Tannemaat, M. R., Malessy, M. J. a, & Verhaagen, J. (2011). Gene therapy for the peripheral nervous system: a strategy to repair the injured nerve? *Current Gene Therapy*, *11*(2), 75–89. doi:10.2174/156652311794940764

Masri, M. S., & Friedman, M. (1988). Protein reactions with methyl and ethyl vinyl sulfones. *Journal of Protein Chemistry*, *7*(1), 49–54. doi:10.1007/BF01025413

Maxfield, J., & Shepherd, I. W. (1975). Conformation of poly(ethylene oxide) in the solid state, melt and solution measured by Raman scattering. *Polymer, 16*(7), 505–509. doi:10.1016/0032-3861(75)90008-7

Maxwell, D. J., Hicks, B. C., Parsons, S., & Sakiyama-Elbert, S. E. (2005). Development of rationally designed affinity-based drug delivery systems. *Acta Biomaterialia*, *1*(1), 101–113. doi:10.1016/j.actbio.2004.09.002

McPherson, T. B., Shim, H. S., & Park, K. (1997). Grafting of PEO to glass, nitinol, and pyrolytic carbon surfaces by gamma irradiation. *Journal of Biomedical Materials Research*, *38*(4), 289–302. Retrieved from http://www.ncbi.nlm.nih.gov/pubmed/9421750

Merrill, E. W., & Salzman, E. W. (1983). Polyethylene oxide as a biomaterial. *Asaio*, *6*(2), 60–64. Retrieved from http://cat.inist.fr/?aModele=afficheN&cpsidt=9324632

Merrill, E. W., Salzman, E. W., Wan, S., Mahmud, N., Kushner, L., Lindon, J. N., & Curme, J. (1982). Platelet-compatible hydrophilic segmented polyurethanes from polyethylene glycols and cyclohexane diisocyanate. *Transactions - American Society for Artificial Internal Organs*, *28*, 482–487. Retrieved from http://www.ncbi.nlm.nih.gov/pubmed/7164286

Miller, J. S., Shen, C. J., Legant, W. R., Baranski, J. D., Blakely, B. L., & Chen, C. S. (2010). Bioactive hydrogels made from step-growth derived PEG-peptide macromers. *Biomaterials*, *31*(13), 3736–3743. doi:10.1016/j.biomaterials.2010.01.058

Moon, J. J., Saik, J. E., Poché, R. a., Leslie-Barbick, J. E., Lee, S. H., Smith, A. a., … West, J. L. (2010). Biomimetic hydrogels with pro-angiogenic properties. *Biomaterials*, *31*(14), 3840–3847. doi:10.1016/j.biomaterials.2010.01.104

Moore, A. M., Kasukurthi, R., Magill, C. K., Farhadi, F. H., Borschel, G. H., & Mackinnon, S. E. (2009). Limitations of conduits in peripheral nerve repairs. *Hand*, *4*(2), 180–186. doi:10.1007/s11552-008-9158-3

Moore, A. M., Wood, M. D., Chenard, K., Hunter, D. a, Mackinnon, S. E., Sakiyama-Elbert, S. E., & Borschel, G. H. (2010). Controlled delivery of glial cell line-derived neurotrophic factor enhances motor nerve regeneration. *The Journal of Hand Surgery*, *35*(12), 2008–2017. doi:10.1016/j.jhsa.2010.08.016

Moore, K., MacSween, M., & Shoichet, M. (2006). Immobilized concentration gradients of neurotrophic factors guide neurite outgrowth of primary neurons in macroporous scaffolds. *Tissue Engineering*, *12*(2), 267–278. doi:10.1089/ten.2006.12.ft-42

Moradzadeh, A., Borschel, G. H., Luciano, J. P., Whitlock, E. L., Hayashi, A., Hunter, D. a., & Mackinnon, S. E. (2008). The impact of motor and sensory nerve architecture on nerve regeneration. *Experimental Neurology*, *212*(2), 370–376. doi:10.1016/j.expneurol.2008.04.012

Mori, Y., Nagaoka, S., Takiuchi, H., Kikuchi, T., Noguchi, N., Tanzawa, H., & Noishiki, Y. (1982). A new antithrombogenic material with long polyethyleneoxide chains. *Transactions - American*

*Society for Artificial Internal Organs*, *28*, 459–463. Retrieved from http://www.ncbi.nlm.nih.gov/pubmed/7164281

Morimoto, K., Katsumata, H., Yabuta, T., Iwanaga, K., Kakemi, M., Tabata, Y., & Ikada, Y. (2000). Gelatin microspheres as a pulmonary delivery system: evaluation of salmon calcitonin absorption. *The Journal of Pharmacy and Pharmacology*, *52*(6), 611–617. doi:10.1211/0022357001774444

Moroder, P., Runge, M. B., Wang, H., Ruesink, T., Lu, L., Spinner, R. J., … Yaszemski, M. J. (2011). Material properties and electrical stimulation regimens of polycaprolactone fumarate-polypyrrole scaffolds as potential conductive nerve conduits. *Acta Biomaterialia*, *7*(3), 944–953. doi:10.1016/j.actbio.2010.10.013

Mukhatyar, V. J., Salmerón-Sánchez, M., Rudra, S., Mukhopadaya, S., Barker, T. H., García, A. J., & Bellamkonda, R. V. (2011). Role of fibronectin in topographical guidance of neurite extension on electrospun fibers. *Biomaterials*, *32*(16), 3958–3968. doi:10.1016/j.biomaterials.2011.02.015

Muller, E., & Rasmussen, P. (1991). Densities and excess volumes in aqueous poly(ethylene glycol) solutions. *Journal of Chemical and Engineering Data*, *36*(2), 214–217. doi:10.1021/je00002a019

Nagano, M., Sakai, A., Takahashi, N., Umino, M., Yoshioka, K., & Suzuki, H. (2003). Decreased expression of glial cell line-derived neurotrophic factor signaling in rat models of neuropathic pain. *British Journal of Pharmacology*, *140*(7), 1252–1260. doi:10.1038/sj.bjp.0705550

Neal, R. a., Tholpady, S. S., Foley, P. L., Swami, N., Ogle, R. C., & Botchwey, E. a. (2012). Alignment and composition of laminin-polycaprolactone nanofiber blends enhance peripheral nerve regeneration. *Journal of Biomedical Materials Research - Part A*, *100 A*(2), 406–423. doi:10.1002/jbm.a.33204

Nectow, A. R., Marra, K. G., & Kaplan, D. L. (2012). Biomaterials for the Development of Peripheral Nerve Guidance Conduits. *Tissue Engineering Part B: Reviews*, *18*(1), 40–50. doi:10.1089/ten.teb.2011.0240

Ng, K. W., Hutmacher, D. W., Schantz, J. T., Ng, C. S., Too, H. P., Lim, T. C., … Teoh, S. H. (2001). Evaluation of ultra-thin poly(epsilon-caprolactone) films for tissue-engineered skin. *Tissue Engineering*, *7*(4), 441–55. doi:10.1089/10763270152436490

Nguyen, P. K., Snyder, C. G., Shields, J. D., Smith, A. W., & Elbert, D. L. (2013). Clickable poly(ethylene glycol)-microsphere-based cell scaffolds. *Macromolecular Chemistry and Physics*, *214*(8), 948–956. doi:10.1002/macp.201300023

Nichols, M. D., Scott, E. a., & Elbert, D. L. (2009). Factors affecting size and swelling of poly(ethylene glycol) microspheres formed in aqueous sodium sulfate solutions without surfactants. *Biomaterials*, *30*(29), 5283–5291. doi:10.1016/j.biomaterials.2009.06.032

Nie, T., Baldwin, A., Yamaguchi, N., & Kiick, K. L. (2007). Production of heparin-functionalized hydrogels for the development of responsive and controlled growth factor delivery systems. *Journal of Controlled Release*, *122*(3), 287–296. doi:10.1016/j.jconrel.2007.04.019

NINDS. (2014). Peripheral Neuropathy Fact Sheet. In *Disorders*.

Nwe, K., & Brechbiel, M. W. (2009). Growing applications of "click chemistry" for bioconjugation in contemporary biomedical research. *Cancer Biotherapy & Radiopharmaceuticals*, *24*(3), 289–302. doi:10.1089/cbr.2008.0626

Oh, S. H., Kim, J. R., Kwon, G. B., Namgung, U., Song, K. S., & Lee, J. H. (2012). Effect of Surface Pore Structure of Nerve Guide Conduit on Peripheral Nerve Regeneration. *Tissue Engineering Part C: Methods*, *19*(3), 120913061739004. doi:10.1089/ten.tec.2012.0221

Oh, S. H., Kim, T. H., & Lee, J. H. (2011). Creating growth factor gradients in three dimensional porous matrix by centrifugation and surface immobilization. *Biomaterials*, *32*(32), 8254–8260. doi:10.1016/j.biomaterials.2011.07.027

Oppenheim, R. W., Houenou, L. J., Parsadanian, a S., Prevette, D., Snider, W. D., & Shen, L. (2000). Glial cell line-derived neurotrophic factor and developing mammalian motoneurons: regulation of programmed cell death among motoneuron subtypes. *The Journal of Neuroscience : The Official Journal of the Society for Neuroscience*, *20*(13), 5001–5011. doi:20/13/5001 [pii]

Ostuni, E., Chapman, R. G., Holmlin, R. E., Takayama, S., & Whitesides, G. M. (2001). A survey of structure-property relationships of surfaces that resist the adsorption of protein. *Langmuir*, *17*(18), 5605–5620. doi:10.1021/la010384m

Panyam, J., & Labhasetwar, V. (2003). Biodegradable nanoparticles for drug and gene delivery to cells and tissue. *Advanced Drug Delivery Reviews*, *55*(3), 329–347. doi:10.1016/S0169-409X(02)00228-4

Parent, C. a, & Devreotes, P. N. (1999). A cell's sense of direction. *Science (New York, N.Y.)*, *284*(5415), 765–770. doi:10.1126/science.284.5415.765

Park, H., Temenoff, J. S., Holland, T. a., Tabata, Y., & Mikos, A. G. (2005). Delivery of TGF-??1 and chondrocytes via injectable, biodegradable hydrogels for cartilage tissue engineering applications. *Biomaterials*, *26*(34), 7095–7103. doi:10.1016/j.biomaterials.2005.05.083

Park, H. Y., Kloxin, C. J., Scott, T. F., & Bowman, C. N. (2010). Stress relaxation by addition-fragmentation chain transfer in highly cross-linked thiol-yne networks. *Macromolecules*, *43*(24), 10188–10190. doi:10.1021/ma1020209

Park, S. Y., Ki, C. S., Park, Y. H., Lee, K. G., Kang, S. W., Kweon, H. Y., & Kim, H. J. (2012). Functional recovery guided by an electrospun silk fibroin conduit after sciatic nerve injury in rats. *Journal of Tissue Engineering and Regenerative Medicine*. doi:10.1002/term.1615

Patterson, J., & Hubbell, J. a. (2010). Enhanced proteolytic degradation of molecularly engineered PEG hydrogels in response to MMP-1 and MMP-2. *Biomaterials*, *31*(30), 7836–7845. doi:10.1016/j.biomaterials.2010.06.061

Patterson, J., & Hubbell, J. a. (2011). SPARC-derived protease substrates to enhance the plasmin sensitivity of molecularly engineered PEG hydrogels. *Biomaterials*, *32*(5), 1301–1310. doi:10.1016/j.biomaterials.2010.10.016

Pawar, K., Mueller, R., Caioni, M., Prang, P., Bogdahn, U., Kunz, W., & Weidner, N. (2011). Increasing capillary diameter and the incorporation of gelatin enhance axon outgrowth in alginate-based anisotropic hydrogels. *Acta Biomaterialia*, *7*(7), 2826–2834. doi:10.1016/j.actbio.2011.04.006

Peppas, N. a., Hilt, J. Z., Khademhosseini, A., & Langer, R. (2006). Hydrogels in biology and medicine: From molecular principles to bionanotechnology. *Advanced Materials*, *18*(11), 1345–1360. doi:10.1002/adma.200501612

Pfister, B. J., Gordon, T., Loverde, J. R., Kochar, A. S., Mackinnon, S. E., & Cullen, D. K. (2011). Biomedical engineering strategies for peripheral nerve repair: surgical applications, state of the art, and future challenges. *Critical Reviews in Biomedical Engineering*, *39*(2), 81–124. doi:10.1615/CritRevBiomedEng.v39.i2.20

Place, E. S., George, J. H., Williams, C. K., & Stevens, M. M. (2009). Synthetic polymer scaffolds for tissue engineering. *Chemical Society Reviews*, *38*(4), 1139–1151. doi:10.1039/b811392k

Polizzotti, B. D., Fairbanks, B. D., & Anseth, K. S. (2008). Three-dimensional biochemical patterning of click-based composite hydrogels via thiolene photopolymerization. *Biomacromolecules*, *9*(4), 1084–1087. doi:10.1021/bm7012636

Porte, H. L., Jany, T., Akkad, R., Conti, M., Gillet, P. a., Guidat, A., & Wurtz, A. J. (2001). Randomized controlled trial of a synthetic sealant for preventing alveolar air leaks after lobectomy. *Annals of Thoracic Surgery*, *71*(5), 1618–1622. doi:10.1016/S0003-4975(01)02468-7

Preul, M. C., Campbell, P. K., Bichard, W. D., & Spetzler, R. F. (2007). Application of a hydrogel sealant improves watertight closures of duraplasty onlay grafts in a canine craniotomy model. *Journal of Neurosurgery*, *107*(3), 642–650. doi:10.3171/JNS-07/09/0642

Pu, L. L., Syed, S. a, Reid, M., Patwa, H., Goldstein, J. M., Forman, D. L., & Thomson, J. G. (1999). Effects of nerve growth factor on nerve regeneration through a vein graft across a gap. *Plastic and Reconstructive Surgery*, *104*(5), 1379–1385. doi:10.1097/00006534-199910000-00021

Quan, D., & Bird, S. J. (1999). Nerve conduction studies and electromyography in the evaluation of peripheral nerve injuries. *The University of Pennsylvania Orthopedic Journal*, *12*, 45–51.

Raeber, G. P., Lutolf, M. P., & Hubbell, J. a. (2005). Molecularly engineered PEG hydrogels: a novel model system for proteolytically mediated cell migration. *Biophysical Journal*, *89*(2), 1374–1388. doi:10.1529/biophysj.104.050682

Ramburrun, P., Kumar, P., Choonara, Y., Bijukumar, D., du Toit, L., & Pillay V. (2014). A Review of Bioactive Release from Nerve Conduits as a Neurotherapeutic Strategy for Neuronal Growth in Peripheral Nerve Injury. *Biomed Res Int*, 132350.

Ratner, B. D., Hoffman, A. S., Schoen, F. J., & Lemons, J. E. (2013). Biomaterials Science: An Evolving, Multidisciplinary Endeavor. In *Biomaterials Science* (pp. xxv–xxxix). doi:10.1016/B978-0-08-087780-8.00153-4

Ribeiro-Resende, V. T., Koenig, B., Nichterwitz, S., Oberhoffner, S., & Schlosshauer, B. (2009). Strategies for inducing the formation of bands of B??ngner in peripheral nerve regeneration. *Biomaterials*, *30*(29), 5251–5259. doi:10.1016/j.biomaterials.2009.07.007

Richardson, J. a, Rementer, C. W., Bruder, J. M., & Hoffman-Kim, D. (2011). Guidance of dorsal root ganglion neurites and Schwann cells by isolated Schwann cell topography on poly(dimethyl siloxane) conduits and films. *Journal of Neural Engineering*, *8*(4), 046015. doi:10.1088/1741-2560/8/4/046015

Rivest, C., Morrison, D., Ni, B., Rubin, J., Yadav, V., Mahdavi, A., … Khademhosseini, A. (2007). Microscale hydrogels for medicine and biology: synthesis, characteristics and applications. *Journal of Mechanics of Materials and Structures*. doi:10.2140/jomms.2007.2.1103

Roam, J. L., Nguyen, P. K., & Elbert, D. L. (2014). Controlled release and gradient formation of human glial-cell derived neurotrophic factor from heparinated poly(ethylene glycol) microsphere-based scaffolds. *Biomaterials*, *35*(24), 6473–6481. doi:10.1016/j.biomaterials.2014.04.027

Roam, J. L., Xu, H., Nguyen, P. K., & Elbert, D. L. (2010). The formation of protein concentration gradients mediated by density differences of poly(ethylene glycol) microspheres. *Biomaterials*, *31*(33), 8642–8650. doi:10.1016/j.biomaterials.2010.07.085

Robinson, L. R. (2000). Traumatic injury to peripheral nerves. *Muscle and Nerve*, *23*(6), 863–873. doi:10.1002/(SICI)1097-4598(200006)23:6<863::AID-MUS4>3.0.CO;2-0

Rosoff, W. J., Urbach, J. S., Esrick, M. a, McAllister, R. G., Richards, L. J., & Goodhill, G. J. (2004). A new chemotaxis assay shows the extreme sensitivity of axons to molecular gradients. *Nature Neuroscience*, *7*(6), 678–682. doi:10.1038/nn1259

Sa Da Costa, V., Brier-Russell, D., Salzman, E. W., & Merrill, E. W. (1981). Esca studies of polyurethanes: blood platelet activation in relation to surface composition. *Journal of Colloid and Interface Science*, *80*(2), 445–452. doi:10.1016/0021-9797(81)90203-4

Saarma, M. (2000). GDNF - A stranger in the TGF-?? superfamily? *European Journal of Biochemistry*, *267*(24), 6968–6971. doi:10.1046/j.1432-1327.2000.01826.x

Sahin, C., Karagoz, H., Kulahci, Y., Sever, C., Akakin, D., Kolbasi, B., … Peker, F. (2014). Minced nerve tissue in vein grafts used as conduits in rat tibial nerves. *Annals of Plastic Surgery*, *73*(5), 540–6. doi:10.1097/SAP.0000000000000060

Sakiyama, S. E., Schense, J. C., & Hubbell, J. a. (1999). Incorporation of heparin-binding peptides into fibrin gels enhances neurite extension: an example of designer matrices in tissue engineering. *The FASEB Journal : Official Publication of the Federation of American Societies for Experimental Biology*, *13*(15), 2214–2224. Retrieved from http://www.fasebj.org/content/13/15/2214.short

Sakiyama-Elbert, S. E., & Hubbell, J. a. (2000). Development of fibrin derivatives for controlled release of heparin- binding growth factors. *Journal of Controlled Release*, *65*(3), 389–402. doi:10.1016/S0168-3659(99)00221-7

Salek-Ardakani, S., Arrand, J. R., Shaw, D., & Mackett, M. (2000). Heparin and heparan sulfate bind interleukin-10 and modulate its activity. *Blood*, *96*(5), 1879–1888. Retrieved from http://www.bloodjournal.org/content/96/5/1879.abstract

Saltzman, W. M., Radomsky, M. L., Whaley, K. J., & Cone, R. a. (1994). Antibody diffusion in human cervical mucus. *Biophysical Journal*, *66*(2), 508–515. doi:10.1016/S0006-3495(94)80802-1

Santosa, K. B., Jesuraj, N. J., Viader, A., Macewan, M., Newton, P., Hunter, D. a., … Johnson, P. J. (2013). Nerve allografts supplemented with schwann cells overexpressing glial-cell-line-derived neurotrophic factor. *Muscle and Nerve*, *47*(2), 213–223. doi:10.1002/mus.23490

Sawhney, a S., Pathak, C. P., & Hubbell, J. a. (1993). Interfacial photopolymerization of poly(ethylene glycol)-based hydrogels upon alginate-poly(l-lysine) microcapsules for enhanced biocompatibility. *Biomaterials*, *14*(13), 1008–1016. doi:10.1016/0142-9612(93)90194-7

Schmidt, C. E., & Leach, J. B. (2003). Neural tissue engineering: strategies for repair and regeneration. *Annual Review of Biomedical Engineering*, *5*, 293–347. doi:10.1146/annurev.bioeng.5.011303.120731

Schonauer, F., Marlino, S., Avvedimento, S., & Molea, G. (2012). *Peripheral Nerve Reconstruction with Autologous Grafts*. InTech.

Scott, D. C., & Hollenbeck, R. G. (1991). Design and manufacture of a zero-order sustained-release pellet dosage form through nonuniform drug distribution in a diffusional matrix. *Pharmaceutical Research*, *8*(2), 156–161. doi:10.1023/A:1015823532764

Scott, E. a., Nichols, M. D., Kuntz-Willits, R., & Elbert, D. L. (2010). Modular scaffolds assembled around living cells using poly(ethylene glycol) microspheres with macroporation via a non-cytotoxic porogen. *Acta Biomaterialia*, *6*(1), 29–38. doi:10.1016/j.actbio.2009.07.009

Scott, R. a., Elbert, D. L., & Willits, R. K. (2011). Modular poly(ethylene glycol) scaffolds provide the ability to decouple the effects of stiffness and protein concentration on PC12 cells. *Acta Biomaterialia*, *7*(11), 3841–3849. doi:10.1016/j.actbio.2011.06.054

Scott, R., Marquardt, L., & Willits, R. K. (2010). Characterization of poly(ethylene glycol) gels with added collagen for neural tissue engineering. *Journal of Biomedical Materials Research - Part A*, *93*, 817–823. doi:10.1002/jbm.a.32775

Seliktar, D., Zisch, a H., Lutolf, M. P., Wrana, J. L., & Hubbell, J. a. (2004). MMP-2 sensitive, VEGF-bearing bioactive hydrogels for promotion of vascular healing. *Journal of Biomedical Materials Research. Part A*, *68*(4), 704–716. doi:10.1002/jbm.a.20091

Serban, M. a., & Prestwich, G. D. (2008). Modular extracellular matrices: Solutions for the puzzle. *Methods*, *45*(1), 93–98. doi:10.1016/j.ymeth.2008.01.010

Shakhbazau, A., Mohanty, C., Shcharbin, D., Bryszewska, M., Caminade, A. M., Majoral, J. P., … Midha, R. (2013). Doxycycline-regulated GDNF expression promotes axonal regeneration and functional recovery in transected peripheral nerve. *Journal of Controlled Release*, *172*(3), 841–851. doi:10.1016/j.jconrel.2013.10.004

Shepard, J. a., Wesson, P. J., Wang, C. E., Stevans, A. C., Holland, S. J., Shikanov, A., … Shea, L. D. (2011). Gene therapy vectors with enhanced transfection based on hydrogels modified with affinity peptides. *Biomaterials*, *32*(22), 5092–5099. doi:10.1016/j.biomaterials.2011.03.083

Shi, J.-Y., Liu, G.-S., Liu, L.-F., Kuo, S.-M., Ton, C.-H., Wen, Z.-H., … Tai, M.-H. (2011). Glial cell line-derived neurotrophic factor gene transfer exerts protective effect on axons in sciatic nerve following constriction-induced peripheral nerve injury. *Human Gene Therapy*, *22*(6), 721–731. doi:10.1089/hum.2010.036

Shi, Y., Zhou, L., Tian, J., & Wang, Y. (2009). Transplantation of neural stem cells overexpressing glia-derived neurotrophic factor promotes facial nerve regeneration. *Acta Oto-Laryngologica*, *129*(8), 906–914. doi:10.1080/00016480802468153

Siemionow, M., & Sonmez, E. (2007). Nerve allograft transplantation: A review. *Journal of Reconstructive Microsurgery*, *23*(8), 511–520. doi:10.1055/s-2007-1022694

Singh, M., Morris, C. P., Ellis, R. J., Detamore, M. S., & Berkland, C. (2008). Microsphere-based seamless scaffolds containing macroscopic gradients of encapsulated factors for tissue engineering. *Tissue Engineering. Part C, Methods*, *14*(4), 299–309. doi:10.1089/ten.tec.2008.0167

Song , H., & Poo , M. (2001). The cell biology of neuronal navigation. *Nature Cell Biology*, *3*(3), E81–E88. doi:10.1038/35060164

Song, H. J., Ming, G. L., & Poo, M. M. (1997). cAMP-induced switching in turning direction of nerve growth cones. *Nature*, *388*(6639), 275–279. doi:10.1038/40864

Stefonek, T. J., & Masters, K. S. (2007). Immobilized gradients of epidermal growth factor promote accelerated and directed keratinocyte migration. *Wound Repair and Regeneration*, *15*(6), 847–855. doi:10.1111/j.1524-475X.2007.00288.x

Strauch, B., Ferder, M., Lovelle-Allen, S., Moore, K., Kim, D. J., & Llena, J. (1996). Determining the maximal length of a vein conduit used as an interposition graft for nerve regeneration. *Journal of Reconstructive Microsurgery*, *12*(8), 521–527. doi:10.1055/s-2007-1006624

Stroncek, J. D., & Reichert, W. M. (2007, January 1). Overview of Wound Healing in Different Tissue Types. *Indwelling Neural Implants: Strategies for Contending with the In Vivo Environment*. CRC Press, Boca Raton (FL). doi:NBK3938 [bookaccession]

Suri, S., Han, L.-H., Zhang, W., Singh, A., Chen, S., & Schmidt, C. E. (2011). Solid freeform fabrication of designer scaffolds of hyaluronic acid for nerve tissue engineering. *Biomedical Microdevices*, *13*(6), 983–993. doi:10.1007/s10544-011-9568-9

Swindle-Reilly, K. E., Papke, J. B., Kutosky, H. P., Throm, A., Hammer, J. a, Harkins, A. B., & Willits, R. K. (2012). The impact of laminin on 3D neurite extension in collagen gels. *Journal of Neural Engineering*, *9*(4), 046007. doi:10.1088/1741-2560/9/4/046007

Szynkaruk, M., Kemp, S. W. P., Wood, M. D., Gordon, T., & Borschel, G. H. (2012). Experimental and Clinical Evidence for Use of Decellularized Nerve Allografts in Peripheral Nerve Gap Reconstruction. *Tissue Engineering Part B: Reviews*, *19*(1), 121003062440003. doi:10.1089/ten.teb.2012.0275

Tae, G., Scatena, M., Stayton, P. S., & Hoffman, A. S. (2006). PEG-cross-linked heparin is an affinity hydrogel for sustained release of vascular endothelial growth factor. *Journal of Biomaterials Science. Polymer Edition*, *17*(1-2), 187–197. doi:10.1163/156856206774879090

Tannemaat, M. R., Eggers, R., Hendriks, W. T., De Ruiter, G. C. W., Van Heerikhuize, J. J., Pool, C. W., … Verhaagen, J. (2008). Differential effects of lentiviral vector-mediated overexpression of nerve growth factor and glial cell line-derived neurotrophic factor on regenerating sensory and motor axons in the transected peripheral nerve. *European Journal of Neuroscience*, *28*(8), 1467–1479. doi:10.1111/j.1460-9568.2008.06452.x

Taylor, C. a, Braza, D., Rice, J. B., & Dillingham, T. (2008). The incidence of peripheral nerve injury in extremity trauma. *American Journal of Physical Medicine & Rehabilitation / Association of Academic Physiatrists*, *87*(5), 381–385. doi:10.1097/PHM.0b013e31815e6370

Tessmar, J. K., & Göpferich, A. M. (2007). Customized PEG-derived copolymers for tissue-engineering applications. *Macromolecular Bioscience*, *7*(1), 23–39. doi:10.1002/mabi.200600096

Tranquillo, R. T. (1988). A stochastic model for leukocyte random motility and chemotaxis based on receptor binding fluctuations. *The Journal of Cell Biology*, *106*(2), 303–309. doi:10.1083/jcb.106.2.303

Trumble, T. E., & Shon, F. G. (2000). The physiology of nerve transplantation. *Hand Clinics*, *16*(1), 105–122. doi:10.1037/h0075210

Uchida, E., Uyama, Y., & Ikada, Y. (1994). Grafting of Water-Soluble Chains onto a Polymer Surface. *Langmuir*, *2*(2), 481–485. doi:10.1021/la00014a023

Um, E., Lee, D. S., Pyo, H. B., & Park, J. K. (2008). Continuous generation of hydrogel beads and encapsulation of biological materials using a microfluidic droplet-merging channel. *Microfluidics and Nanofluidics*, *5*(4), 541–549. doi:10.1007/s10404-008-0268-6

V Sa da Costa, D Brier-Russell, G Trudel, D.F Waugh, E.W Salzman, E. . M. (1980). Polyether—polyurethane surfaces: Thrombin adsorption, platelet adsorption, and ESCA scanning. *Journal of Colloid and Interface Science*, *76*(2), 594–596.

Van Dijk, M., Van Nostrum, C. F., Hennink, W. E., Rijkers, D. T. S., & Liskamp, R. M. J. (2010). Synthesis and characterization of enzymatically biodegradable peg and peptide-based hydrogels prepared by click chemistry. *Biomacromolecules*, *11*(6), 1608–1614. doi:10.1021/bm1002637

Vepari, C. P., & Kaplan, D. L. (2006). Covalently immobilized enzyme gradients within three-dimensional porous scaffolds. *Biotechnology and Bioengineering*, *93*(6), 1130–1137. doi:10.1002/bit.20833

Vulic, K., & Shoichet, M. S. (2012). Tunable growth factor delivery from injectable hydrogels for tissue engineering. *Journal of the American Chemical Society*, *134*(2), 882–5. doi:10.1021/ja210638x

Wacker, B. K., Scott, E. a., Kaneda, M. M., Alford, S. K., & Elbert, D. L. (2006). Delivery of Sphingosine 1-phosphate from poly(ethylene glycol) hydrogels. *Biomacromolecules*, *7*(4), 1335–1343. doi:10.1021/bm050948r

Walton, R. L., Brown, R. E., Matory, W. E., Borah, G. L., & Dolph, J. L. (1989). Autogenous vein graft repair of digital nerve defects in the finger: a retrospective clinical study. *Plastic and Reconstructive Surgery*, *84*(6), 944–949; discussion 950–952. doi:10.1097/00006534-198912000-00014

Wang, H., Leeuwenburgh, S. C. G., Li, Y., & Jansen, J. a. (2012). The Use of Micro- and Nanospheres as Functional Components for Bone Tissue Regeneration. *Tissue Engineering Part B: Reviews*, *18*(1), 24–39. doi:10.1089/ten.teb.2011.0184

Wang, S., & Cai, L. (2010). Polymers for Fabricating Nerve Conduits. *International Journal of Polymer Science*, *2010*.

Wang, X., Wenk, E., Matsumoto, A., Meinel, L., Li, C., & Kaplan, D. L. (2007). Silk microspheres for encapsulation and controlled release. *Journal of Controlled Release*, *117*(3), 360–370. doi:10.1016/j.jconrel.2006.11.021

Wang, X., Wenk, E., Zhang, X., Meinel, L., Vunjak-Novakovic, G., & Kaplan, D. L. (2009). Growth factor gradients via microsphere delivery in biopolymer scaffolds for osteochondral tissue engineering. *Journal of Controlled Release*, *134*(2), 81–90. doi:10.1016/j.jconrel.2008.10.021

Wen, X., Peng, X., Fu, H., Dong, Y., Han, K., Su, J., … Wu, C. (2011). Preparation and in vitro evaluation of silk fibroin microspheres produced by a novel ultra-fine particle processing system. *International Journal of Pharmaceutics*, *416*(1), 195–201. doi:10.1016/j.ijpharm.2011.06.041

West, J. L., & Hubbell, J. a. (1999). Polymeric biomaterials with degradation sites for proteases involved in cell migration. *Macromolecules*, *32*(1), 241–244. doi:10.1021/ma981296k

Whicher, S. J., & Brash, J. L. (1978). Platelet-foreign surface interactions: release of granule constituents from adherent platelets. *Journal of Biomedical Materials Research*, *12*(2), 181–201. doi:10.1002/jbm.820120205

Whitesides, G. M. (1993). *Poly(ethylene glycol) chemistry biotechnical and biomedical applications J. Milton Harris, Ed. Applied Biochemistry and Biotechnology* (Vol. 41). Springer Science & Business Media. doi:10.1007/BF02916424

Whitlock, E. L., Tuffaha, S. H., Luciano, J. P., Yan, Y., Hunter, D. a., Magill, C. K., … Borschel, G. H. (2009). Processed allografts and type I collagen conduits for repair of peripheral nerve gaps. *Muscle and Nerve*, *39*(6), 787–799. doi:10.1002/mus.21220

Wolford, L. M., & Stevao, E. L. L. (2003). Considerations in nerve repair. *Proceedings (Baylor University. Medical Center)*, *16*(2), 152–156. Retrieved from http://www.pubmedcentral.nih.gov/articlerender.fcgi?artid=1201001&tool=pmcentrez&rendertype=abstract

Wood, M. D., Borschel, G. H., & Sakiyama-Elbert, S. E. (2009). Controlled release of glial-derived neurotrophic factor from fibrin matrices containing an affinity-based delivery system. *Journal of Biomedical Materials Research - Part A*, *89*(4), 909–918. doi:10.1002/jbm.a.32043

Wood, M. D., Gordon, T., Kim, H., Szynkaruk, M., Phua, P., Lafontaine, C., … Borschel, G. H. (2013). Fibrin gels containing GDNF microspheres increase axonal regeneration after delayed peripheral nerve repair. *Regenerative Medicine*, *8*(1), 27–37. doi:10.2217/rme.12.105

Wood, M. D., Kim, H., Bilbily, A., Kemp, S. W. P., Lafontaine, C., Gordon, T., … Borschel, G. H. (2012). GDNF released from microspheres enhances nerve regeneration after delayed repair. *Muscle and Nerve*, *46*(1), 122–124. doi:10.1002/mus.23295

Wood, M. D., MacEwan, M. R., French, A. R., Moore, A. M., Hunter, D. a., Mackinnon, S. E., … Sakiyama-Elbert, S. E. (2010). Fibrin matrices with affinity-based delivery systems and neurotrophic factors promote functional nerve regeneration. *Biotechnology and Bioengineering*, *106*(6), 970–979. doi:10.1002/bit.22766

Wood, M. D., Moore, A. M., Hunter, D. a., Tuffaha, S., Borschel, G. H., Mackinnon, S. E., & Sakiyama-Elbert, S. E. (2009). Affinity-based release of glial-derived neurotrophic factor from

fibrin matrices enhances sciatic nerve regeneration. *Acta Biomaterialia*, *5*(4), 959–968. doi:10.1016/j.actbio.2008.11.008

Wu, J., Liao, C., Zhang, J., Cheng, W., Zhou, N., Wang, S., & Wan, Y. (2011). Incorporation of protein-loaded microspheres into chitosan-polycaprolactone scaffolds for controlled release. *Carbohydrate Polymers*, *86*(2), 1048–1054. doi:10.1016/j.carbpol.2011.05.060

Xiao, J.-H., & Zhang, M.-N. (2010). Neuroprotection of retinal ganglion cells with GDNF-Loaded biodegradable microspheres in experimental glaucoma. *International Journal of Ophthalmology*, *3*(3), 189–91. doi:10.3980/j.issn.2222-3959.2010.03.01

Xie, J., MacEwan, M. R., Li, X., Sakiyama-Elbert, S. E., & Xia, Y. (2009). Neurite outgrowth on nanofiber scaffolds with different orders, structures, and surface properties. *ACS Nano*, *3*(5), 1151–1159. doi:10.1021/nn900070z

Xie, J., Willerth, S. M., Li, X., Macewan, M. R., Rader, A., Sakiyama-Elbert, S. E., & Xia, Y. (2009). The differentiation of embryonic stem cells seeded on electrospun nanofibers into neural lineages. *Biomaterials*, *30*(3), 354–362. doi:10.1016/j.biomaterials.2008.09.046

Xu, H., Yan, Y., & Li, S. (2011). PDLLA/chondroitin sulfate/chitosan/NGF conduits for peripheral nerve regeneration. *Biomaterials*, *32*(20), 4506–4516. doi:10.1016/j.biomaterials.2011.02.023

Yan, Q., Matheson, C., & Lopez, O. T. (1995). In vivo neurotrophic effects of GDNF on neonatal and adult facial motor neurons. *Nature*, *373*(6512), 341–344. doi:10.1038/373341a0

Yang, Y., De Laporte, L., Zelivyanskaya, M. L., Whittlesey, K. J., Anderson, A. J., Cummings, B. J., & Shea, L. D. (2009). Multiple channel bridges for spinal cord injury: cellular characterization of host response. *Tissue Engineering. Part A*, *15*(11), 3283–3295. doi:10.1089/ten.tea.2009.0081

Yeh, J., Ling, Y., Karp, J. M., Gantz, J., Chandawarkar, A., Eng, G., … Khademhosseini, A. (2006). Micromolding of shape-controlled, harvestable cell-laden hydrogels. *Biomaterials*, *27*(31), 5391–5398. doi:10.1016/j.biomaterials.2006.06.005

Yu, X., Dillon, G. P., & Bellamkonda, R. B. (1999). A laminin and nerve growth factor-laden three-dimensional scaffold for enhanced neurite extension. *Tissue Engineering*, *5*(4), 291–304. doi:10.1089/ten.1999.5.291

Yu, X., Dillon, G. P., Bellamkonda, R. V, & Ph, D. (1999). A Laminin and Nerve Growth Factor-Laden Three-, *5*(4).

Zaari, N., Rajagopalan, P., Kim, S. K., Engler, A. J., & Wong, J. Y. (2004). Photopolymerization in microfluidic gradient generators: Microscale control of substrate compliance to manipulate cell response. *Advanced Materials*, *16*(23-24), 2133–2137. doi:10.1002/adma.200400883

Zhang, G., Wang, X., Wang, Z., Zhang, J., & Suggs, L. (2006). A PEGylated fibrin patch for mesenchymal stem cell delivery. *Tissue Engineering*, *12*(1), 9–19. doi:10.1089/ten.2006.12.ft-25

Zhou, W., Blewitt, M., Hobgood, A., & Willits, R. K. (2012). Comparison of neurite growth in three dimensional natural and synthetic hydrogels. *Journal of Biomaterials Science, Polymer Edition*, *24*(3), 1–14. doi:10.1080/09205063.2012.690277

Zhu, Y., Wang, A., Patel, S., Kurpinski, K., Diao, E., Bao, X., … Li, S. (2011). Engineering bi-layer nanofibrous conduits for peripheral nerve regeneration. *Tissue Engineering. Part C, Methods*, *17*, 705–715. doi:10.1089/ten.tec.2010.0565

Zisch, A. H., Lutolf, M. P., Ehrbar, M., Raeber, G. P., Rizzi, S. C., Davies, N., … Hubbell, J. a. (2003). Cell-demanded release of VEGF from synthetic, biointeractive cell ingrowth matrices for vascularized tissue growth. *The FASEB Journal : Official Publication of the Federation of American Societies for Experimental Biology*, *17*(15), 2260–2262. doi:10.1096/fj.02-1041fje

Zustiak, S. P., Durbal, R., & Leach, J. B. (2010). Influence of cell-adhesive peptide ligands on poly(ethylene glycol) hydrogel physical, mechanical and transport properties. *Acta Biomaterialia*, *6*(9), 3404–3414. doi:10.1016/j.actbio.2010.03.040